Copyright Warning & Restrictions

The copyright law of the United States (Title 17, United States Code) governs the making of photocopies or other reproductions of copyrighted material.

Under certain conditions specified in the law, libraries and archives are authorized to furnish a photocopy or other reproduction. One of these specified conditions is that the photocopy or reproduction is not to be "used for any purpose other than private study, scholarship, or research." If a, user makes a request for, or later uses, a photocopy or reproduction for purposes in excess of "fair use" that user may be liable for copyright infringement,

This institution reserves the right to refuse to accept a copying order if, in its judgment, fulfillment of the order would involve violation of copyright law.

Please Note: The author retains the copyright while the New Jersey Institute of Technology reserves the right to distribute this thesis or dissertation

Printing note: If you do not wish to print this page, then select "Pages from: first page # to: last page #" on the print dialog screen

ABSTRACT

ANTI-SOLVENT PRECIPITATION AND SUBSEQUENT FILM FORMATION OF HYDROPHOBIC DRUGS FOR DRUG DELIVERY

by
Xiangxin Meng

It is estimated that about forty percent of the drug molecules being developed by the pharmaceutical industry are hydrophobic in nature, leading to poor water solubility and bioavailability in the gastrointestinal tract. Dissolution is a limiting factor in their in vivo performance, and increasing their dissolution rate is a major challenge. It has been proven that the dissolution rate is directly proportional to the specific surface area, which can be effectively increased by reducing the particle size. Therefore, considerable efforts have gone into developing reliable and efficient methods for the manufacture of fine particles. Particle size reduction technologies such as milling or high-pressure homogenization have been used over the years. However, controlling of size distribution, morphology, and surface properties can be challenging.

In recent years, bottom up processes have emerged as methods for the synthesis of drug particles for hydrophobic drugs. As many hydrophobic drugs are soluble in various water miscible organic solvents, an effective approach is the precipitation of fine particles from solution phase while mixing with an anti-solvent. The formation, stabilization and sedimentation of these particles depend upon the discreet steps of nucleation, condensation and coagulation into larger particles. Nucleation and condensation tend to be competing factors as both consume solute molecules, and the coagulation step involves the aggregation, often leading to bimodal particle size distribution. Therefore,

suspension stabilization involves the optimization of the above mentioned competing factors.

The objective of this study is the anti-solvent synthesis of micron-size drug particles, their stabilization and subsequent self-assembly into polymer films suitable for drug delivery. The drug particles were produced with anti-solvent precipitation, while different stabilizers were used to stabilize the suspensions, and encapsulation into polymer films was carried out with hydroxypropyl methyl cellulose. The process was effective under low power ultrasonic agitation. The mean diameter of the small particles grew with time, while the overall particle size distribution showed a decrease in average particle size due to sedimentation. The results showed that a combination of polymers and surfactant reduced the average particle size more effectively than either only polymers or surfactant. The particles were distributed uniformly throughout the drug-loaded polymer films and the release profiles from films showed marked improvements. Most importantly, the redispersion of the drug-loaded films in an aqueous matrix showed that the crystallinity remained unaltered, and there was no appreciable increase in the particle size distribution.

ANTI-SOLVENT PRECIPITATION AND SUBSEQUENT FILM FORMATION OF HYDROPHOBIC DRUGS FOR DRUG DELIVERY

by
Xiangxin Meng

A Dissertation
Submitted to the Faculty of
New Jersey Institute of Technology
in Partial Fulfillment of the Requirements for the Degree of
Doctor of Philosophy in Chemistry

Department of Chemistry and Environmental Science

May 2011

APPROVAL PAGE

ANTI-SOLVENT PRECIPITATION AND SUBSEQUENT FILM FORMATION OF HYDROPHOBIC DRUGS FOR DRUG DELIVERY

Xiangxin Meng

Dr. Somenath Mitra, Dissertation Advisor — Date
Professor of Chemistry and Environmental Science, NJIT

Dr. Piero M. Armenante, Committee Member — Date
Distinguished Professor of Chemical Engineering, NJIT

Dr. Rajesh N. Dave, Committee Member — Date
Distinguished Professor of Chemical Engineering, NJIT

Dr. Tamara Gund, Committee Member — Date
Professor of Chemistry and Environmental Science, NJIT

Dr. Zafar Iqbal, Committee Member — Date
Research Professor of Chemistry and Environmental Science, NJIT

BIOGRAPHICAL SKETCH

Author: Xiangxin Meng

Degree: Doctor of Philosophy

Date: May 2011

Undergraduate and Graduate Education:

- Doctor of Philosophy in Chemistry,
  New Jersey Institute of Technology, Newark, NJ, 2011

- Bachelor of Science in Chemistry,
  Northwest University, Xi'an, Shaanxi, P.R. China, 2003

Major: Chemistry

Selected Publications and Presentations:

Meng, X., Sae-Khow, O., Yang, D., Mitra, S., 2011. Two stage precipitation for simultaneous synthesis, stabilization and casting of micro-scale drug particles in polymer films. (in preparation)

Meng, X., Yang, D., Keyvan, G., Michniak-Kohn, B., Mitra, S., 2011. Synthesis and immobilization of micro-scale drug particles in presence of cyclodextrins. Colloids and Surfaces B: Biointerfaces. (under review)

Meng, X., Yang, D., Keyvan, G., Michniak-Kohn, B., Mitra, S., 2011. Synthesis and immobilization of micro-scale drug particles in cellulosic films. Colloids and Surfaces B: Biointerfaces. In press, accepted manuscript.

Meng, X., Yang, D., Mitra, S., 2011. Simultaneous synthesis, stabilization, and self-assembly of microscale drug particles in polymer films. Journal of Applied Polymer Science. 120, 2082-2089.

Desai, C., Meng, X., Yang, D., Wang, X., Akkunuru, V., Mitra, S., 2011. Effect of solvents on stabilization of micro drug particles. Journal of Crystal Growth. 314, 353-358.

Zhu, W., Romanski, F.S., Meng, X., Mitra, S., Tomassone, M.S., 2011. Atomistic simulation study of surfactant and polymer interactions on the surface of a fenofibrate crystal. European Journal of Pharmaceutical Sciences. In Press, Corrected Proof.

Meng, X., Chen, Y., Chowdhury, S.R., Yang, D., Mitra, S., 2009. Stabilizing dispersions of hydrophobic drug molecules using cellulose ethers during anti-solvent synthesis of micro-particulates. Colloids and Surfaces B: Biointerfaces. 70, 7-14.

Meng, X., Dalvi, S.V., Dave, R.N., Mitra, S., Simultaneous antisolvent synthesis stabilization and solvent casting of hydrophobic drug molecules in biological polymers. ACS National Meeting, Washington, DC, August 16-20, 2009.

Meng, X., Mitra, S., Polymer films for the delivery of hydrophobic Drugs. ISPE Meeting, Newark, April 28, 2009.

Meng, X., Benedetto, G.D., Armenate, P.M., Dave, R.N., Mitra, S., Simultaneous microparticle formation, suspension stabilization with cellulose and subsequent film formation. ACS National Meeting, Salt Lake City, UT, March 22-26, 2009.

Meng, X., Mitra, S., Integration of particle formation and film formation for delivery. ISPE Meeting, Piscataway, May 28, 2008.

This dissertation is dedicated to my beloved family, for their love and support

ACKNOWLEDGMENT

I would like to extend my deepest appreciation and respect to my doctoral dissertation advisor, Dr. Somenath Mitra, who has provided a tremendous amount of advisement, guidance and support during the time of my doctoral studies. I am also very grateful to Dr. Piero M. Armenante, Dr. Rajesh N. Dave, Dr. Tamara Gund and Dr. Zafar Iqbal for serving on my committee and providing valuable feedback.

I gratefully acknowledge the funding support financial support from National Science Foundation grants, the Center for Structured Organic Composites for Pharmaceutical, Nutraceutical, and Agrochemical applications (NSF ERC: EEC-0540855), NanoPharmaceutical Engineering and Science (NSF IGERT: DGE-0504497) and Computation and Communication: Promoting Research Integration in Science and Mathematics (NSF C2PRISM: DGE-0638423).

Special thanks go to the Department of Chemistry and Environmental Science for providing the teaching assistantship. I greatly appreciate the help that Ms. Clarisa González-Lenahan and Dr. Marino Xanthos, as well as the staff of the Graduate Studies Office and the Office of International Students and Faculty have offered to me during my study. I would also like to thank my colleagues for their friendship, assistance and suggestions.

Lastly, I would like to thank my whole beloved family: my parents, my husband and my daughter, who patiently stood by me during my doctoral studies.

TABLE OF CONTENTS

TABLE OF CONTENTS
(Continued)

TABLE OF CONTENTS
(Continued)

LIST OF TABLES

LIST OF FIGURES

LIST OF FIGURES
(Continued)

LIST OF FIGURES
(Continued)

Figure **Page**

LIST OF FIGURES
(Continued)

CHAPTER 1

INTRODUCTION

1.1 Objective

The enhancement of aqueous solubility and the dissolution rate of hydrophobic drugs is one of the major challenges during the drug development process. The dissolution rate and the bioavailability of hydrophobic drug are dependent on the particle size. The smaller particles have more surface area, which lead to an increase in dissolution rate. With increase in surface area, the newly formed particles need to be stabilized to prevent subsequent agglomeration due to interparticulate interactions. Agglomeration of the particles lowers the stability of drug suspension systems. Therefore, it is necessary to use stabilizers to overcome the stability problem.

The objective of this research is micron-scale particles formation, their stabilization and subsequent self-assembly as homogeneous polymer films suitable for drug delivery. Biopharmaceutics Classification System (BCS) class II drugs such as Fenofibrate and Griseofulvin were used as the model drugs in this project. The objectives of this project are listed as follows:

- Study of micro-scale drug particle formation with anti-solvent precipitation;
- Stabilization of drug suspensions by using cellulose ethers, β-cyclodextrins and surfactants;
- Understanding of stability of drug suspension based on the characterization for different suspension systems;
- Formation of drug-loaded polymer film by using both low and high molecular weight hydroxypropyl methyl cellulose (HPMC);
- Characterization of drug-loaded polymer films;

- Drug release study for drug loaded polymer films.

1.2 Hydrophobic Drug Molecules

"Hydrophobic Drugs" describes a heterogeneous group of drug compounds that exhibit poor solubility in water but are typically soluble in various organic solvents. The degree of water solubility for drug compounds can be defined as slightly soluble (1-10mg/ml), very slightly soluble (0.1-1 mg/ml), and practically insoluble (<0.1mg/ml) (Wischke and Schwendeman, 2008). It has been proven that low solubility in water may cause low dissolution rate, thus result in low absorption across biological barriers. The Biopharmaceutics Classification System (BCS) is a guide for predicting the intestinal drug absorption provided by the U.S. Food and Drug Administration. It classifies the Active Pharmaceutical Ingredients (API) based upon the aqueous solubility related to dose at three relevant pHs and intestinal permeability (Yasuji et al., 2008). According to the BCS, active pharmaceutical ingredients are classified into four groups: class I (high solubility and high permeability), class II (low solubility and high permeability), class III (high solubility and low permeability) and class IV (low solubility and low permeability) (Table 1.1). It has been reported that about 40% of the drug candidates in the pipeline are hydrophobic. The oral bioavailability of these drug compounds is limited due to slow drug dissolution in the gastrointestinal tract. Therefore, it is desirable to improve the solubility of these drug compounds by using various pharmaceutical technologies (Merisko-Liversidge et al., 2003).

Table 1.1 Biopharmaceutics Classification System

		Permeability	
		High	Low
Solubility	High	Class I	Class III
	Low	Class II	Class IV

Although some prodrug technologies have been employed to address drug structure design in drug discovery step, it might be too difficult to change the chemical structure of the drug compound after development of drug products. Several formulation approaches have been developed over years to address the solubility issue and it has been proved that formation of fine drug particles has been a well-established approach for solubility improvement and enhancing bioavailability (Kesisoglou et al., 2007).

1.3 Drug Particle Formation

1.3.1 Dissolution Enhancement through Drug Particle Formation

The solubilization of drug from the micro- or nano-particles is of interest nowadays. Drug must first be dissolved in the medium at the absorption site. The process that a drug particle dissolves is called dissolution. As the drug undergoes dissolution, the drug molecules on the surface enter into solution, creating a diffusion layer. The drug molecules from diffusion layer pass throughout the dissolving fluid and contact with the biologic membranes, and absorption occurs (Allen et al., 2005). Hydrophobic drugs can be formulated as micro- or nano-particles with high surface area, which enhances dissolution rates in accordance with the Noyes-Whitney equation (Sanganwar et al., 2010):

$$dc/dt = kS(Cs - Ct) \quad (1.1)$$

Where dc/dt is the rate of dissolution, k is the dissolution rate constant, S is the surface area of the dissolving solid, Cs is the saturation concentration of drug in the diffusion layer and Ct is the concentration of the drug in the dissolution medium at time. Based on this principle, the reduction of particle size leads to a significant increase in the surface area, which in turn can lead to substantial increase in dissolution rate and bioavailability.

In addition to the dissolution rate enhancement described above, forming fine particles also improves the saturation solubility of drug substances. It was described by the Ostwald-Freundlich equation, which demonstrates that solubility increases exponentially as a function of particle size (Kesisoglou et al., 2007):

$$S = S_{\infty} \exp(\frac{2\gamma M}{r\rho RT}) \quad (1.2)$$

Where S is the saturation solubility of the drug substance, S_{∞} is the saturation solubility of an infinitely large drug crystal, γ is the crystal medium interfacial tension, M is the compound molecular weight, r is the particle radius, ρ is the density, R is a gas constant and T is the temperature. The increase in solubility results in a further increase in dissolution rate, as a result, the bioavailability for drug can be enhanced through forming fine drug particles (Merisko-Liversidge et al., 2003).

1.3.2 Drug Particle Formation Technologies

Micro- or nano-particles can be produces by bottom-up or top-down technologies. Top-down technologies start with coarse materials and apply forces to break down into micro- or nano-particles, while bottom-up technologies start with the molecules in solution and the molecules are aggregated to form the solid particles (Muller et al., 2006).

1.3.2.1 Top-down Technologies. Milling and homogenization are the traditional top-down methods for size reduction of large quantities of particulate materials. In the milling operation, the applied stress is applied on the material, which causes the breakage of the particle. Nowadays, most of the pharmaceutical size reduction operations use Ball/Pearl milling for the production of fine drug particles. For instance, Rapamune® coated tablet is based on the ball-milling technology by the company NANOSYSTEMS ELAN and it showed 27% higher of bioavailability than the solution form (Kipp, 2004). During the milling, surfactants or stabilizers were used for the physical stability of the produced drug nanoparticles. The choice of surfactant/stabilizers depends on the properties of the particles, physical principles and the route of administration. SDS, which has excellent dispersion properties and can adsorb on the particle surface was used in the formulation of Emend® (Kipp, 2004). Although milling process is effective for producing nano-particles, erosion of the milling material may cause certain contamination for the products. Also, milling process requires grinding for hours to days in order to reach a desired size range (Ward and Schultz, 1995). Moreover, prolonged milling may induce the formation of amorphous material (Willart et al., 2001).

High-pressure homogenization has been utilized for many years for production of emulsion and suspensions. This technology is easy to scale up, even with very large volumes. Piston-gap principle and jet-stream technology are the two basic technologies for most homogenizers. For instance, in the piston-gap homogenizer, the macrosuspension coming from the sample container is forced to pass through a tiny gap and particle diminution is affected by shear force, cavitation and impaction. In jet-stream homogenizers, the collision of two streams leads to particle diminution mainly by impact forces. Intralipid® and Lipofundin® are the two commercial products which have mean droplet diameter with the range of 200-400nm (Akkar and Müller, 2003). For lab scale study, Muller et al developed batch Micon Lab 40 which has relatively small batch volume and the homogenizer is equipped with two product containers having a maximum volume of 1000 ml (Grau et al., 2000).

1.3.2.2 Bottom-up Technologies. In recent years, bottom-up processes such as emulsification and precipitation methods have emerged as methods for the synthesis of submicron or micro-particles from the liquids. As many hydrophobic drugs are soluble in various water immiscible organic solvents, one of the simple methods to form drug particles is emulsification method. In a typical emulsification process, the drug and polymer are first dissolved in a water immiscible solvent and are added into aqueous solution containing an emulsifier. The solvent removal then took place by evaporation to a gas phase or by extraction to the continuous phase (Sawalha et al., 2008). The emulsification method has been applied for forming fine particles for a large number of drug compounds, including neuroleptics thioridazine, chlorpromazine and bromperidol (Maulding et al., 1986; Suzuki and Price, 1985; Wischke and Schwendeman, 2008).

Precipitation methods such as anti-solvent precipitation have been utilized for many years in the preparation of submicron particles for drug delivery (Xia et al., 2010; Zimmermann et al., 2007). Typically, the drug is first dissolved in an organic solvent and the drug solution is mixed with a miscible anti-solvent (Figure 1.1). The ultrasonic agitation was used to assist particle precipitation during mixing. Precipitation processes that form particles directly may provide more control of particle size distribution and morphology. Recently we have reported sonication assisted anti-solvent precipitation for the formation of submicron and micro-particles of hydrophobic drugs, where appropriate combination use of cellulose ethers and surfactants could enhance the rate of particle formation as well as the reduction of the overall particle size (Desai et al., 2011; Meng et al.; Meng et al., 2009; Zhu et al.). The stabilization of these suspensions is of great importance for both controlling the particle size and developing manufacturing processes. The latter could include conventional methods such as spray drying or incorporation into final drug delivery vehicles like polymer films and control release formulations.

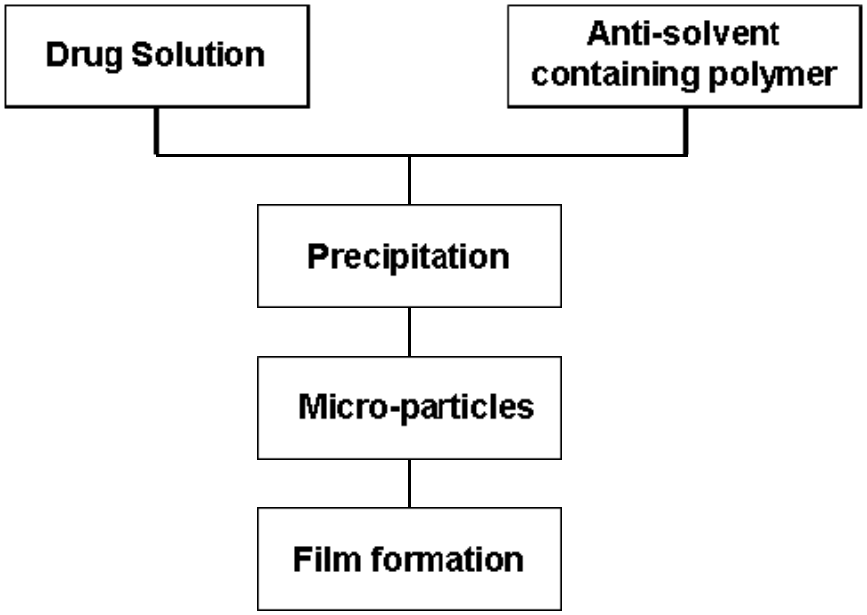

Figure 1.1 Approach for anti-solvent precipitation.

Precipitation method has also been used with high shear processing. NANOEDGE process is accomplished by a combination of rapid precipitation and high-pressure homogenization (Kipp, 2004). During the process, sudden supersaturation is achieved by rapid addition of drug solution to an anti-solvent which leads to fine crystalline or amorphous solids. High supersaturation often causes the formation of needle like crystals, which is because supersaturation favors nucleation rather than crystal growth. Nowadays, supercritical technology has been combined with anti-solvent precipitation method for particle formation. The high diffusive supercritical fluid can rapidly extract the solvent and precipitate the drug particles that are mainly under 15 μm (Martin et al., 2002; Yu. Shekunov et al., 2001).

The particle precipitation and growth involve nucleation, condensation of solute molecules, and coagulation of particles. (Figure 1.2) The nucleation rate depends on the degree of supersaturation. The increase of supersaturation can give rise to a sharp increase in the nucleation rate. Nucleation occurs when a critical number of molecules join together to form nuclei. The formed small nuclei can be absorbed on the surface by the single molecules through the condensation process. Nucleation and condensation are two processes consuming the solute molecules. Thus, they compete with each other and result in the particle size during the precipitation process. Generally, high nucleation rate can result in small particles and low nucleation rate can result in large particles (Helfgen et al., 2001; Weber and Thies, 2002). The coagulation process usually occurs after particle precipitation, resulting in particles collide and stick together to form bigger particles. Coagulation does not consume solute molecules, leaving unchanged the total particle mass (Young et al., 2003). It is initiated and accelerated by the nucleation and

condensation process. Coagulation can also affect these processes indirectly. For instance, coagulation can reduce the condensation rate, which reduces the number of particles and thus increase overall available particle surface area. Condensation competes with coagulation and weakens it by lowering coagulation's driving force. Therefore, coagulation tends to favor nucleation (Marchisio et al., 2006; Matteucci et al., 2006; Weber and Thies, 2002).

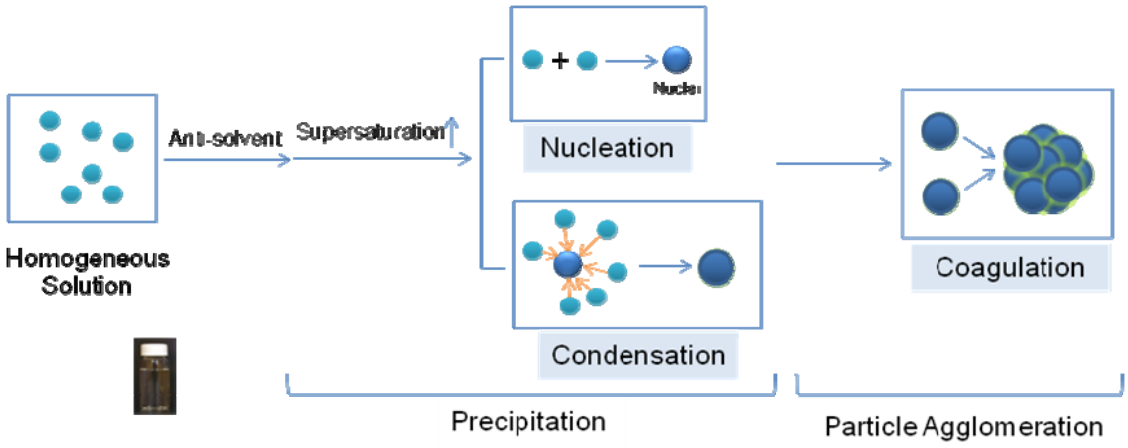

Figure 1.2 Mechanism of particle precipitation and growth.

The Damkhöler number (Da) can be defined that the ratio between the mixing time (τ_{mix}) and overall precipitation time (τ_{precip}). The degree of supersaturation is low with slow mixing rate. The consequent nucleation rates may be slow and result in the formation of large particles. On the other hand, time of condensation and coagulation that contribute to the overall precipitation time can be long to produce smaller particles (Da<<1). With anti-solvent precipitation, the addition of stabilizer is known to slow the condensation and coagulation due to lower Da (Matteucci et al., 2006).

$$D_a = \frac{\tau_{mix}}{\tau_{precip}} \tag{1.3}$$

1.4 Drug Particle Stabilization in Aqueous Media

The stabilizers are usually added for the stabilization of drug particles during particle formation. It is known that the increased surface area creates a positive gain in free energy, thus small particles will tend to agglomerate to a less energetic state. Stabilizers are needed to stabilize the micro- or nano-particles against inter-particle forces and prevent them from agglomeration. Generally, stabilizers are amphiphilic having both hydrophobic and hydrophilic properties so that the surface of solid particles can be properly wetted and then stabilized in the aqueous phase. Stabilization can be achieved by steric, electrostatic or a combination of both types of interactions. Those interactions can provide imparting repulsive forces to a colloidal system. Steric stabilization can be achieved by adsorbing polymers on the particle surface, while electrostatic stabilization is obtained by adsorbing charged molecules (eg. ionic surfactants or charged polymers) on the particle surface (Merisko-Liversidge and Liversidge). Common pharmaceutical stabilizers include cellulose ethers, cyclodextrins, polyvinylpyrrolidone (PVP), polyethylene glycol (PEG) and polyvinylalcohol (PVA). Here, we only discuss the cellulose ethers and cyclodextrins, which are used in the present work.

1.4.1 Celluloses Ethers

Cellulose ethers are high molecular weight compounds produced by replacing the hydrogen atoms of hydroxyl groups in the anhydroglucose units of cellulose with alkyl or substituted alkyl groups. They are widely used as stabilizers, binders and film-forming

agents in the pharmaceutical industry nowadays (Ferrero et al., 2010; Sasa et al., 2006; Scherlund et al., 2000). The properties of cellulose ethers are determined by the molecular weight, the substituent groups and the degree of substitution. The most commonly used cellulose ethers include methylcellulose (MC), hydroxypropyl methylcellulose (HPMC), hydroxyethyl cellulose (HEC), hydroxypropyl cellulose (HPC) and ethyl cellulose (EC). A variety of studies have recently been focused on the usage of cellulose ethers for stabilizing aqueous drug suspensions. Hideo Terayama has studied the aqueous suspensions of 5-(3-ethoxy-4-pentyloxyphenyl)-2,4-thiazolidinedione (CT112) prepared by neutralization of alkaline solutions of CT112 in the presence of HPMC. HPMC is found to adsorb onto the particle surface and lead to a highly stable drug suspension with homogenous particle size (Terayama et al., 2001; Terayama et al., 2004). Moreover, it has been found that mixed systems of the HPMC and SDS can enhanced the rate of particle formation and reduce the particle size effectively. Surfactant and polymers are able to absorb on the hydrophobic drug particle surface and form protective colloid which can lead to rapid wetting, resulting in enhancement of dispersion stability (Terayama et al., 2002).

Three cellulose ethers, namely, methyl cellulose (MC), hydroxyethyl cellulose (HEC) and hydroxypropyl methyl cellulose (HPMC) are used for the stabilization of drug particles during anti-solvent precipitation in the present study. The nature of the substituent and the degree of substitution are known to have direct effect on the polarity exhibited by the various cellulose ethers. The relative polarity of cellulose ethers chosen in this work are in the order HEC>HPMC>MC. The hydrophilicity, as assessed by partial solubility parameters, as well as by hygroscopicity, is in the as increasing order

MC<HPMC<HEC. This correlates well with polarity (Rodriguez et al., 2000). The physicochemical properties of cellulose ethers are also affected by their molecular weight. The chemical structures for the cellulose ethers are shown in Figure 1.3 (Bodvik et al., 2010).

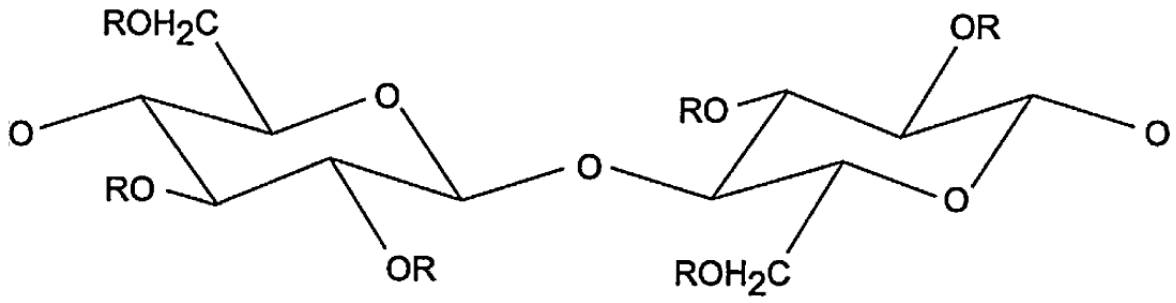

Figure 1.3 Chemical structure of cellulose ethers: in methyl cellulose (MC), R=H, CH_3; in hydroxyethyl cellulose (HEC), R=H, $CH_2CH_2(OH)$; in hydroxypropyl methyl cellulose (HPMC), R= H, CH_3, $CH_2CH(OH)CH_3$.

1.4.2 Cyclodextrins

Cyclodextrins are functional excipients that are widely used in the pharmaceutical industry as drug carriers, solubilizers and tablet excipients. Cyclodextrins are cyclic oligosaccharides consisting of six to eight glucose units, which are linked by α-1,4-glycosidic bonds (Figure1.4) (Brewster et al., 2008). Cyclodextrins have a molecular structure of truncated cone with a hydrophilic outer surface and a hydrophobic cavity, which enables them to form host-guest inclusion complexes with a size compatible drug molecule (Charoenchaitrakool et al., 2002). In aqueous solutions, the inclusion complex formation occurs through a process in which water molecules located inside the cavity are replaced by partial or whole drug molecule, thus lowering the energy of system during the release of enthalpy-rich water molecules from the cyclodextrin cavity

(Loftsson and Masson, 2001). The drug/cyclodextrin inclusion complex can be formed either during formulation or *in situ* from physical mixture to provide increased solubility.

While complexation describes many cases of drug/cyclodextrin formulations, there are growing evidences that other non-complex factors are also involved, such as surfactant-based effects in drug/cyclodextrin systems (Loftsson et al., 2004; Loftsson et al., 2005). Cyclodextrins were found to interact with growing crystals and act as an inhibitor for crystal growth, thus contribute the stabilization of drug/cyclodextrin system. It has been shown that the mechanism of stabilization for cyclodextrins via nucleation and crystal growth inhibition in supersaturated systems. Cyclodextrins can serve as a stabilizer that adsorbs on the crystal interface and accumulates in the water layer resulting in an increase resistance for diffusion of drug molecules (Brewster et al., 2008). For instance, it has been reported the ability of hydroxypropyl-β-cyclodextrin to inhibit crystal growth in spray-dried dispersion of nifedipine. They drug dissolution and bioavailability didn't change compared with freshly prepared dispersions due to the inhibition of crystal growth by hydroxypropyl-β-cyclodextrin (Uekama et al., 1992). It has been also suggested that the interaction of ibuprofen with hydroxypropyl-β-cyclodextrin changes the metastable zone as a function of drug-cyclodextrin interaction and solubilization (Iervolino et al., 2001).

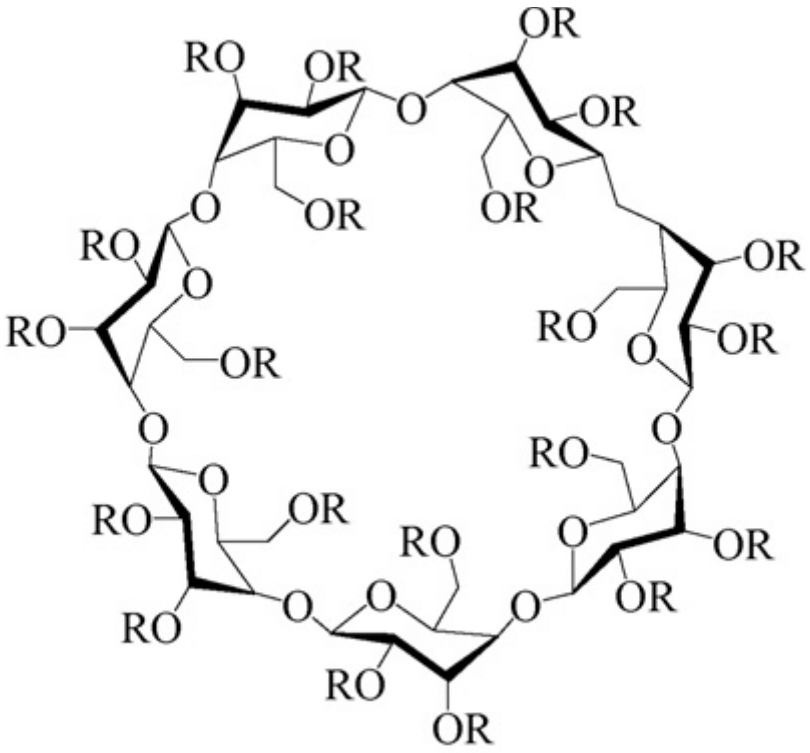

Figure 1.4 Chemical structure of β-cyclodextrin (BCD).

1.5 Drug Delivery

Drug delivery system (DDS) is the formulation by which a pharmaceutical compound is administrated to achieve a therapeutic effect in humans or animals. The drug delivery process includes the administration of the drug product, the release of the active pharmaceutical ingredients by the products, and the transport of the active ingredients across the biological membranes to the site of action. Drug delivery system is an interface between the patient and the drug (Jain, 2008b). Based on the disease, the effect desired and the product available, the drugs can be introduced into the human body by various administration routes, such as oral, parenteral, transdermal and pulmonary routes (Figure 1.5) (Mitragotri, 2005; Mitragotri, 2008).

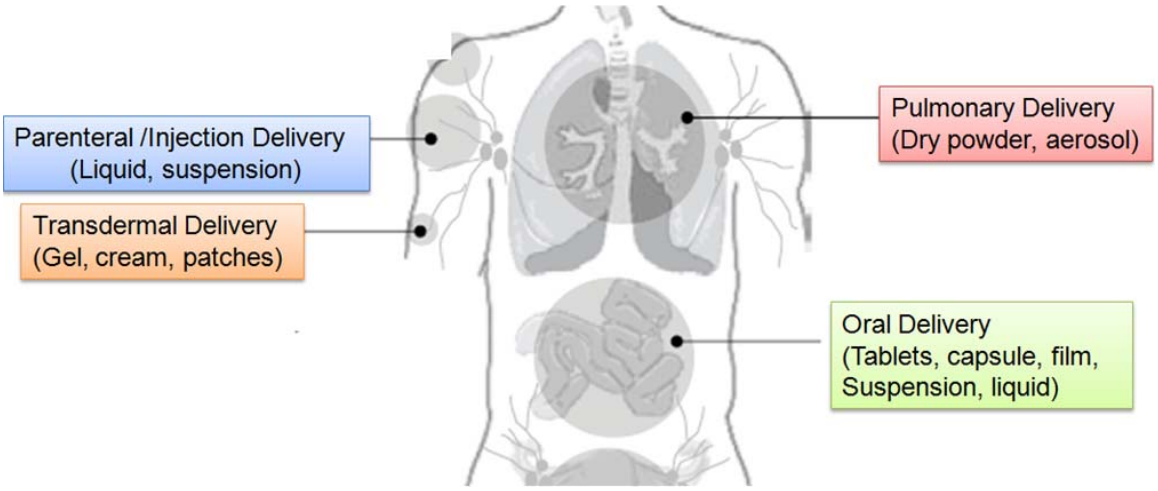

Figure 1.5 Drug delivery systems.

Source: Mitragotri, S., 2008. Recent development in needle-free drug delivery Frontiers of engineering. 38, 5-12.
http://www.nae.edu/Publications/Bridge/FrontiersofEngineering12256/RecentDevelopmentinNeedleFreeDrugDelivery.aspx accessed April 12, 2011

Oral drug delivery has been known for decades as the mostly used route of administration among all the routes. The reasons that the oral route achieved such popularity are the ease of administration as well as the acceptance by patients. Generally, pharmaceutical products designed for oral delivery include immediate-release, sustained-release and controlled-release products. Immediate-release (IR) products provide immediate release of drug for rapid absorption, while sustained release (SR) products provide long acting or delayed release compared with IR products. Controlled release technology has been recognized as new generation of pharmaceutical products nowadays (Chien, 1992). Since different drug compounds have variable absorption rates and serum concentrations that are unpredictable, it is necessary to develop controlled release drug delivery system. Typically, controlled release delivery aims at delivering the drug at the specific rate for a definite period of time. The period of delivery are usually much longer than SR products and vary from days to years (Kewal, 2008). All the pharmaceutical

products designed for oral administration must be developed based on the thorough understanding of the anatomy and physiology of the GI tract. This includes the fundamental understanding of various disciplines of drug absorption, GI transit, microenvironment of GI tract, pharmacokinetics and pharmacodynamics (Chien, 1992).

In addition to the commonly used oral administration routes, drugs can also be administered through other means, including parenteral and transdermal. Parenteral administration involves of injection of drug substance through the skin or mucous membrane. Unlike oral administration, in which the bioavailability of the drug is often subjected to the variations in GI transit, parenteral administration can access to the systemic circulation directly and therefore reach the site of drug action. Parenteral administration has now emerged as an established method for drug delivery and it has various advantages compared with other administration routes. For instance, it provides the rapid onsite of action and almost complete drug bioavailability. It can also provide the alternative administration route for the patients who are not able to ingest anything orally. Transdermal drug delivery system (TDDS) is an alternative delivery methods to oral and parenteral delivery and it deliver drugs though the skin to achieve the therapeutic effect. For a drug to be delivered through the skin it needs to have certain lipophilicity and molecular weight less than 500 Da (Brown et al., 2006). Because those requirements the number of commercially transdermal products are limited. In order to enhance the poor permeability across the skin, the use of penetration enhancers and prodrugs is necessary. Recently, there is considerable interest in usage of physical techniques such as iontophoresis, electroporation, sonophoresis, and reverse iontophoresis to improve

transdermal permeability of drugs of differing lipophilicity and molecular weight, including proteins, peptides and oligonucletides (Jain, 2008a).

The lung is an attractive target for drug delivery because it provides not only local lung effects but also possibly high systemic bioavailability. The local pulmonary deposition and delivery of the drug substances facilitates a targeted treatment of many diseases and chronic medical conditions (Beck-Broichsitter et al., 2009). Inhalation systems for pulmonary delivery have made significant advances in recent years and its technologies fall into three categories, which are pressurized metered-dose inhalers (MDIs), nebulizers and dry powder inhalers (DPIs) (Seppälä et al., 1998). Vaginal/rectal delivery shows advantages such as avoidance of the gut and hepatic first-pass metabolism and reduction in gastrointestinal and hepatic side effects. This route is being developed mainly to provide the protection against microbial infections and uterine targeting.

Incorporating the drug compound into a drug delivery system can significantly improve its performance. Drug delivery has been greatly improved over the years by means of particulate systems that increase bioavailability, reduce toxicities, improve the timed release of drug molecules and enable precision drug targeting (Italia et al., 2009). The particulate drug delivery system can be applied not only for common oral delivery but also for other delivery routes such as parenteral, transdermal or pulmonary. For instance, fine particles can interact with skin at a cellular level and the interaction between the particles and skin can be used to enhance immune reactivity for topical vaccine applications (Prow et al.). Typically, drug carriers are needed to incorporate into particulate drug delivery system for the design of delivery systems for those drug compounds. Biopolymer materials show desired properties such as biocompatibility,

biodegradability and functionalization capability as drug carrier and are most widely used in the pharmaceutical industry (Nair and Laurencin). Drug molecules can be entrapped or encapsulated within the polymer matrix, which provides the modified release of the drug molecules through the matrix to the onsite of action. The drug can be delivered through different dosage forms, including solids (tablets, capsules and thin films), semi-solids (gels and creams) and liquids (solutions, colloids and emulsions). The selection of drug delivery dosage forms is based on the route of administration and other factors, such as solubility and stability of drug compounds.

Nowadays, the pharmaceutical industry faces many challenges and innovative drug delivery technologies are needed to keep up with drug discovery technologies that help to reduce adverse effects, improve patient compliance and shorten the drug development time. There are 30 main drug delivery products on the market now and the number of those products has significantly increased in the past few years. This growth is expected to continue in the near future (Pierigè et al., 2008).

1.6 Drug-loaded Polymer Film for Drug Delivery

The aqueous suspensions formed via different particle formation technologies such as anti-solvent precipitation can be incorporated into a variety of final dosage forms, including biocompatible films, which have shown enormous potential (Akhgari et al., 2006; Schmidt and Bodmeier, 1999; Zheng et al., 2005). Edible films dissolve rapidly in saliva without the need for water and, thereby, improve patient compliance and acceptance. Films can also be designed to improve the onset of action for sublingual and buccal delivery and to provide controlled and sustained drug release and can be

optimized on the basis of the mechanical properties, permeability, and water vapor transmission (Akhgari et al., 2006; Nagarsenker, 1999).

Hydroxypropyl methyl cellulose (HPMC), a semi-synthetic derivative of cellulose, has been widely used in the pharmaceutical industry because of its nontoxic nature and ease of processing (Cao et al., 2004; Hiremath, 2008). HPMC also has excellent film-forming properties such as toughness and flexibility. The mechanical properties of HPMC are significantly dependent on the molecular weight of HPMC and the optimization of film formulation can be carried out by using different grades of HPMCs (Hardy et al., 2006). Nagarsenker et al. have studied mechanical and water-vapor transmission of films containing both low and high molecular weight HPMCs (Nagarsenker and Hegde, 1999). Moreover, HPMC can be used in combination with a secondary polymer such as polyvinylpyrrolidone (PVP), which has good solubility in water and a variety of organic solvents. The latter can improve the wettability of the dispersed particles and, therefore, improve the dissolution rate. PVP also has good adhesive/binding properties, which help in the formation of a continuous matrix with the drug particles dispersed in it. PVP-based films have been fabricated for controlled delivery through the skin, and it has been reported that the release rates increase linearly with the PVP fraction. This was attributed to the leaching of PVP, which resulted in the formation of pores in films (Rao and Diwan, 1998; Ye et al., 2007).

CHAPTER 2

ANTI-SOLVENT PARTICLE FORMATION WITH CELLULOSE ETHERS

2.1 Introduction

Drug molecules that exhibit poor aqueous solubility and bioavailability often end up as therapeutic failures (Gao et al., 2008; Mehta et al., 2007; Yuan et al., 2008). Therefore, the enhancement of solubility and the dissolution rate are major challenges in the drug development involving such compounds. Dissolution rate and bioavailability of hydrophobic molecules are known to be dependent on particle size and the morphology. Finer particles have more surface area per unit mass for van der Waals attraction, which can show strong adhesion. Therefore, considerable efforts have gone into developing reliable and efficient methods for the manufacture of stable and fine particles (Perrut et al., 2005). Conventional methods for the synthesis of micron and submicron particles include milling and homogenization in order to reduce the particle size. However, controlling of size, morphology, surface properties and electrostatic charge is often difficult (Wong et al., 2006). Precipitation processes that form particles directly may provide more control of these parameters.

Anti-solvent methods have been used extensively in the synthesis of submicron and micron size particles of insoluble drug moieties (Zimmermann et al., 2007). The formation, stabilization and sedimentation of these particles depend upon the discreet steps of nucleation, condensation and coagulation into larger particles (Helfgen et al., 2001; Weber and Thies, 2002; Young et al., 2003). Nucleation and condensation tend to be competing factors as both consume solute molecules (Marchisio et al., 2006), and the

coagulation step involves the aggregation, often leading to bimodal particle size distribution (Weber and Thies, 2002). Therefore, suspension stabilization involves the optimization of the above mentioned competing factors.

During anti-solvent precipitation, the addition of stabilizer is known to slow the condensation and coagulation due to lower Damkhöler number (Da) (Matteucci et al., 2006). The nano/micron particles suspension have been stabilized using biocompatible proteins such as human serum albumin, and polymers such as polycaprolactone (Dreis et al., 2007; Zili et al., 2005). Both steric and electrostatic stabilization can be carried out to stabilize a suspension. Several studies have recently focused on the usage of polymers for stabilizing aqueous dispersions (Chacón et al., 1999; Duro et al., 1998; Martinac et al., 2005). Polyvinylpyrrolidone (PVP) has been reported to improve the wettability of the dispersed particles and therefore improve the dissolution rate (Broman et al., 2001; Tantishaiyakul et al., 1999). Drug-PVP and Drug-PVP-SDS have been used to improve stability and dissolution properties of several hydrophobic drugs (Pongpeerapat et al., 2004; Yagi et al., 1996). The combined use of a polymer and surfactant is known to contribute to enhanced rate of particle formation, and reduce the overall particle size by the sorption of a polymer-surfactant complex on the particle surface (Itoh et al., 2003; Terayama et al., 2001; Terayama et al., 2002). Cellulose ethers have been used with water-insoluble drugs as they reduce surface tension and sterically inhibit water-insoluble particles from aggregating. Studies with fluorometholone and indomethacin, poorly soluble ophthalmic active ingredients have shown that the surface tension could be decreased by using HPMC in suspensions. It was further demonstrated that the adsorption of HPMC occurred on the surface of suspended particles which resulted in a good re-

dispersibility (Yasueda et al., 2004). Furthermore, when cellulose ether was used in combination with other stabilizer, it was able to provide smaller particle size compared to those containing only cellulose ether (Ain-Ai and Gupta, 2008).

The objective of this study is the anti-solvent synthesis of micro scale drug particles with simultaneous stabilization using different cellulose ethers and SDS. The anionic surfactant can adsorb effectively on drug particles to control the nucleation process, while the cellulose ethers forms a protective colloid. The process was found quite effective even under low power ultrasonic agitation.

2.2 Experimental Section

2.2.1 Materials

Fenofibrate (FNB, 99% purity) and Griseofulvin (GF, 95% purity) were purchased from Sigma Aldrich, USA. Fenofibrate is used to lower triglyceride levels and cholesterol levels in the blood. Griseofulvin is an antifungal agent which is widely used for the treatment of mycotic diseases. Fenofibrate and Greiseofulvin were chosen as the model drugs because of their poor solubility in water resulting in a poor absorption in the gastrointestinal tract. Methyl cellulose or MC (molecular weight of 40,000, and viscosity of 400 cP, 2 wt. % in H2O), hydroxyethyl cellulose or HEC (molecular weight of 90,000, and viscosity of 145 cP, 1 wt. % in H2O), hydroxypropyl methyl cellulose or HPMC (molecular weight of 10,000, and viscosity of 5 cP, 2 wt. % in H2O) and sodium dodecyl sulphate or SDS were obtained from Sigma Aldrich, USA. All chemicals were used as received. The water used in the experiments was purified with a Milli-Q Plus system. The melting points of MC, HEC, HPMC and SDS are 290 °C, 140 °C, 230 °C and 206 °C,

respectively. The glass transition temperature of MC, HEC and HPMC are 165 °C, 125 °C and 151 °C, respectively.

2.2.2 Methods

All precipitation experiments were carried out at room temperature. Model drugs were dissolved in acetone to form a clear solution. The cellulose ethers and SDS were dissolved in Milli-Q water by stirring. The ratio of drug, cellulose ether and SDS was 3:1:1. The drug solution was added into the aqueous phase slowly during sonication. The final drug concentration in the suspension was 0.4 % w/w. The pH of the aqueous dispersions was approximately 7.

Sedimentation was monitored as a function of time by measuring the weight percentage of the solid remaining in the suspension. This was accomplished as follows. Each suspension was divided equally into four subsamples and transferred to separate tubes and stored at 25°C. The solid sediments were collected at 2, 4, 7 and 9 hour intervals, dried in the oven at 35 °C in a vacuum to remove the solvent. The solid sediments were thoroughly rinsed with Milli-Q water to remove the excess cellulose ethers/SDS and then dried before weighing and further characterization.

Particle size analysis was carried out by static and dynamic light scattering. The former provided an estimate of the overall particle size distribution of the stabilized suspension, while the latter provided a selective picture of the relatively smaller particles that underwent significant Brownian motion. Static light scattering was carried out using Coulter Particle Size Analyzer LS230 (Beckman Coulter Inc., Miami, FL). Dynamic light scattering was carried out using Beckman Coulter, N4 Plus Submicron Particle Size

Analyzer (Beckman Coulter Inc., Miami, FL) at 23^{o} fixed detector angle. The nanoparticles nucleation and growth in the suspension was successfully monitored by measuring the change of particle diameter as a function of time. Zeta potential values were calculated from the electrophoretic mobilities of particles by using the Smoluchowski equation. Differential scanning calorimetry (DSC) was used to determine the melting point of GF particles. Approximately 6 mg of samples were weighed and sealed in an aluminum pan and then scanned using a Pyris-1 DSC instrument (Perkin Elmer Inc., San Jose, CA) with a temperature speed of 5 °C /min from 25 to 300 °C.

Scanning electron microscopy (SEM) was performed using a LEO 1530 (LEO Electron Microscopy Inc., Thornwood, NY) to study the morphology of particles and films. The samples were placed onto an aluminum stub with carbon conductive double-sided tape and then coated with carbon using a MED 020 HR sputtering coater (Micro Surface Engineering Inc., Los Angeles, CA) to improve conductivity. A Nicolet Almege XR Dispersive Raman with Olympus BX51 Confocal Microscope (Thermo Fisher Scientific Corp., Madison, WI) using a laser at 532nm was applied in the Raman imaging mode. The samples were placed onto the glass slide for the detection using 100× optical lens.

2.3 Results and Discussion

The characteristics of the two drug molecules are presented in Table 2.1. The solubility is known to correlate with melting point, enthalpy of fusion and partition coefficient (Yalkowsky and Valvani, 1980). Crystal energy related with Tm (melting point) and Hf (enthalpy of fusion), which refers to the energy a compound must overcome to dissolve

(Vippagunta et al., 2007). FNB had higher aqueous solubility than GF, while the latter had higher values of Tm and ΔHf and thus higher crystal energy. FNB had higher octanol/water partition coefficient (cLog P), thus a lower hydrophilicity. It also had higher molecular weight and molecular volume than GF.

Table 2.1 Physicochemical Properties of Model Drugs

	Structure	MF	FW	Water solubility (µg/ml)	ΔHf (kJ/mol)	Molar Volume (ml/gmol)	cLog P (n-Octanol Water)
Fenofibrate (FNB)	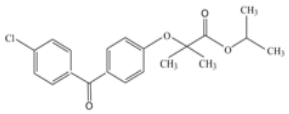	$C_{20}H_{21}ClO_4$	360.8	0.1	34.0	310.7	4.43
Griseofulvin (GF)	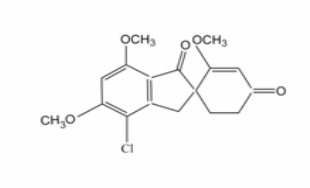	$C_{17}H_{17}ClO_6$	352.8	12	41.0	255.0	3.53

The cellulose ethers were found to be effective in stabilizing drug suspensions. A clear blank solution of HPMC and SDS is shown in Figure 2.1a. Figure 2.1b-e show an unstable suspension of FNB, stabilized FNB suspension with HPMC and SDS, unstable suspension of GF and stabilized GF suspension with HPMC and SDS, respectively. Other systems are not shown here for brevity. The unstable suspension clearly shows particles settling down, but the stable suspension was a homogenous suspension. Depending upon the conditions, the suspensions were found to be stable for as long as 30 hours without any reagitation. In absence of stabilization with cellulose ether and the surfactant, the suspensions settled down rather quickly as shown in Figure 2.1b and 2.1d. The kinematic viscosity of these solutions were measured and were found to be in the range of 1.20 and 1.86 cSt, therefore its role might have been limited.

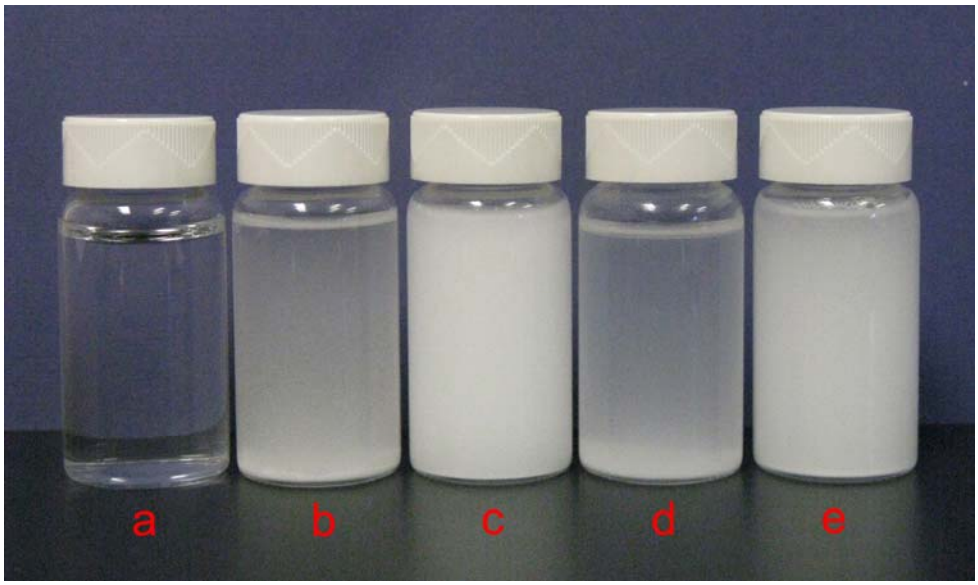

Figure 2.1 Suspensions of FNB and GF: (a) blank containing HPMC and SDS; (b) unstable suspension of FNB; (c) stabilized suspension of FNB with HPMC and SDS; (d) unstable suspension of GF; (e) stabilized suspension of GF with HPMC and SDS.

2.3.1 Particle Size Distribution

Dynamic light scattering or photon correlation spectroscopy (PCS) was used to selectively monitor the growth of the smaller particles. The upper size limit of PCS measurement is typically of the order of a few microns which are primarily determined by the sedimentation limit (Gun'ko et al., 2003). For the relatively larger or dense particles, the sedimentation rate may exceed the Brownian motion and the diffusion of the particle becomes increasingly limited. Thus, PCS provided a more accurate measure of the relatively smaller particles in the suspension. Figure 2.2 shows the change of the diameter of the smaller particles as a function of time for 50 hours. It is seen that the small particles grew with time, as the nanoparticles agglomerated into larger ones. The growth of the smaller particles was faster in presence of SDS when MC or HPMC was used as the stabilizing polymer. The trend was similar for other cellulose ethers. The decrease in particle size in the GF/HPMC and GF/HPMC/SDS systems may be attributed to Ostwald ripening (Van Eerdenbrugh et al., 2008). The growth of the submicron particles implies a higher nucleation rate, which ought to lead to a stable suspension.

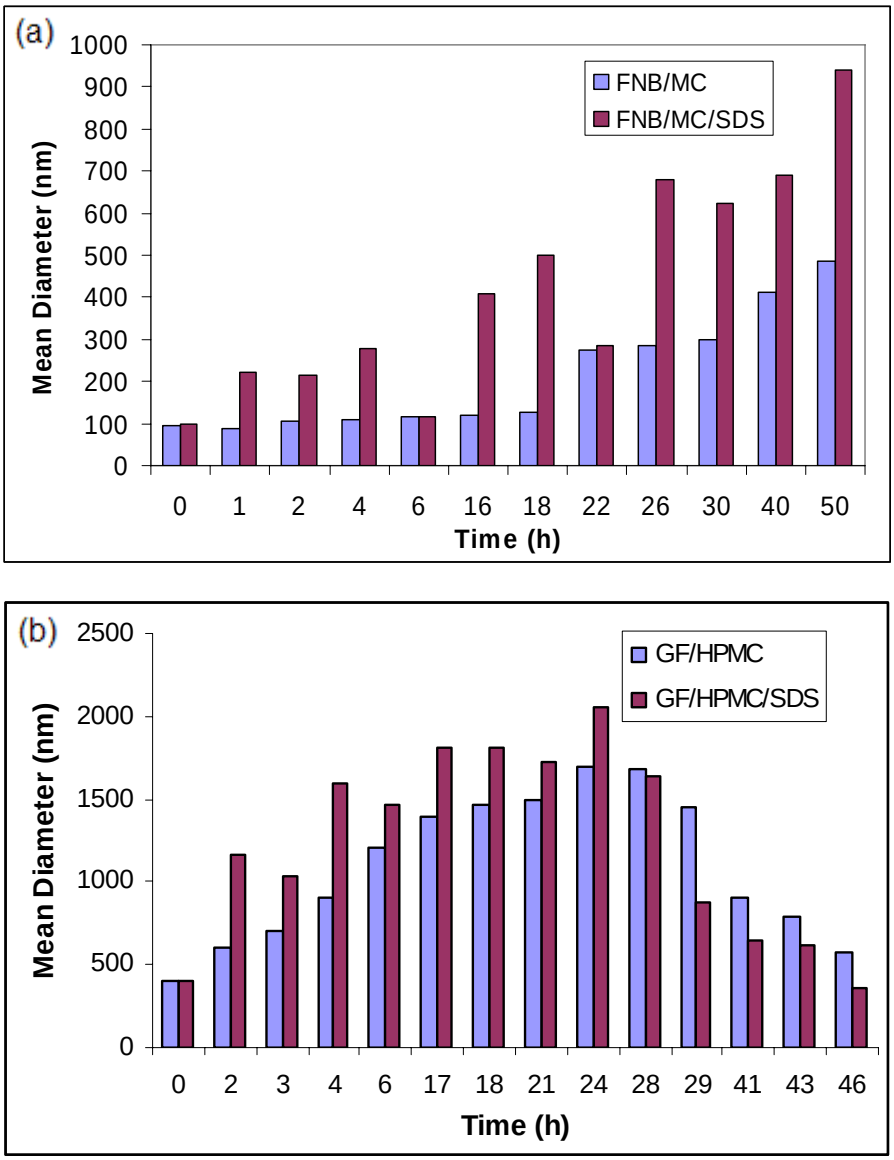

Figure 2.2 Dynamic light scattering measurement of stabilized suspension as a function of time: (a) FNB stabilized with MC, FNB stabilized with MC and SDS; (b) GF stabilized with HPMC, GF stabilized with HPMC and SDS.

The overall particle size distribution (PSD) was monitored using laser diffractometry, where the intensity of the diffracted light increases with the particle size. It used both Faunhofer and Mie theories to deduce PSD from spatial scattering distribution (Larson et al., 2002). The measurement in the submicron range was possible

using Polarization Intensity Differential Scattering system. However, since the suspensions had large amount of relatively larger particles, it provided a more accurate measure of the overall PSD than PCS. While PCS measurement provided a better picture of the condensation, the PSD was a better measure of coagulation growth and sedimentation.

Typical particle size distribution in stabilized suspension of FNB/GF in HPMC and SDS at the time of initial synthesis is shown in Figure 2.3. It is evident that beyond 10 microns, the particles settled rapidly. In some cases (Figure 2.3b) bimodal distribution was achieved, which clearly showed the coagulation of particles. The mean diameters of particle for different drug/cellulose/SDS systems are presented in Table 2.2 at the initiation of anti-solvent particle formation and four hours hence. All the cellulose ethers used here were effective in reducing the particle size. Cellulose ethers with alkyl-substituents such as MC and HPMC are known to interact with the newly formed particles and prevent particle growth. MC and HPMC which contain methoxyl or hydroxypropyl groups are able to adsorb onto hydrophobic solid surfaces, while polar cellulose ether (HEC) were found to be less effective (Allen et al., 2005; Rasenack and Müller, 2002). It was observed that the addition of SDS to the cellulose ether reduced the particle size between 20-50%. The trend in particle diameter appeared to be in the order HPMC<MC<HEC. For example, the suspension of FNB stabilized by HPMC and SDS produced smaller particles (4.7μm) compared with the one stabilized only by HPMC (6.3 μm). Among the FNB systems studied, the combination of HPMC/SDS generated the smallest average dp of 4.7 μm.

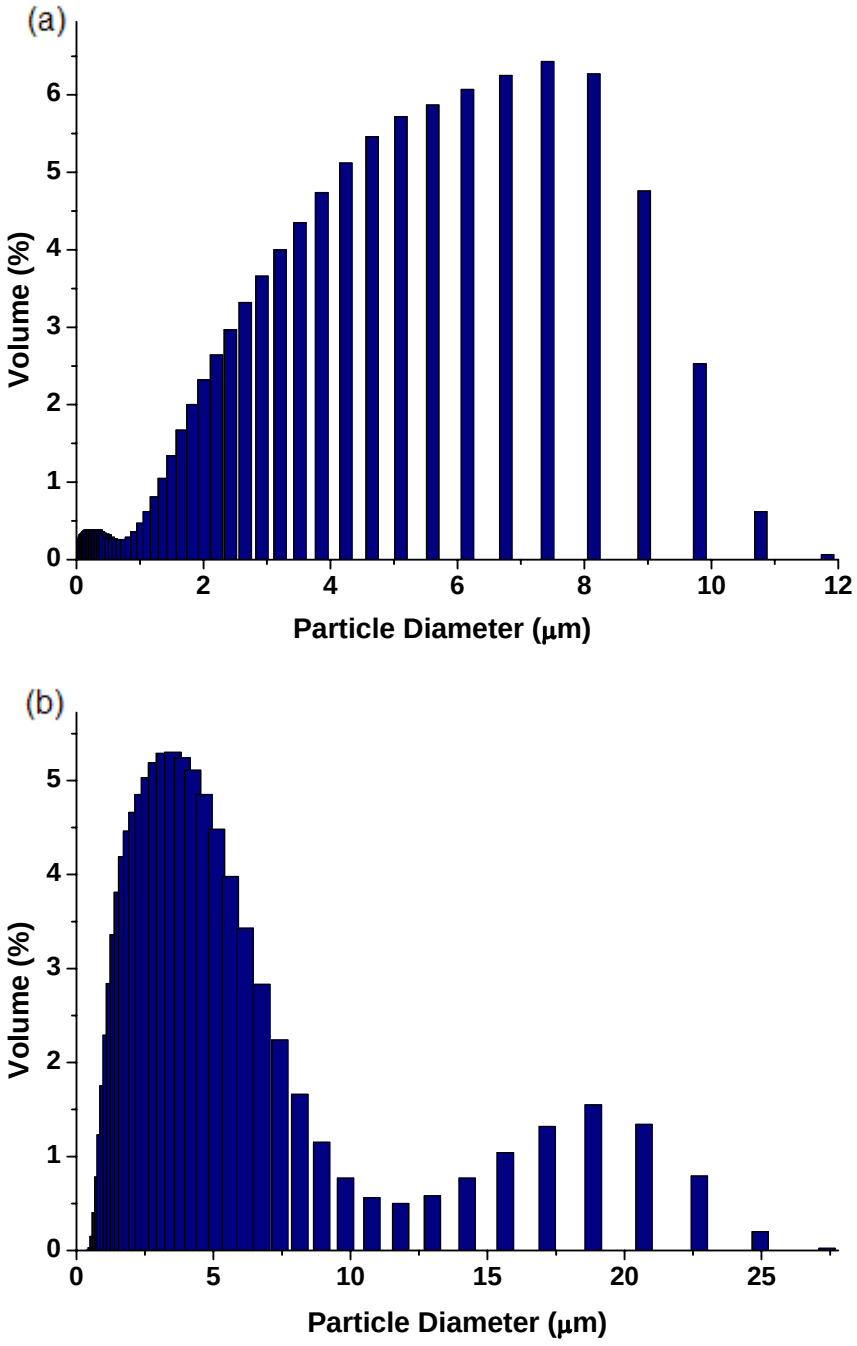

Figure 2.3 Particle size distribution (a) FNB stabilized by HPMC and SDS; (b) GF stabilized by HPMC and SDS.

Table 2.2 Stabilizing GF and FNB with Cellulose Ethers and Surfactant

Suspension	Mean diameter (μm)		Percentage of particles in suspension (%)		Sedimentation rate (w %/h)		Melting point (°C)
	0 hour	4 hour	4 hour	9 hour	2 hour	7 hour	
FNB/HPMC/SDS	4.7	3.4	83.0	74.6	4.8	1.7	73
FNB/HPMC	6.3	3.8	74.5	65.2	9.3	2.3	74
FNB/MC/SDS	5.1	3.5	81.6	73.2	6.2	1.5	72
FNB/MC	8.2	3.2	74.2	68.2	9.0	1.5	74
FNB/HEC/SDS	6.8	4.1	76.4	65.0	6.8	2.4	75
FNB/HEC	8.6	4.7	75.0	64.3	9.3	2.2	73
GF/HPMC/SDS	3.4	1.9	68.3	56.0	11.6	3.6	201
GF/HPMC	6.7	2.5	28.2	27.0	25.2	0.1	203
GF/MC/SDS	5.1	3.5	56.4	50.4	13.0	1.3	200
GF/MC	8.7	2.2	32.4	31.0	23.4	0.1	204
GF/HEC/SDS	7.3	3.7	50.1	43.1	21.6	1.7	198
GF/HEC	10.5	3.9	44.9	34.0	23.1	2.7	202

Note: Melting point (Tm) of pure FNB = 77 °C, GF = 206 °C.

Also seen from Table 2.2 is that as the suspension was allowed to stand, the larger particles settled, reducing the average particle diameter (dp) in the suspension. It is evident from Figure 4a that the presence of the cellulose ether and surfactant had stabilizing effect. In presence of SDS, the variation in dp was significantly less because the settling rate was slower. In its absence dp dropped rapidly from 8 to 2 micron. While cellulose ether provides a non-electrical stabilization, SDS provides an electrostatic energy barrier. Together they help maintain the distance between closely approaching solid particles in a suspension (Ain-Ai and Gupta, 2008). The selection of cellulose ethers was also important. According to Figure 2.4b, HPMC showed a stronger stabilizing effect

than HEC. The trend was similar for all the cellulose ethers and the average dp in this suspension dropped to between 2-3 microns in 6-8 hours. Typically the drops were maximum in case of HEC and minimum for HPMC. The presence of both hydrophilic and hydrophobic functional groups as well as lower molecular weight may account for the smallest dp in the HPMC suspensions.

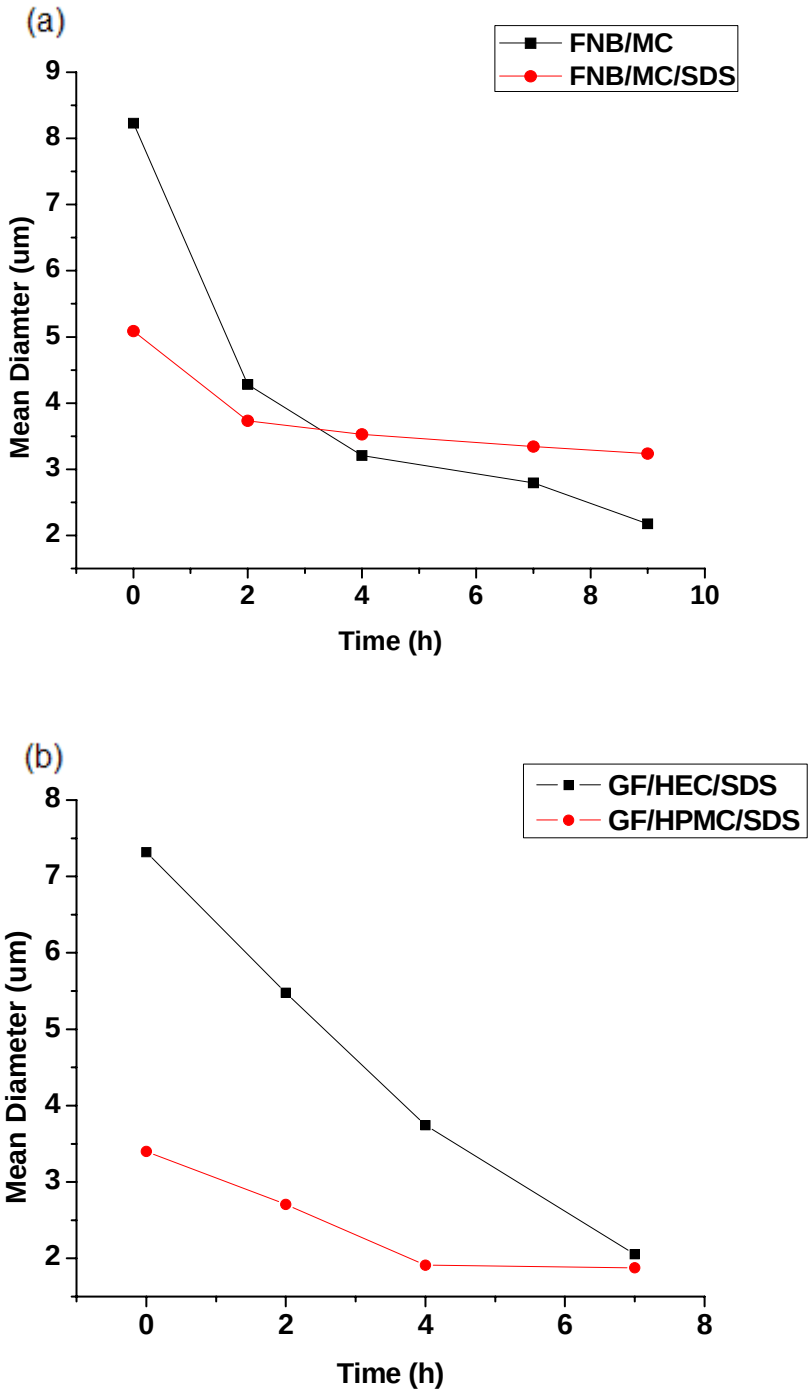

Figure 2.4 Mean diameter of drug particles as a function of time: (a) FNB stabilized with MC, FNB stabilized with MC and SDS; (b) GF stabilized with HEC and SDS, GF stabilized with HPMC and SDS.

Zeta-potential measurements were used to study the stability of the drug suspension. The zeta potential values were measured 24 hours after the preparation of the drug suspensions. Both cellulose ethers and SDS has been found to contribute the stabilization of drug particles in the suspension. The zeta potential values ranged between -3.24 and -24.61 mV (Table 2.3). These numbers imply that the suspension was not highly stable from an electrostatic consideration, but rather prone to agglomeration. SDS did not enhance zeta potentials, but clearly led to overall stability. In case of FNB, the addition of SDS led to a more negative zeta potential.

Table 2.3 Zeta Potential of FNB and GF Particles in Different Systems

Suspension	Zeta potential (mV)	Melting point (°C)
FNB/HPMC/SDS	-19.25	73
FNB/HPMC	-7.44	74
FNB/MC/SDS	-15.11	72
FNB/MC	-6.52	74
FNB/HEC/SDS	-11.55	75
FNB/HEC	-3.24	73
GF/HPMC/SDS	-15.16	201
GF/HPMC	-18.01	203
GF/MC/SDS	-13.06	200
GF/MC	-24.61	204
GF/HEC/SDS	-14.06	198
GF/HEC	-17.96	202

2.3.2 Sedimentation Rate

According to Stokes equation the rate of sedimentation depends upon the diameter of the dispersed particles, and the density and viscosity of the medium (Allen et al., 2005). Sedimentation rate was measured by calculating the weight percentage (w%) of solid drug particles remaining in the suspension as a function of time.

The solid particles were uniformly distributed after the preparation of the suspension. The amount of the solid particles in the suspension decreased with time as they began to settle. These are presented in Figure 2.5. The results appear to be consistent with the Stokes Equation that the smaller diameter particles have slower settling rate. However, the rate of settling varied depending upon the cellulose ether and the surfactant used. It was found that the rate of settling of the drug/cellulose/SDS systems were slower than that of the drug/cellulose systems. At the end of 9 hours, 74.6% of the particles in the FNB/HPMC/SDS were still in suspension as compared to 65.2% when the SDS was not added. As shown in Figure 2.5b, among HPMC, MC and HEC, the first two were most suitable polymers where 74.6%/73.2% of the drug stayed stabilized at the end of nine hours as compared to only 65.0% in presence of HEC for FNB systems. As seen from Table 2.2 and Figure 2.5a, b and c, GF was less stable than FNB. The effect of SDS was more pronounced for GF than FNB. For example, in presence of SDS with HPMC in GF system at four hours, 68.3% of the particles were still in suspension where as only 28.2% stayed suspended when SDS was not used. The corresponding numbers were 83.0% and 74.5% for FNB. From Table 2.2, it can be seen that as much as 74.6% of FNB and 56.0% of GF were still in stable suspensions at the end of nine hours in drug/HPMC/SDS systems. However, trend in the settling rate for the different cellulose

ethers were not as obvious, as they were for the particle diameter. According to the Stokes equation, the density of the particles along with the medium plays an important role and may affect the precipitation of the particles.

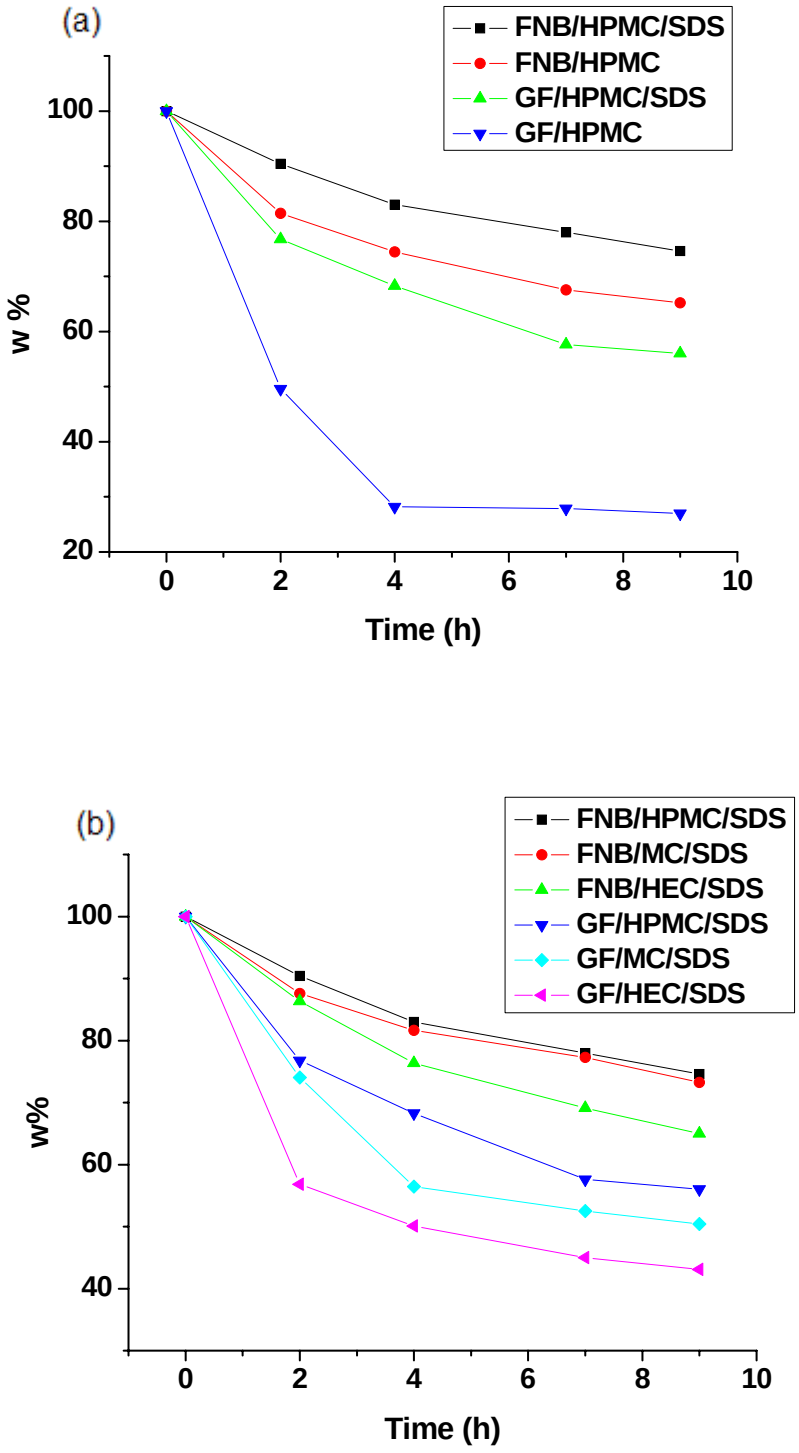

Figure 2.5 Weight percentage of stabilized drug particles in suspension: (a) FNB and GF in presence of HPMC and SDS; (b) FNB and GF in presence of different cellulose ethers and SDS; (c) FNB and GF in presence of different cellulose ethers without SDS.

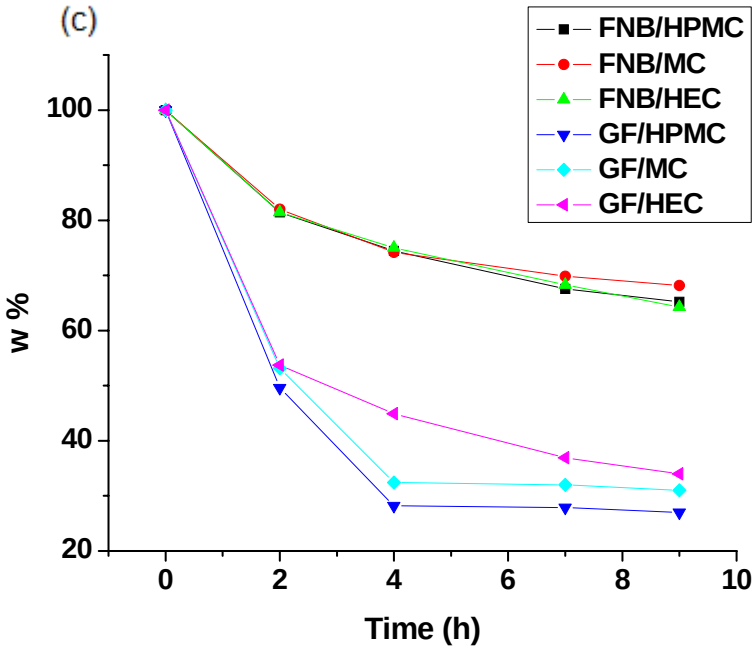

Figure 2.5 Weight percentage of stabilized drug particles in suspension: (a) FNB and GF in presence of HPMC and SDS; (b) FNB and GF in presence of different cellulose ethers and SDS; (c) FNB and GF in presence of different cellulose ethers without SDS. (Continued)

The settling rate was computed as a function of time for all systems (Figure 2.6). It was evident that the settling rate increased rapidly to 5-25% per hour within the first two hours and then dropped to 1-2%. The rate of settling was slowest for HPMC and fastest for HEC. In all cases, SDS was effective in lowering the settling rate. For example, in the case of GF/HPMC/SDS system, the settling rate was reduced by more than 50% by the addition of SDS.

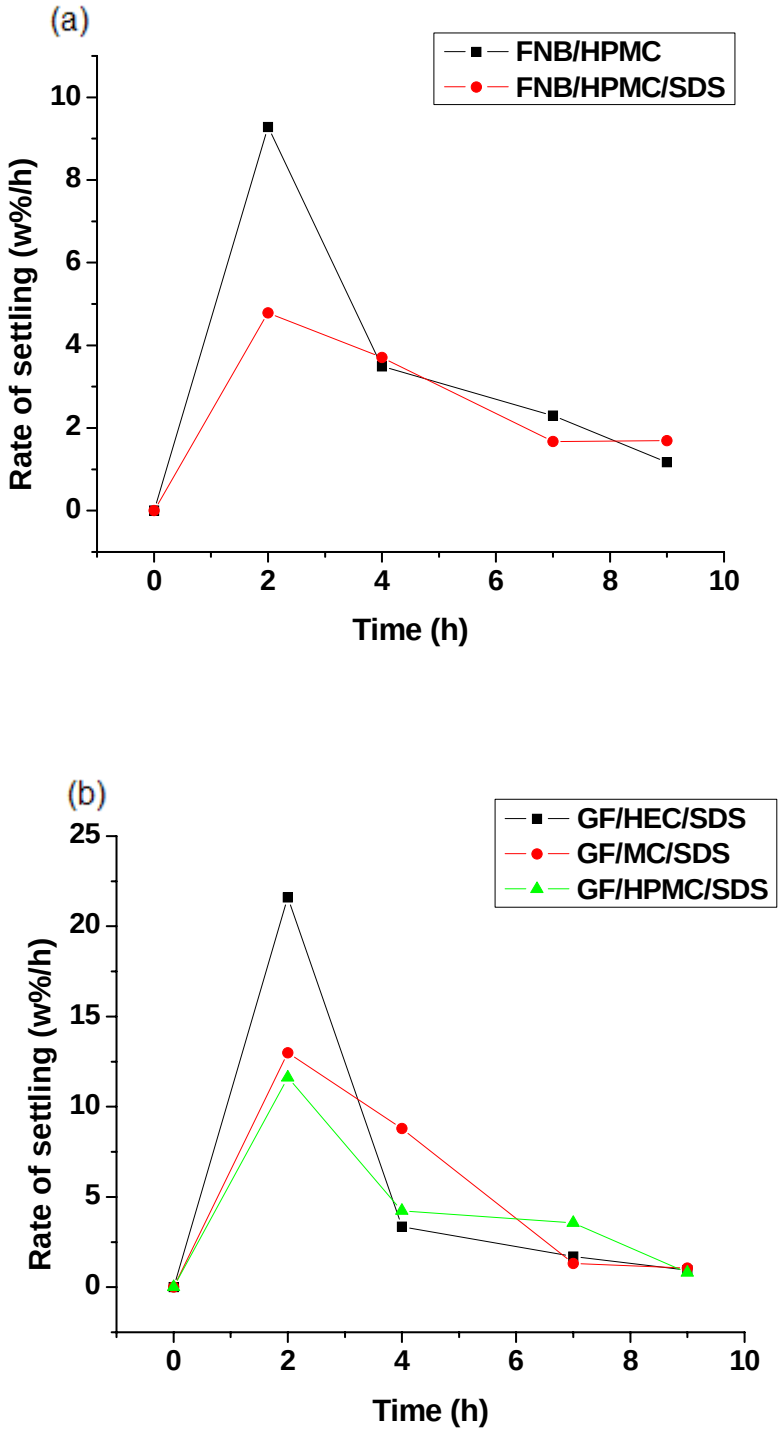

Figure 2.6 Rate of settling as a function of time for GF and FNB: (a) FNB in presence of HPMC and SDS; (b) GF in presence of different cellulose ethers and SDS.

2.3.3 Melting Point and Particle Morphology

Melting point of the precipitated particles was measured as a means to study the co-precipitating of the cellulose ethers with the drug particles (Table 2.2). In all cases, the melting point did not increase significantly. This implied that the cellulose ethers only formed a protective layer on the particle surface and was not a major component of the particle itself. On the other hand, a marginal decrease (2-8 °C) in melting point was observed. This is because the drug particles in polymer systems had less affinity toward each other due to decreased inter-molecular forces (Terayama et al., 2004).

Figure 2.7 shows the comparison of SEM images of drug/cellulose/SDS systems and drug/cellulose systems. It was found that FNB and GF particles had different crystal shapes. In drug/cellulose/SDS systems, the particles had relatively smaller diameter compared with those in drug/cellulose systems. The presence of agglomerates can be observed in the drug/cellulose systems.

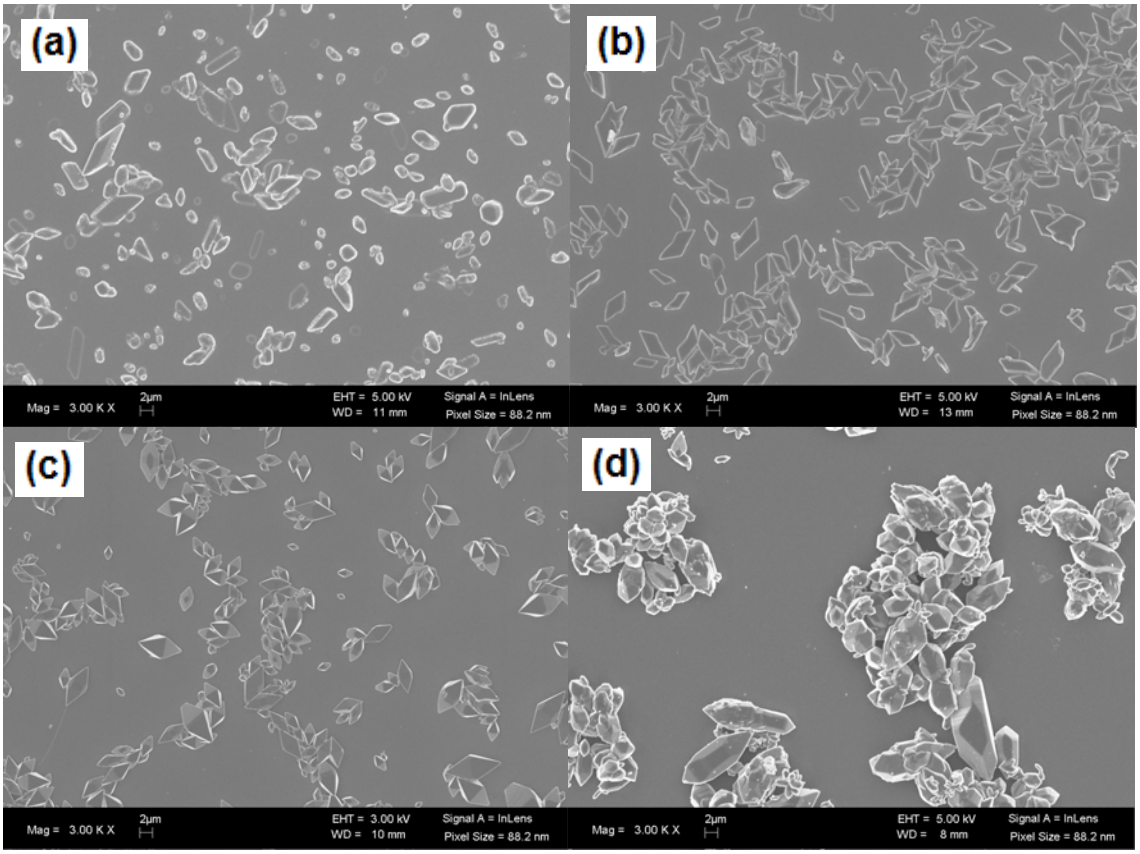

Figure 2.7 SEM images of drug particles**:** (a) FNB stabilized by HPMC and SDS; (b) FNB stabilized by HPMC; (c) GF stabilized by HEC and SDS (d) GF stabilized by HEC.

Some of the large particles (8 to 10 microns) were analyzed by Confocal Raman Microscopy. Figures 2.8 and 2.9 show the Raman images of FNB and GF drug particles stabilized with HPMC and SDS. The Raman spectra of HPMC, pure drug and drug particles stabilized with HPMC and SDS were compared. The C-O stretching in the region 1050-1200 cm^{-1}, C=O stretching in the region 1500-1700 cm^{-1} and C-H stretching in the region of 2800-3200 cm^{-1} were found in both pure FNB and its stabilized analog. Meanwhile, the C=O stretching of benzofuran ring of GF in the region 1550-1800cm^{-1} and C-H stretching in the region of 2800-3200 cm^{-1} were observed in both pure GF and it stabilized analog (Bolton and Prasad, 1981). It is clear from the Raman scattering data

that the crystals contained the respective drugs, and there was no significant interaction between the drug, cellulose ethers and SDS.

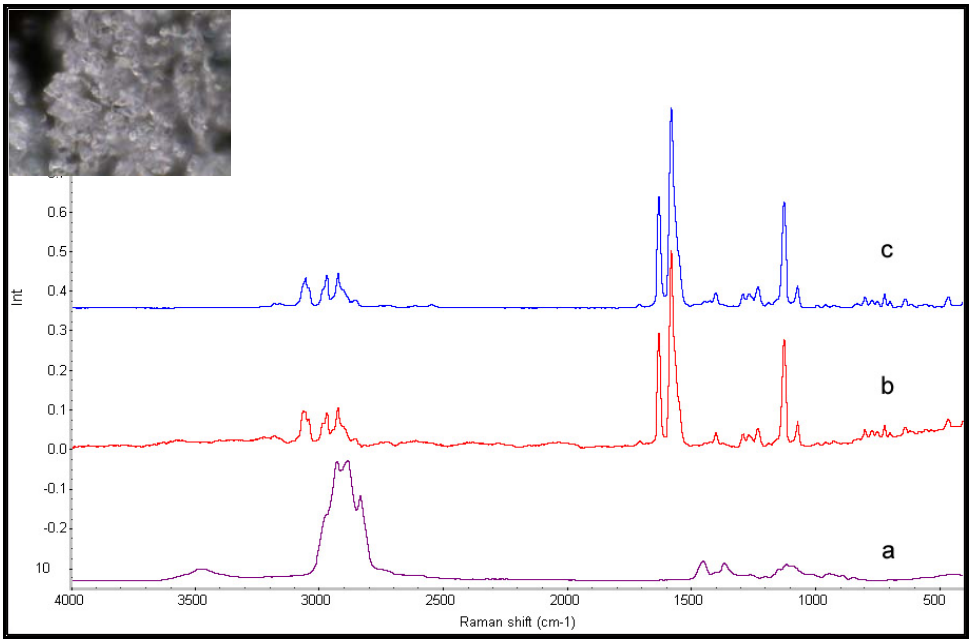

Figure 2.8 Raman spectra of (a) Pure HPMC (b) Pure FNB (c) FNB stabilized by HPMC and SDS. Image in set shows FNB stabilized by HPMC and SDS.

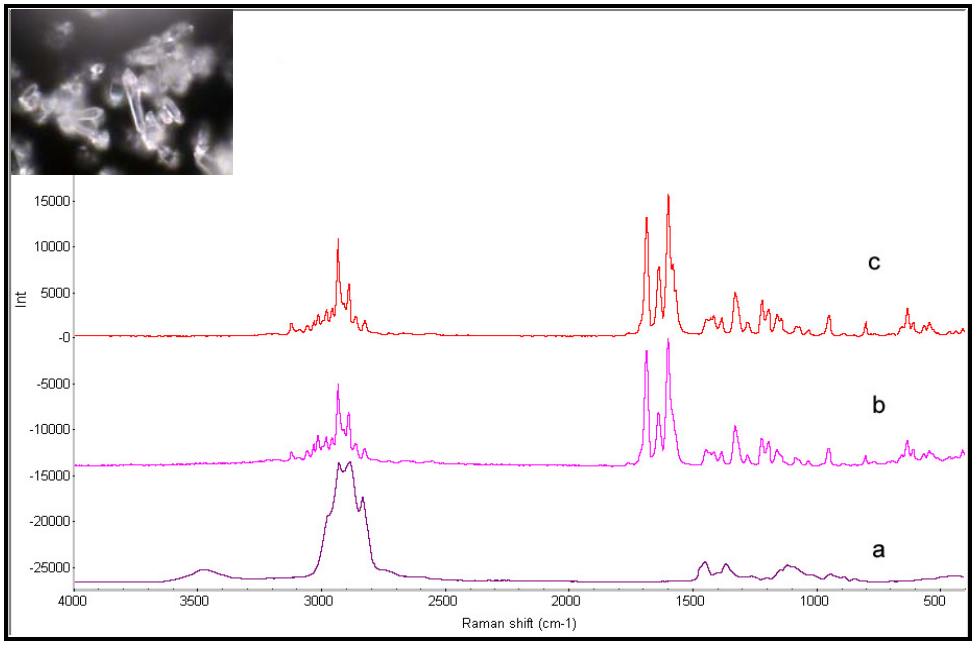

Figure 2.9 Raman spectra of (a) pure HPMC (b) pure GF (c) GF stabilized by HPMC and SDS. Image in set shows GF stabilized by HPMC and SDS.

2.4 Summary

Anti-solvent synthesis of micro scale drug particles with simultaneous stabilization was quite effective under ultrasonic agitation. At the end of four hours, the average diameters of particles in suspension were between 1.9 to 4.7 microns depending upon the drug and the conditions used. A combined use of cellulose ether and SDS was more effective than either of the two components being used alone in lowering the particle diameter, keeping a larger percentage of the particles in suspension and decreasing the sedimentation rate. Raman Spectroscopy confirmed the presence of the drug molecule in these crystals.

CHAPTER 3

ANTI-SOLVENT PARTICLE FORMATION AND FILM FORMATION WITH LOW MOLECULAR WEIGHT HYDROXYPROPYL METHYL CELLULOSE

3.1 Introduction

Potential drug molecules that exhibit poor aqueous solubility often end up as therapeutic failures (Gao et al., 2008). The insolubility is normally attributed to the inability to hydrogen bond with water and high lattice energy (Kipp, 2004). Particle size reduction and incorporation within drug carriers are often used to increase the dissolution rate and bioavailability of such compounds. Conventional methods for the synthesis of micron or submicron particles include milling and homogenization, where the controlling of size, morphology, and surface properties are difficult (Wong et al., 2006). Precipitation processes have emerged as effective methods for the synthesis of particulates of hydrophobic drugs. Typically, the molecule is first dissolved in a solvent and then mixed with a miscible anti-solvent. This leads to the precipitation of micro- or nano-particles that may be directly incorporated into a drug delivery vehicle.

Nucleation and growth need to be controlled for obtaining micron and submicron particles during a precipitation process. Polymers and surfactants are used as stabilizers to enhance colloidal stability (Itoh et al., 2003; Terayama et al., 2002; Yasueda et al., 2004). Different celluloses such as hydroxypropyl methyl cellulose (HPMC) and polymers such as chitosan have been used as biomaterials and microencapsulating agents. While polymers such as polyethylene glycol (PEG) can serve as plasticizers, HPMC imparts a more hydrophilic characteristic and controls of its porosity (Fulzele et al., 2002; Zili et al., 2005). HPMC can be used in combination with secondary polymer such as

polyvinylpyrrolidone (PVP), which has good solubility in water and a variety of organic solvents. The latter can improve the wettability of the dispersed particles and therefore improve the dissolution rate.

The objective of this study was to integrate the anti-solvent synthesis of micron-scale particles, their stabilization in the aqueous suspensions and subsequent synthesis of polymer films for drug delivery. The particular interest is the antifungal agent Griseofulvin (GF) whose aqueous solubility is only 12 μg/ml.

3.2 Experimental Section

3.2.1 Materials

Griseofulvin (GF, 95% purity), Hydroxypropyl methyl cellulose or HPMC (molecular weight of 10,000, and viscosity of 5 cP), sodium dodecyl sulphate or SDS, polyvinylpyrrolidone 40 or PVP 40 were purchased from Sigma Aldrich, USA. All these materials were used without further purification. The water used in the experiments was purified with a Milli-Q Plus system.

3.2.2 Methods

Anti-solvent precipitation was carried out at room temperature. The anti-solvent was prepared by dissolving HPMC in water. The solvent solution was prepared by dissolving Griseofulvin in acetone. The mixing of anti-solvent and solvent was carried out under ultrasonic agitation for 30 min. This was followed by 30 min stirring to remove air bubbles. Film precursors were obtained by adding additional polymers such as HPMC and PVP into the stabilized drug suspensions with stirring. Typical film suspension consisted of 0-6 wt% of GF, 0-8 wt% of HPMC, 0-20 wt% of PVP, 0-0.2 wt% of SDS,

60-85% anti-solvent and 0-25% solvent. Film suspensions were cast on Teflon plate and then dried at 40 °C in a vacuum oven for 5 hours, followed by an additional 4 hours at room temperature. Finally, the films were peeled off and stored in a dessicator. The films were redispersed after four months of storage. This was carried out by dissolving the GF film in the water, which was followed by 1hour of stirring.

Particle size analysis was carried out by static light scattering with a particle size analyzer LS230 (Beckman Coulter Inc., Miami, FL, USA). The atomic force microscopy (AFM) measurements were carried out with a Nanoscope II microscope (Digital Instruments Inc., Santa Barbara, CA, USA) in tapping mode at room temperature. The film morphology was studied with a LEO 1530 VP scanning electron microscopy (LEO Electron Microscopy Inc., Thornwood, NY, USA). Samples were mounted on aluminum stubs with adhesive tape and coated with carbon with a MED 020 sputtering coater (Micro Surface Engineering Inc., Los Angeles, CA, USA) to improve conductivity. A Nicolet Almege XR Dispersive Raman with Olympus BX51 confocal microscope (Thermo Fisher Scientific Corp., Madison, WI, USA) with a laser at 532 nm was used to obtain the Raman spectra in the imaging mode. X-ray diffraction (XRD) was used to investigate the crystallographic structure of the films. This was performed on a Philips X'Pert MRD X-ray diffractometer (Philips, Almedo, Netherlands) with Cu Ka radiation operated at 45 kV and 40 mA. After redispersion, the particle size distribution (PSD) in the suspension was studied by static light scattering, and the dried GF particles were analyzed by XRD.

3.3 Results and Discussion

In this work, we used cellulose ethers and surfactants to sterically stabilize the drug particles in the suspension, thus preventing the water-insoluble particles from aggregating. Several celluloses including methyl cellulose, hydroxyethyl cellulose were studied in our previous work, and HPMC was found to be the most suitable one for stabilization (Desai et al., 2011; Meng et al., 2009). Initial attempts were aimed at increasing the concentration of cellulose ethers in the aqueous suspension and casting them as films. It was found that these did not form continuous films and were rather brittle. However, the addition of PVP led to the formation of stable, continuous films with reasonable mechanical properties. Therefore both HPMC and PVP needed to be introduced into the suspension which would eventually form a continuous film. We have reported that the combination of HPMC and SDS is excellent for stabilizing a suspension of GF (Meng et al., 2009). The goal was to introduce PVP into the suspension without significant increase in particle size.

The mean diameter of particles in drug suspensions was measured using laser diffractometry, where both Faunhofer and Mie theories were used to deduce particle size distribution (PSD) from spatial scattering (Larson et al., 2002). The measurement in the submicron range was possible using Polarization Intensity Differential Scattering system. Typical PSD of stabilized suspensions of GF in HPMC/SDS and HPMC/SDS/PVP systems are shown in Figure 3.1. The latter contained higher amounts of HPMC and PVP, and showed a shift towards a larger diameter. This was attributed to the higher concentrations of the polymers. While there was a 35%-70% increase in mean particle diameter for the GF/HPMC/SDS/PVP systems, the diameter remained under 10 micron.

Furthermore, the effect of the concentration of HPMC and PVP during the anti-solvent precipitation on the particle size in the suspensions was examined, and the results are shown in Figure 3.2. With the increase in concentration of HPMC, the particle size in the suspension increased and the effects were quite pronounced. The particle size remained relatively constant below 1.0 wt% of PVP, but beyond that there was marked increase. The average particle size increased to as high as 20 microns. The increase is attributed to the fact that at high PVP and HPMC concentrations, the degree of supersaturation decreased leading to low nucleation rate and larger particles.

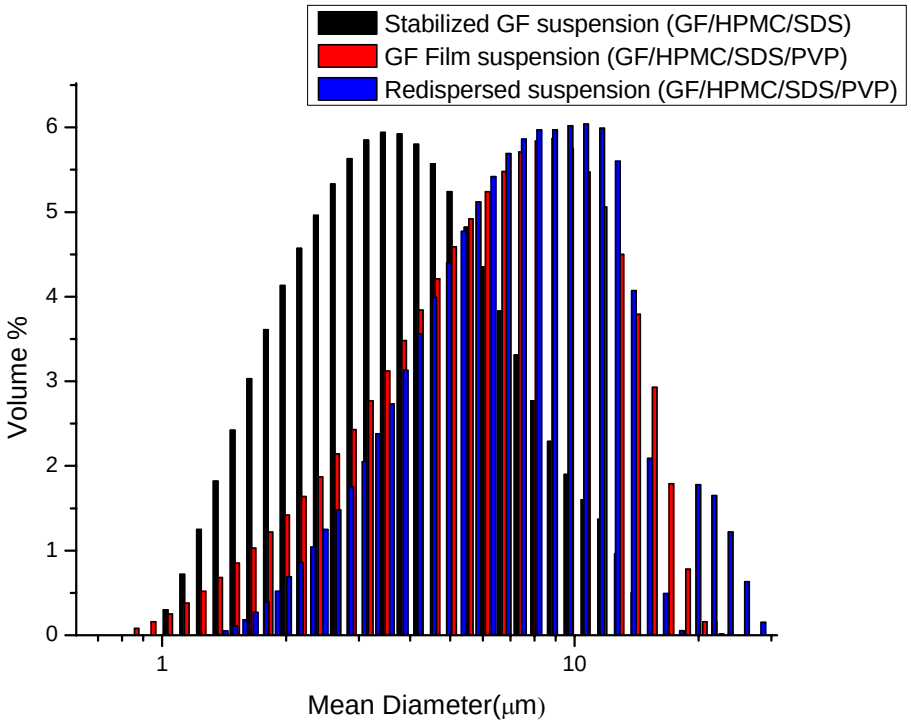

Figure 3.1 Particle size distribution of suspensions: (black) GF stabilized by HPMC and SDS (GF: 0.41%, HPMC: 0.12%, SDS: 0.12 wt% in suspension); (red) GF stabilized by HPMC, SDS and PVP (GF: 0.41%, HPMC: 0.82%, SDS: 0.12% PVP: 0.12 wt% in suspension); (blue) redispersed suspension for the film that casted from GF suspension.

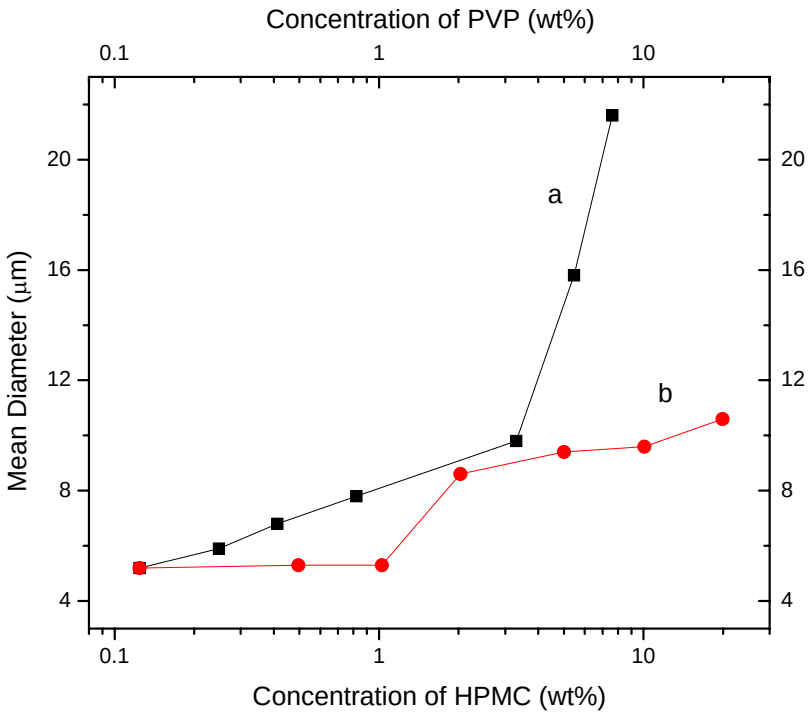

Figure 3.2 Effect of concentration of HPMC or PVP on mean particle size. The starting suspension had the following composition: GF: 0.41%, HPMC: 0.12%, SDS: 0.12%, PVP: 0.12wt%; (a) particle size as a function of HPMC concentration; (b) particle size as a function of PVP concentration.

At higher polymer concentration in the suspensions, there was a marked phase separation as the polymers began to precipitate. It was evident from Figure 3.2 that high concentrations of HPMC would affect particle size in the suspension, and finally in the films. The film formation was carried out according to Figure 3.3. The HPMC could be added either at Stage 1 or at Stage 2, when particles had already been stabilized. Based on Figure 3.1 and 3.2, Stage 2 was selected, and it led to smaller particle size.

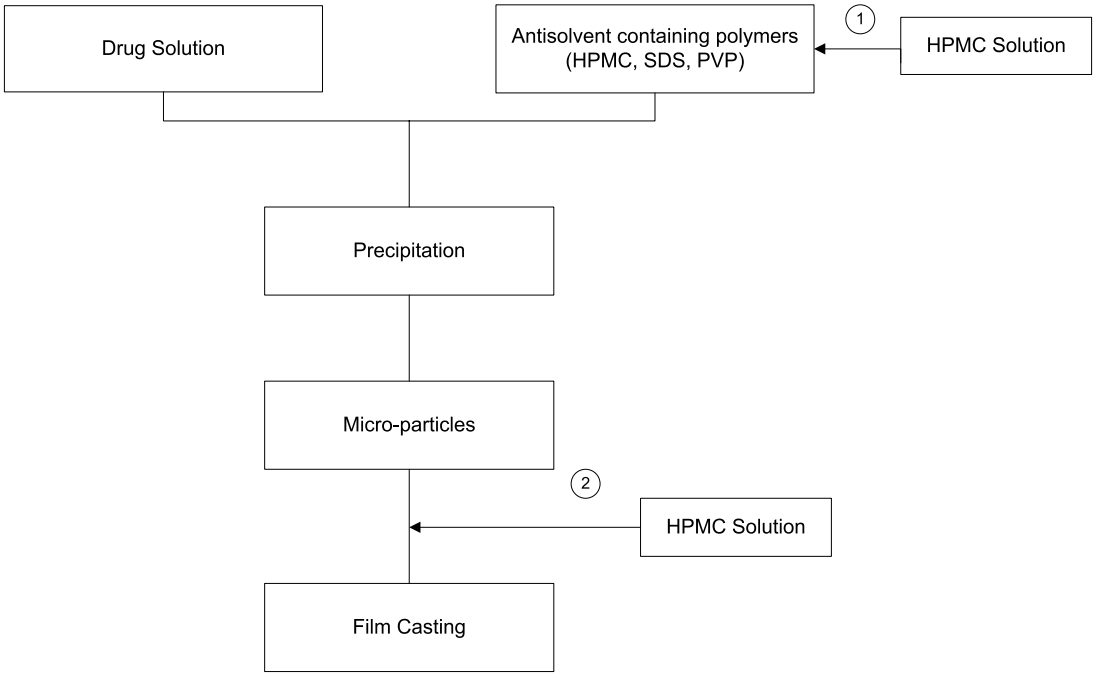

Figure 3.3 Approach to integrating anti-solvent precipitation and film casting.

As mentioned before, the absence of PVP led to the formation of brittle films that were not uniform, where the drug particles and the polymers separated during film formation. The blank film was transparent in color as shown in Figure 3.4, while the one containing the drug was white with a different texture. The thickness of the drug-loaded films could be varied, but in this study we targeted between 300-400 μm. The PVP was the binder used in these films, and no phase separation was observed. A film containing between 5-20% (on a dry basis) of PVP showed good uniformity and mechanical properties. The HPMC-PVP combination was a good one because the ether and the hydroxyl groups of HPMC could interact with the imide and carbonyl group of PVP via hydrogen bonding (Chan et al., 2005).

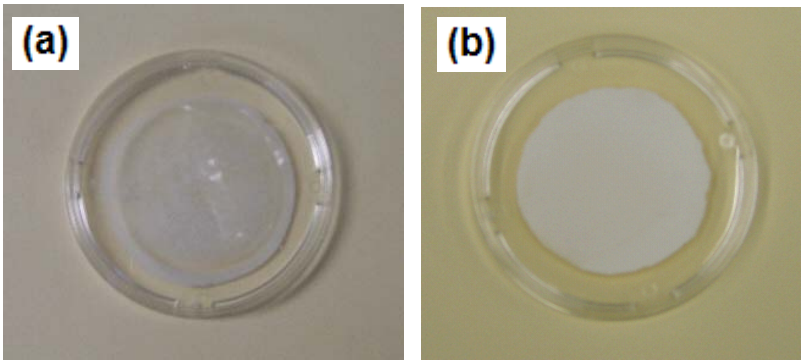

Figure 3.4 Photograph of films: (a) blank polymer film (b) GF-loaded polymer film.

SEM was used to study the surface morphology and GF particle distribution within the films. The goal was to obtain uniform distribution of the GF particles throughout the film. Figure 3.5 a, b, c show SEM images of GF-loaded film containing 6.2% of GF, 84.3% of HPMC, 5.9% of PVP and 3.6% of SDS. This film is referred to as Film A. The distribution of particles was found to be non-uniform. The top surface showed mainly the presence of polymer, while the GF particles settled to the bottom surface. Figure 3.6c shows the SEM of the crossection and non-homogeneous distribution of GF. This was typical when HPMC concentration was high. The SEM images of the surface, bottom and the crossection of the GF-loaded film containing lower concentration of HPMC and relatively higher concentration of PVP are shown in Figure 3.6 a, b and c (film B). It contained 27.8% of GF, 55.6% of HPMC, 10.3% of PVP and 6.3% of SDS. In film B, the particles were uniformly distributed. It can be seen that both top surface and bottom surface showed the presence of large number of GF crystals. The SEM of the crosssection showed that the drug particles were uniformly distributed throughout the film.

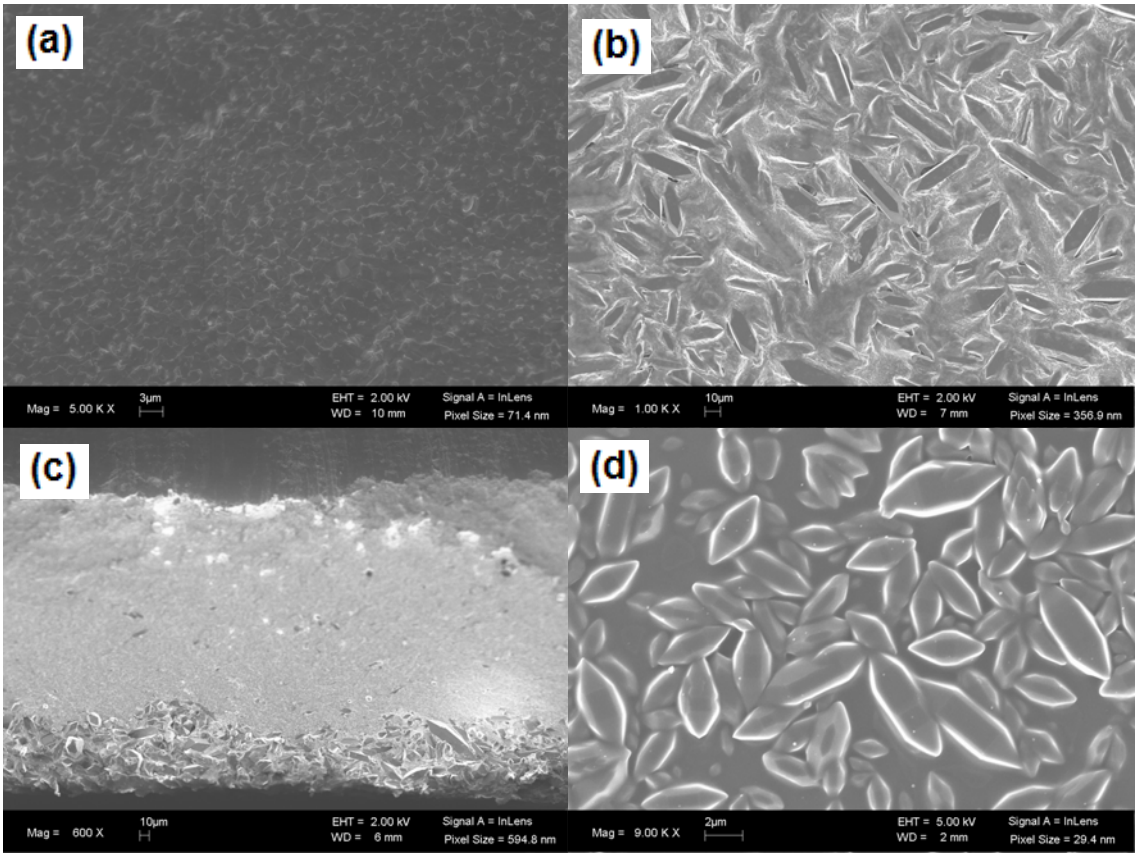

Figure 3.5 SEM images of GF-loaded polymer film: film A containing 6.2% of GF, 84.3% of HPMC and 5.9% of PVP: (a) top surface; (b) bottom surface (c) cross-section (d) GF particles in redispersed suspension.

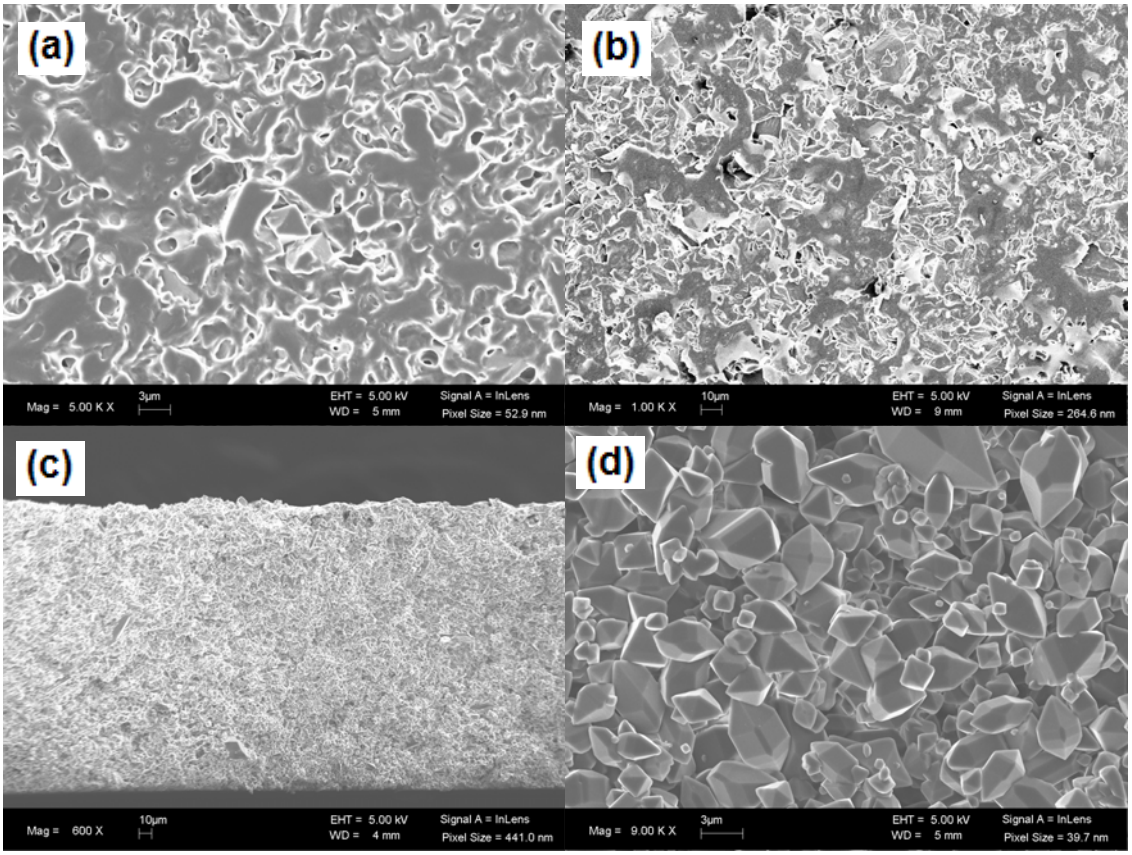

Figure 3.6 SEM images of GF-loaded polymer film: film B containing 27.8% of GF, 55.6% of HPMC and 10.3% of PVP: (a) top surface (b) bottom surface (c) cross-section; (d) GF particles in redispersed suspension.

The surface topography of the non-drug loaded polymer film, and film B were analyzed by AFM in the tapping mode (Figure 3.7). The blank film with no drug loading showed a smooth surface with a Ra of 2.8 nm, where as that for film B was 91.3 nm. This indicated the presence of drug particles on the film surface. Similar images were also obtained for other drug films containing different concentrations of GF. The images show consistence with previous results obtained by SEM measurements, which showed that the drug particles were embedded into the film. The presence of drug particles also altered the surface morphology.

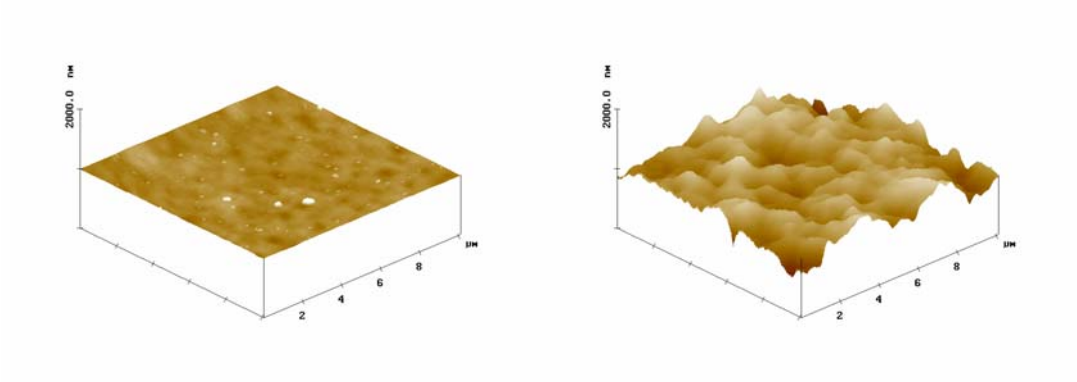

Figure 3.7 A tapping mode 2-dimensional AFM image of the top surfaces (10 μm scans): (a) non-drug loaded polymer film (b) film B.

Raman spectroscopy was used to image the films and the concentration distribution of GF. It provided sensitive GF detection in the expecient matrices and the well-resolved fundamental intra- and/or intermolecular stretching and bending modes allowed determination in solid-state. Figure 3.8 a, b and c shows the Raman spectra of blank film, GF-loaded film (Flim B containing 27.8% of GF) and pure GF. The GF spectra showed strong peaks in the region 1550-1800cm^{-1} and 2800-3200 cm^{-1}, which were attributed to the C=O stretching of benzofuran ring and C-H stretching of GF respectively (Bolton and Prasad, 1981). The same characteristic peaks were also observed in Film B, which indicated the presence of the drug and no significant alteration of the GF molecule.

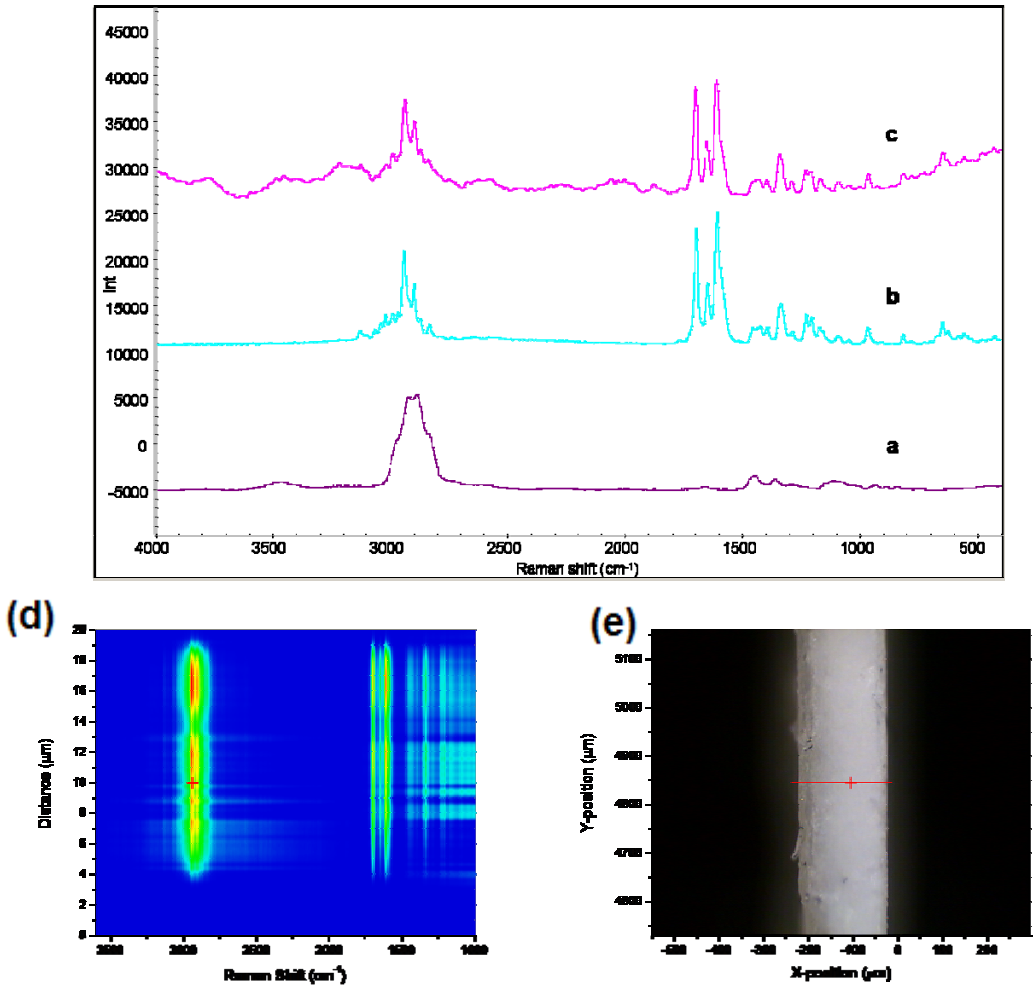

Figure 3.8 Cross-section of the film B containing 27.8% of GF: Raman spectra of (a) blank film, (b) pure GF, (c) Film B; (d) Raman line mapping (e) Raman real image. Scanning was done at 1699cm^{-1}.

Raman Chemical Mapping was used to image the crosssection of the Flim B. The chemical images corresponding to 1699 cm^{-1} were attributed to GF. Figure 3.8d and 8e showed uniform distribution of the drug. The images were consistent with the SEM measurements. The Raman spectroscopy was also able to map the GF concentration in three dimensions. A film containing only 3.7% of GF is shown Figure 3.9. Two particles embedded in the film were mapped and Figures 3.9a, b and c show the distribution of GF.

This was done by plotting the peak area of the selected Raman bands over the entire scanned area. A red color corresponded to a high GF concentration, followed by yellow and green, whereas the blue color signified the background. Strongest Raman bands of GF were identified in the center of the particles, which reduced as one moved away from the central core. This indicated that the drug was coated and distributed in the polymer matrix. Similar results were obtained for different GF films with different GF concentration. These observations agreed with the SEM measurements, suggesting that drug existed in the form of microparticles dispersed in the polymer matrix.

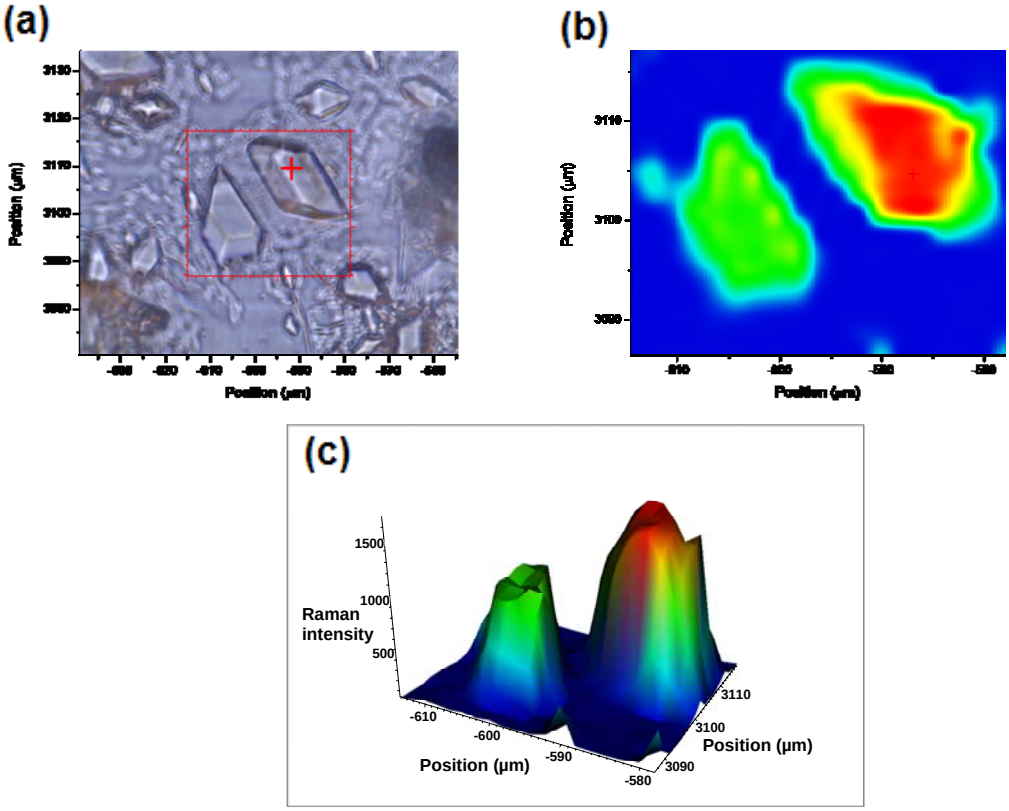

Figure 3.9 Raman mapping of the drug particles on the surface of GF-loaded polymer film containing 3.7% of the GF: (a) microscopic photo of scanned area, (b) GF distribution in scanned area (2D, blue area corresponds to a non-GF background, green and red area to a high GF concentration) (c) 3D Chemical Imaging of the scanned area. Scanning was done at 1699cm^{-1}.

XRD analysis was used to study the crystal structure of the GF in the film (Figure 3.10). It was seen that the crystal structure did not change when the stabilized particles were embedded in the polymer matrix. The spectra of pure GF and in GF-loaded polymer film were identical, and neither splitting nor shifting of the peak was observed for the GF-loaded polymer film, indicating that there was no change in polymorphism.

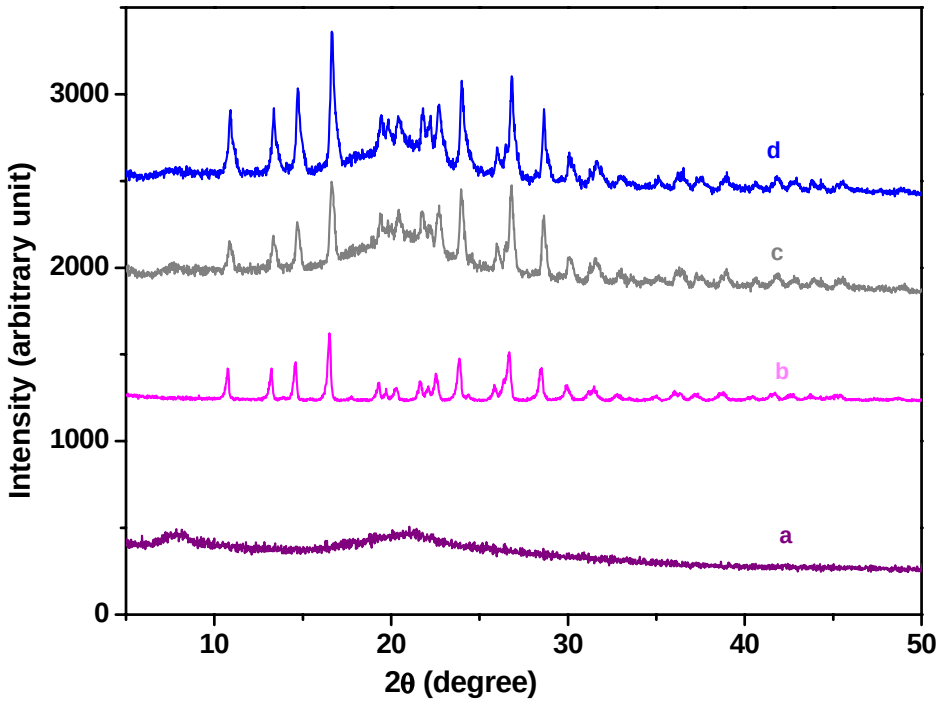

Figure 3.10 XRD patterns of (a) blank polymer film, (b) pure GF, and (c) film B containing 27.8% of GF, (d) redispersed particles.

The GF films were stored at room temperature for four months prior to redispersion in aqueous medium. The particle size distribution of the redispersion was studied, and is shown in Figure 3.1. It is evident that the size distribution was not altered significantly. The SEM analysis (Figure 3.5d and 3.6d) of the dried GF particles from the redispersions of film A and B showed similar crystal shape as the original particles. XRD

pattern of particles from redispersion of film B showed that the pattern remained unchanged (Figure 3.10d). Therefore it is concluded that the multiple steps of film formation, storage and redispersion, did not alter the properties of the drug including its crystallinity.

3.4 Summary

The integration of anti-solvent synthesis of micron-scale particles, their stabilization in the suspension and subsequent film formation was accomplished. While HPMC was an excellent at stabilizing GF in suspension, PVP was necessary to make continuous and films that contained uniform distribution of GF particles. Main particles size in the suspension as well as the solids films were between 1 to 10 microns.

CHAPTER 4

ANTI-SOLVENT PARTICLE FORMATION AND FILM FORMATION WITH LOW AND HIGH MOLECULAR WEIGHT HYDROXYPROPYL METHYL CELLULOSE

4.1 Introduction

The absorption of hydrophobic drugs across biological barriers is limited by their solubility in biological fluids (Gao et al., 2008). Increase in drug dissolution rate is of great importance because it can improve bioavailability and minimize side effects. According to the Noyes-Whitney equation, the dissolution rate of insoluble or sparingly soluble molecules is dependent on the surface area (Al-Hamidi et al., 2010b), and reducing the particle size has been an well-established approach for its improvement and enhancing bioavailability (Al-Hamidi et al., 2010a; Haas Jimoh Akanbi et al., 2010). Direct particle formation via controlled crystallization or anti-solvent precipitation have emerged as useful methods for the synthesis of micron and sub micron drug particles nowadays.

The drug suspension that contains micron drug particles can also be used for the synthesis of drug delivery vehicles including biocompatible films. HPMC is found an excellent film-forming agent in pharmaceutical industry nowadays. The objective of this study is integrating the anti-solvent synthesis of micron-scale particles, their stabilization, and subsequent self-assembly into polymer films suitable for drug delivery. The colloidal particles were stabilized using low molecular weight hydroxypropyl methylcellulose (HPMC), while drug encapsulation was carried out in high molecular weight HPMC and polyvinylpyrrolidone (PVP). Griseofulvin (GF) was used as the model drug compound,

and the polymer films were evaluated in terms of their surface morphology, mechanical properties and in vitro drug release.

4.2 Experimental Section

4.2.1 Materials

Griseofulvin (GF, 95% purity), Sodium dodecyl sulfate or SDS, Polyvinylpyrrolidone K40 or PVP K40 was purchased from Sigma Aldrich (St Louis, MO). Two grades, namely low (E15LV referred to as HPMC-LM) and high (E4M referred to as HPMC-HM) molecular weight HPMCs were purchased from Dow Chemical Company (Midland, MI). All these materials were used as received. The water used in the experiments was purified with a Milli-Q Plus system.

4.2.2 Methods

Anti-solvent precipitation was carried out at room temperature and the anti-solvent was prepared by dissolving HPMC-LM and SDS in water. The drug solution was prepared by dissolving GF in acetone. The drug solution was added dropwise into anti-solvent under ultrasonic agitation in ultrasonic bath (Crest Ultrasonics Corp., Trenton, NJ) for 30 min, which was followed by 15 min magnetic stirring. The final water to acetone ratio was 4:1 on a volumetric basis. The drug suspensions were stored at 25 °C without the removal of acetone. Film-forming suspensions were cast on a stainless steel plate with a Film Casting Knife (BYK Additives & Instruments, Columbia, MD) and then dried at 50 °C in a vacuum oven for 5 hours. This was followed by an additional 4 hours of drying at room temperature. Finally, the films were peeled off and stored in a dessicator.

The mean particle diameter and particle size distribution (PSD) were determined

using a Coulter Particle Size Analyzer LS230 (Beckman Coulter Inc., Miami, FL) based on static light scattering. Size measurements were performed in triplicate for each sample at 25 °C. Zeta potential measurements were determined using a DelsaNano (Beckman Coulter Inc., Miami, FL). Differential scanning calorimetry (DSC) was used to determine the melting point of GF particles. Approximately 6 mg of samples were weighed and sealed in an aluminum pan and then scanned using a Pyris-1 DSC instrument (Perkin Elmer Inc., San Jose, CA) with a temperature speed of 5 °C /min from 25 to 300 °C.

Scanning electron microscopy (SEM) was performed using a LEO 1530 (LEO Electron Microscopy Inc., Thornwood, NY) to study the morphology of particles and films. The samples were placed onto an aluminum stub with carbon conductive double-sided tape and then coated with carbon using a MED 020 HR sputtering coater (Micro Surface Engineering Inc., Los Angeles, CA) to improve conductivity. A Nicolet Almege XR Dispersive Raman with Olympus BX51 Confocal Microscope (Thermo Fisher Scientific Corp., Madison, WI) using a laser at 532nm was applied in the Raman imaging mode. The samples were placed onto the glass slide for the detection using 100× optical lens.

In order to determine the mechanical properties of the GF-loaded polymer film, a puncture test was performed on a TA-XTplus Texture Analyzer (Stable Micro Systems, Surrey, UK). Film samples were positioned in the film holder between two mounting plates followed by tightening of the holding screws to prevent slippage of the film. In the puncture test, a puncturing probe with a spherical end was driven downward through the GF film with a speed of 1.0 mm/s. The puncture force at break and the maximum displacement of the film samples were recorded.

GF-loaded polymer films were stored in a dessicator at 25 °C for two months. Their redispersion was studied by dissolving the GF film in the water with magnetic stirring. The particle size distribution and particle morphology for redispersed particles were determined as described before. The drug release studies were performed using the USP basket method at a rotational speed of 100 rpm using a Varian VK 7010 dissolution apparatus (Varian Inc., Cary, NC). The dissolution medium was 900 ml of 5% SDS solution and the temperature was maintained at 37±0.5 °C. At appropriate time intervals, the samples were directed to analysis using a Cary 50 UV-visible spectrophotometer (Cary Inc., Canoga Park, CA) at 291nm.

4.3 Results and Discussion

The properties of different grades of HPMC are strongly affected by the presence of methoxy/hydroxypropoxy groups and the molecular weight. The stabilizing effects of HPMC of different molecular weight in the production of drug particles have been studied extensively and it has been reported that both low and high molecular weight HPMCs are effective (Sepassi et al., 2007). However, high molecular weight HPMC solutions are highly viscous even at low concentrations, which led to problems during the ultrasonic assisted anti-solvent precipitation. Therefore, low molecular weight HPMC was used for stabilization during particle formation. On the other hand, high molecular weight HPMC formed more continuous and mechanically stronger films, and was used as the film-forming agent. The properties of low and high molecular weight HPMCs used in this study are listed in Table 4.1. Both belonged to the E grade of HPMC (Hypromellose 2910), with a methoxy substitution (-OCH_3) of 28-30% and a hydroxypropyl substitution

(-$OCH_2CH(OH)CH_3$) of 7-12%. Compared with other grades (such as F or K), E grade of HPMC had higher content of methoxy substitution that accounted for a higher degree of hydrophobicity, which was necessary for surface activity (Pérez et al.). Compared to HPMC-LM, HPMC-HM possesed lower percent of methyl, and higher percent of hydroxypropyl substitution. This made the latter less hydrophobic. HPMC-LM had higher methyl/hydroxypropyl ratio (3.1) as well as lower molecular weight and viscosity (Camino et al., 2009; Li et al., 2005; Siepmann and Peppas, 2001).

Table 4.1 Properties of HPMC-LM and HPMC-HM

	HPMC-LM	**HPMC-HM**
%methyl	29.2	28.0
%hydroxypropyl	9.3	10.2
Methyl/hydroxypropyl ratio	3.1	2.3
Viscosity (cp), 2%wt solution, 20 °C	15	4965
Molecular weight (Da)	6000	90000

4.3.1 Characterization of GF Suspensions

Sonication-assisted anti-solvent precipitation was used in the synthesis of submicron and micron size particles of GF (Desai et al., 2011; Meng et al., 2009). Nucleation and condensation tended to be competing factors as both consumed solute molecules, while coagulation led to aggregation (Marchisio et al., 2006; Weber and Thies, 2002; Young et al., 2003). The addition of stabilizer is known to slow the condensation and coagulation (Matteucci et al., 2006), and here we used HPMC-LM and SDS to sterically stabilize the drug particles in the suspension, thus preventing aggregation (Ain-Ai and Gupta, 2008). Several cellulose ethers including methyl cellulose and hydroxyethyl cellulose have been used in our previous work, and a combination of HPMC and SDS was found to be excellent for GF (Meng et al., 2009; Zhu et al.).

Mean diameter of GF particles in presence of HPMC-LM at the initiation of anti-solvent particle formation are presented in Table 4.2. Drug to stabilizer weight ratios used for anti-solvent particle formation are also listed, and were important considerations when producing the submicron or nanoparticles. Merisko-Liversidge et al. has reported that a drug to stabilizer weight ratio in the range of 20:1 to 2:1 is necessary for nanoparticle production (Merisko-Liversidge et al., 2003). The particle size distribution of GF suspensions with different weight ratio of GF to HPMC-LM is presented in Figure 4.1. From Table 4.2 and Figure 4.1, it is clear that there is minimum and maximum concentration of HPMC-LM to produce and stabilize GF particles during anti-solvent precipitation. The mean particle diameter was found to decrease as the HPMC-LM concentration increased. For example, it was found that large sized particles (6.5 μm) were obtained when using 0.07% HPMC compared to 3.7 μm with 0.21% HPMC. Moreover, the particle size distribution of GF suspension with 0.21% HPMC showed narrowest size distribution in the submicron-sized range. It is probable that sufficient polymer present in the system may adsorb on the surface of the drug particles in order to provide a steric barrier against the inter-molecular forces between the drug particles that lead to the agglomeration (Raghavan et al., 2001; Raghavan et al., 2003). The drug:stabilizer ratio of 3:1 is an optimum value where the particles size was found to be the minimum. Too little polymer did not provide adequate stability and too much beyond critical flocculation concentration (CFC) leads to an unbalanced osmotic pressure and initiate the depletion of the adsorbed polymer layer, causing depletion flocculation of particles, thereby resulting less efficient for size reduction (Jongen et al., 2000; Kiratzis et al., 1999).

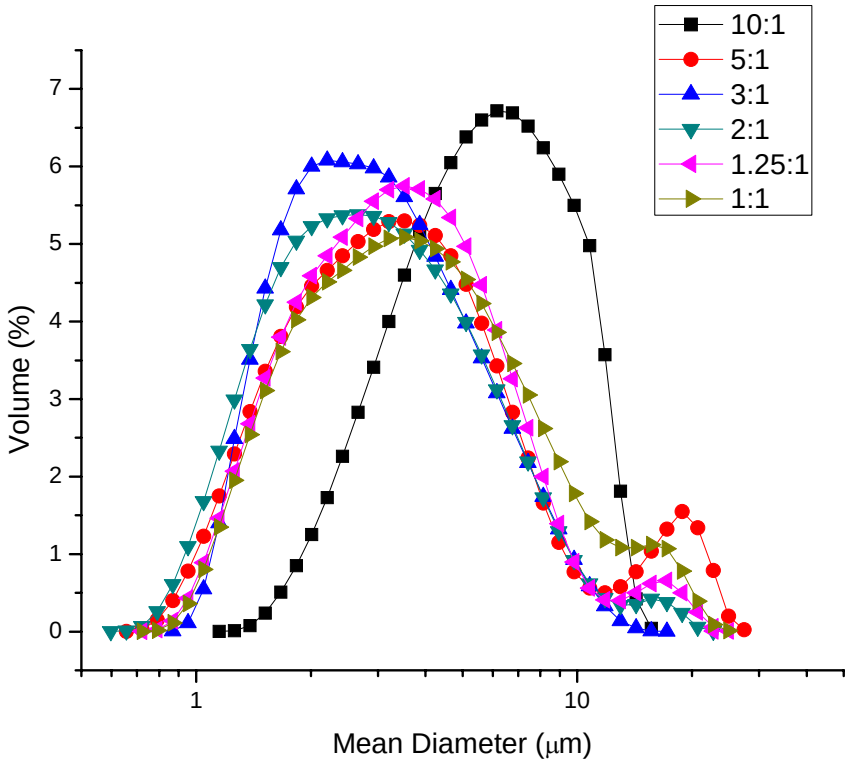

Figure 4.1 Particle size distribution of GF suspensions with different weight ratio of GF to HPMC-LM.

Dispersed GF particles showed negative zeta potential in the range of -5.2 to -19.5 mV (Table 4.2). The addition of the anionic surfactant SDS probably led to a negative zeta potential and the values showed an initial decrease with the addition of HPMC-LM. This data suggested that more HPMC adsorbed on the particle surface and formed a larger interfacial layer between the particles. Melting point of the precipitated particles was measured to see if the HPMC co-precipitated with GF particles. In all cases, the melting point did not increase significantly, which implied that the HPMC only formed a surface layer and was not a major component of the particle itself.

Table 4.2 Mean Particle Size, Zeta Potential and Melting Point of Griseofulvin at Different HPMC-LM Concentrations

HPMC-LM Concentration (wt%)	Weight Ratio of Drug to Polymer	Mean particle Diameter (μm)	Zeta potential (mV)	Melting point (°C)
0.07	10:1	6.5	-5.24	219.6
0.14	5:1	4.9	-10.58	217.8
0.21	3:1	3.7	-18.43	214.3
0.35	2:1	3.8	-19.46	214.8
0.56	1.25:1	4.3	-16.06	216.2
0.70	1:1	4.8	-16.52	215.0

Typical particle size distribution (PSD) of pure GF, stabilized GF and film-forming suspensions are shown in Figure 4.2. Pure GF suspension was obtained by directly dissolving GF powder into water with stirring. The mean diameter in the aqueous suspension was 24.3 μm with a broad size distribution, where particles were as large as 76.4 μm. With anti-solvent precipitation and stabilization with HPMC-LM/SDS, the mean particle diameter decreased to 3.7μm with a significantly narrow particle size distribution. The final film forming suspension, which contained both HPMC-HM and PVP showed a slight shift in the size distribution. It was found that there was a 2-15% increase in mean particle diameter but it remained under 5.0 μm. Figure 4.3 shows the comparison of SEM images of pure GF and GF particles stabilized with 0.21% of HPMC-LM in suspension. It was found that the GF particles formed with anti-solvent method had well defined crystal shape.

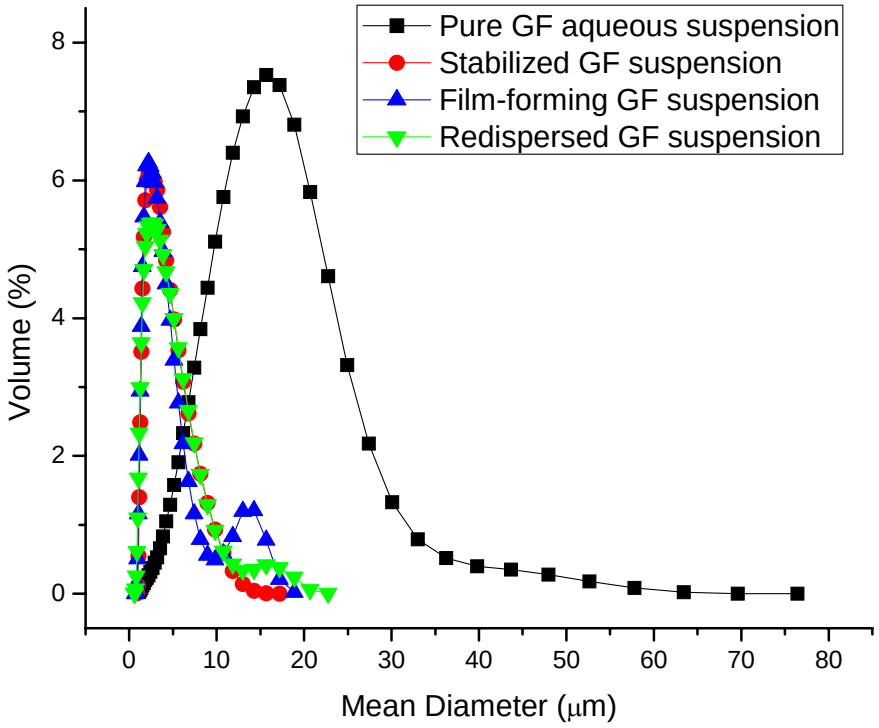

Figure 4.2 Particle Size Distribution of GF suspensions: (black) pure GF aqueous suspension containing 0.71% of GF; (red) stabilized GF suspension containing 0.71% of GF, 0.28% of HPMC-LM and 0.07% of SDS; (blue) film-forming GF suspension containing 0.70% of GF, 0.28% of HPMC-LM, 0.07% of SDS, 1.4% of HPMC-HM and 0.14% of PVP; (green) redispersed GF suspension from the casted film.

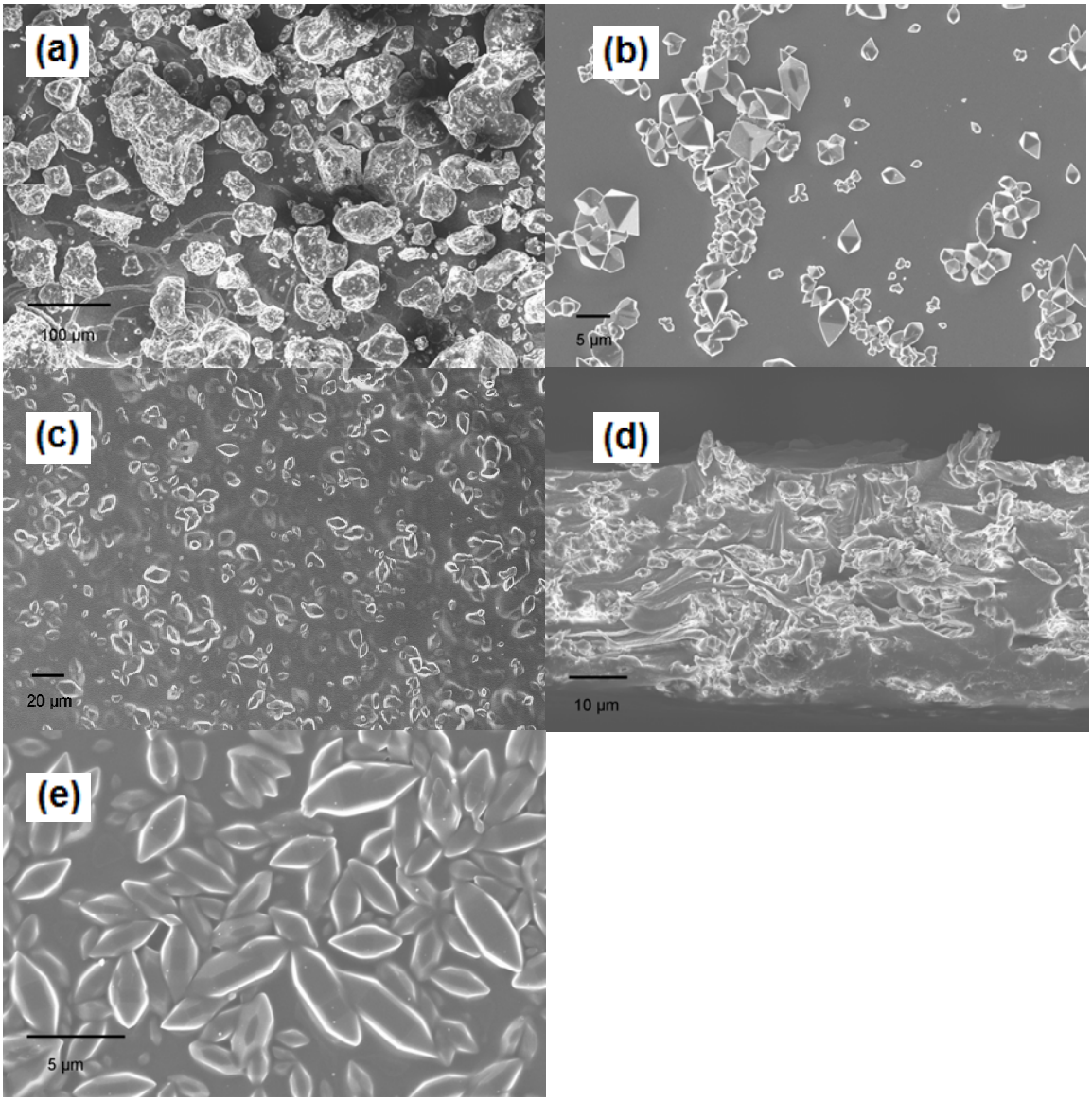

Figure 4.3 SEM images of (a) pure GF; (b) GF particles with anti-solvent precipitation (0.21% HPMC-LM); (c) top surface of GF-loaded polymer film; (d) cross-section of GF-loaded polymer film; (e) GF particles in redispersed suspension.

Since, the film formation was carried out by drying at an elevated temperature for a relatively long period of time, the stability of film-forming suspension as a function of time was studied at different temperatures. The mean diameter of the suspension was measured every one hour at 25, 40 and 50 °C. This is shown in Figure 4.4. The mean

particle size did not change significantly for 6 hours at room temperature. On the other hand suspensions at higher temperature were not as stable but mean particle diameter still remained under 4.3 μm. For example, at 50 °C, the mean particle diameter increased from initial 3.7 μm to 4.3 μm at 6 hours. Higher temperature brought more collisional agglomerations, however, the increase in particle size was less than 20% in all cases.

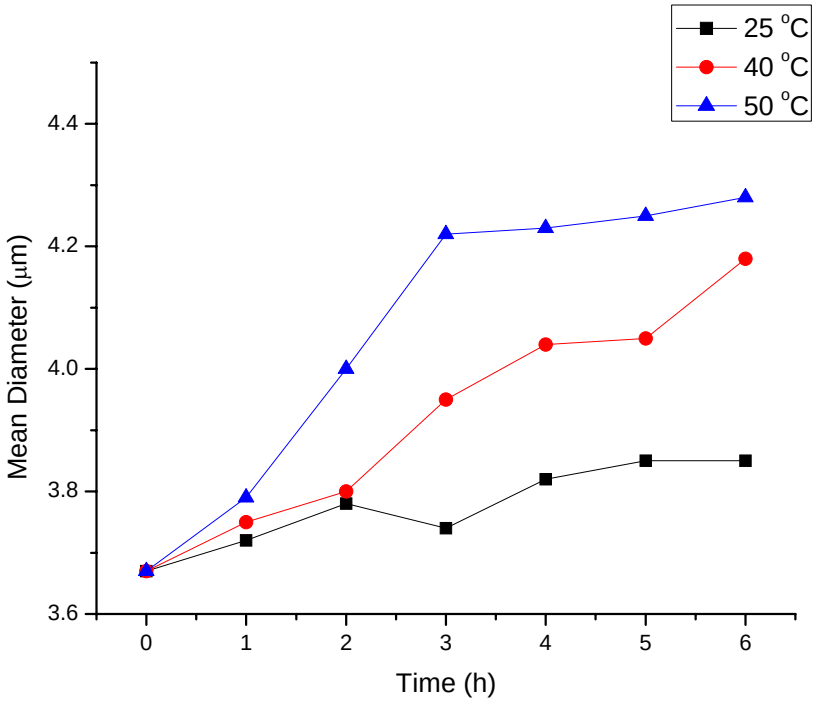

Figure 4.4 Mean particle diameter as a function of time at different temperatures.

4.3.2 Characterization of GF-loaded Polymer Films

It has been reported that HPMC is a good film-forming agent (Meng et al., 2011). In this work, GF-loaded polymer films were cast from GF suspensions and the solvent was removed via solvent evaporation in a vacuum oven. Figure 4.5 shows the photographs of a blank HPMC and a GF-loaded polymer film. The pure HPMC film was smooth and transparent, while the one containing the drug was white with a rougher texture. The

thickness of the GF-loaded films could be varied, but in this study we used thicknesses between 50-100 μm.

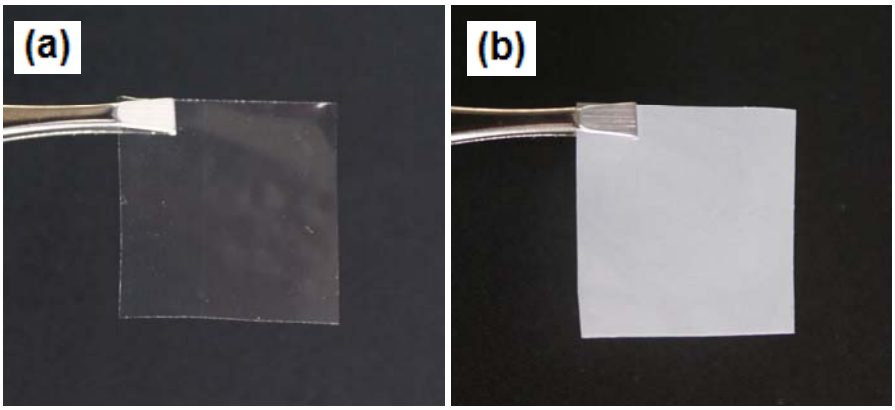

Figure 4.5 Photographs of films: (a) blank polymer film (b) GF-loaded polymer film.

The stability of the drug suspension greatly affected the final microstructure of the film matrix, and it was found that suspensions with large drug particles formed less uniform films with SEM analysis. Stability of the suspension was also important, because this would affect the agglomeration of the particles.

SEM was used to study the film microstructure. Figures 4.3 c and d show SEM images of GF-loaded films containing 27.0% of GF, 10.8% of HPMC-LM, 2.7% of SDS, 54.1% of HPMC-HM and 5.4% of PVP. It can be seen that the top surface showed the presence of GF crystals while the cross-section showed that the GF particles were homogeneously distributed in a continuous polymer matrix.

Raman spectroscopy was used to image the films and the concentration distribution of GF. It provided sensitive GF detection in polymer matrices and the well-resolved fundamental intra- and/or intermolecular stretching and bending modes allowing determination in solid state. Figures 4.6 shows the Raman spectra of blank film, GF-

loaded film containing 27.0% of GF and pure GF. The GF spectra showed strong peaks in the region 1550-1800cm^{-1} and 2800-3200 cm^{-1}, which were attributed to the C=O stretching of benzofuran ring and C-H stretching of GF respectively (Bolton and Prasad, 1981). The same characteristic peaks were also observed in GF-loaded polymer film, which indicated the presence of the drug and no significant alteration of the GF molecule.

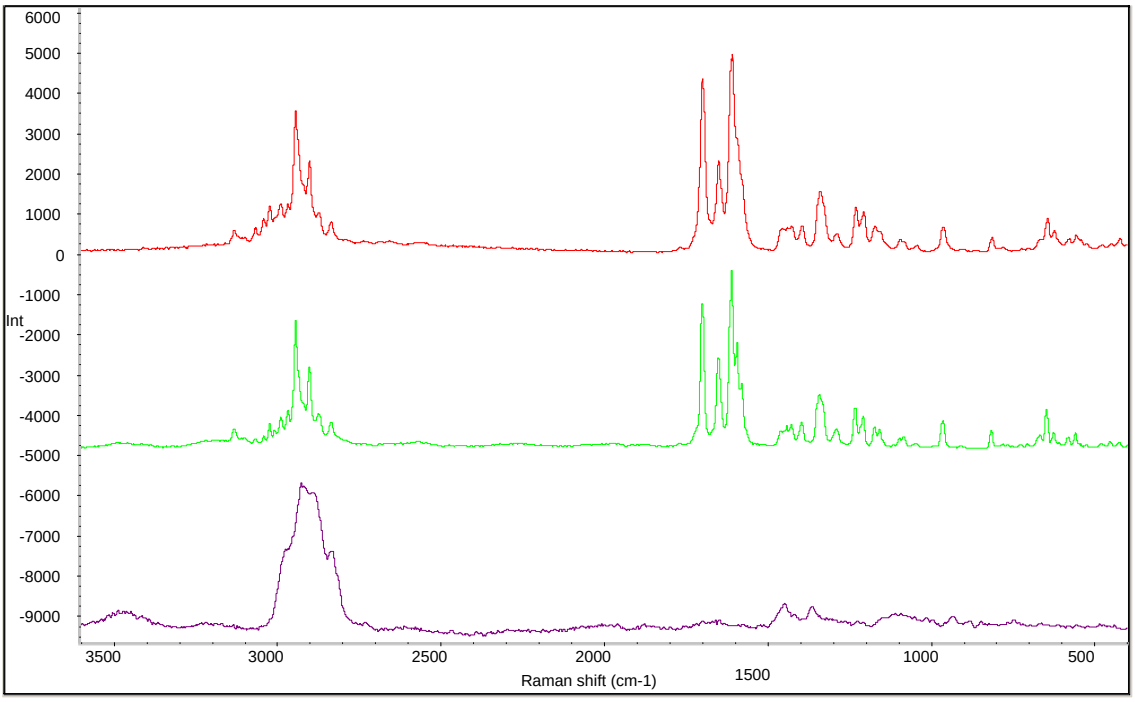

Figure 4.6 Raman spectra of (red) Pure GF, (green) GF-loaded polymer film, (purple) blank film.

Raman Chemical Mapping was used to image and map the top surface of drug film. Two particles embedded in the GF film were mapped and Figures 4.7a, b and c show the distribution of GF. This was done by plotting the peak area of the selected Raman bands over the entire scanned area. A red color corresponded to a high GF concentration, followed by yellow and green, whereas the blue color signified the background. Strongest Raman bands of GF were identified in the center of the particles,

which decreased as one moved away from the central core. This indicated that the drug was coated and distributed in the polymer matrix. Similar results were obtained for films with different GF concentrations. These observations agreed with the SEM measurements, suggesting that drug existed in the form of microparticles dispersed in the polymer matrix.

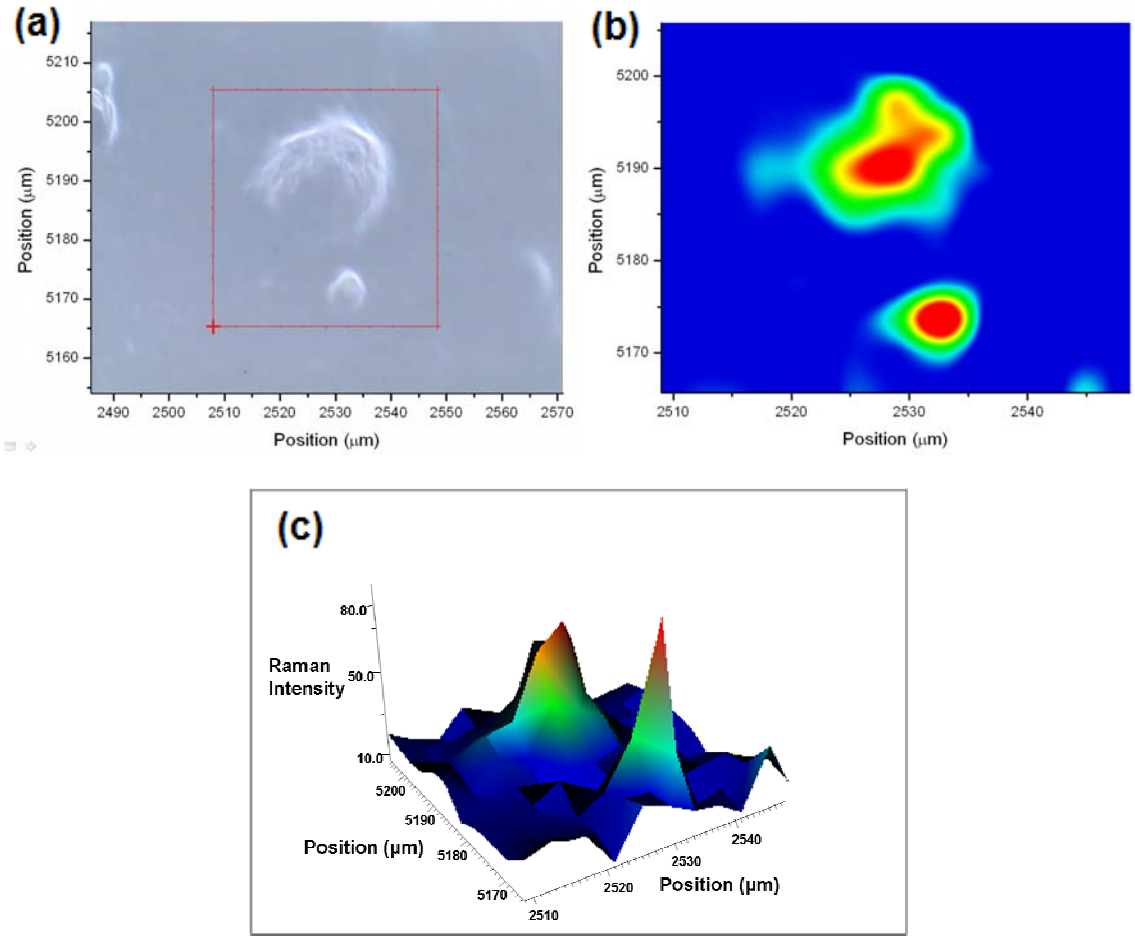

Figure 4.7 Raman mapping of the drug particles on the surface of GF-loaded polymer film containing 27.0 % of the GF: (a) image of the scanned area, (b) GF distribution in scanned area (2D, blue area corresponds to a non-GF background, green and red area to a high GF concentration) (c) 3D Chemical Imaging of the scanned area. Scanning was done at 1699cm^{-1}.

HPMC-HM films provided good mechanical properties compared to HPMC-LM (Hardy et al., 2006). Films formed with HPMC-LM were easy to crack (Nagarsenker and Hegde, 1999). In our study, 7%-14% of HPMC-LM and 41%-71% of HPMC-HM were present in the final film and contributed to the optimization of films and this was in line with previous observations (Meng et al., 2011). The secondary film-forming agent, PVP, served as a binder and its addition enhanced the mechanical properties of these films. It was seen that the addition of 5-20% of PVP provided good uniformity and mechanical properties. The HPMC-PVP combination was optimal because the ether and the hydroxyl groups of HPMC could interact with the imide and carbonyl group of PVP via hydrogen bonding (Chan et al., 2005). Table 4.3 shows the maximum puncture force and displacement of the drug films with varied components. It is found that maximum puncture forces of the films increased with increase in the ratio of HPMC-HM/Drug in the formulation. Films with higher mechanical strength were obtained by addition of PVP in the formulation. As can be seen in Table 4.3, films with weight ratio 5:15:1 of GF, HPMC-HM and PVP has largest puncture force (5438g) and displacement (3.8mm).

Table 4.3 Puncture Force and Maximum Displacement for GF-loaded Polymer Films

Formulation	Weight ratio of GF:HPMC-HM: PVP	Puncture Force at break (g)	Maximum Displacement (mm)
F1	5:10:0	1541	2.2
F2	5:10:1	2748	2.5
F3	5:15:0	3041	2.9
F4	5:15:1	5438	3.8

4.3.3 Redispersion of Drug Particles and Drug Release Profiles

The GF films were stored at room temperature for two months prior to redispersion in aqueous medium. In all cases, the redispersion of the GF films regenerated the original particles, with no increase in particle size (Figure 4.2). The SEM analysis of the dried GF particles from the film redispersions showed similar crystal shape (Figure 4.3e). Therefore it is concluded that the multiple steps of film formation, storage and redisperion did not alter the main properties of the drug.

The drug release profiles for pure drug substance and films were studied and are shown in Figure 4.8. It was evident that 100% of GF in the film released at the end of 50 minutes for 57% of HPMC-HM films. As the amount of HPMC-HM increased from 57% to 70%, the drug release decreased with distinct differences in the release profiles were observed (Figure 4.8a). This could be attributed to the fact that the pores of high molecular weight HPMC probably block up quickly and inhibit further liquid uptake, decreasing dilution and erosion and subsequently resulting in slower drug diffusion and release rates (Talukdar et al., 1996; Wan et al., 1991). For the films prepared with addition of PVP in the formulation, the drug release profiles did not change significantly compared with those without PVP (Figure 4.8b).

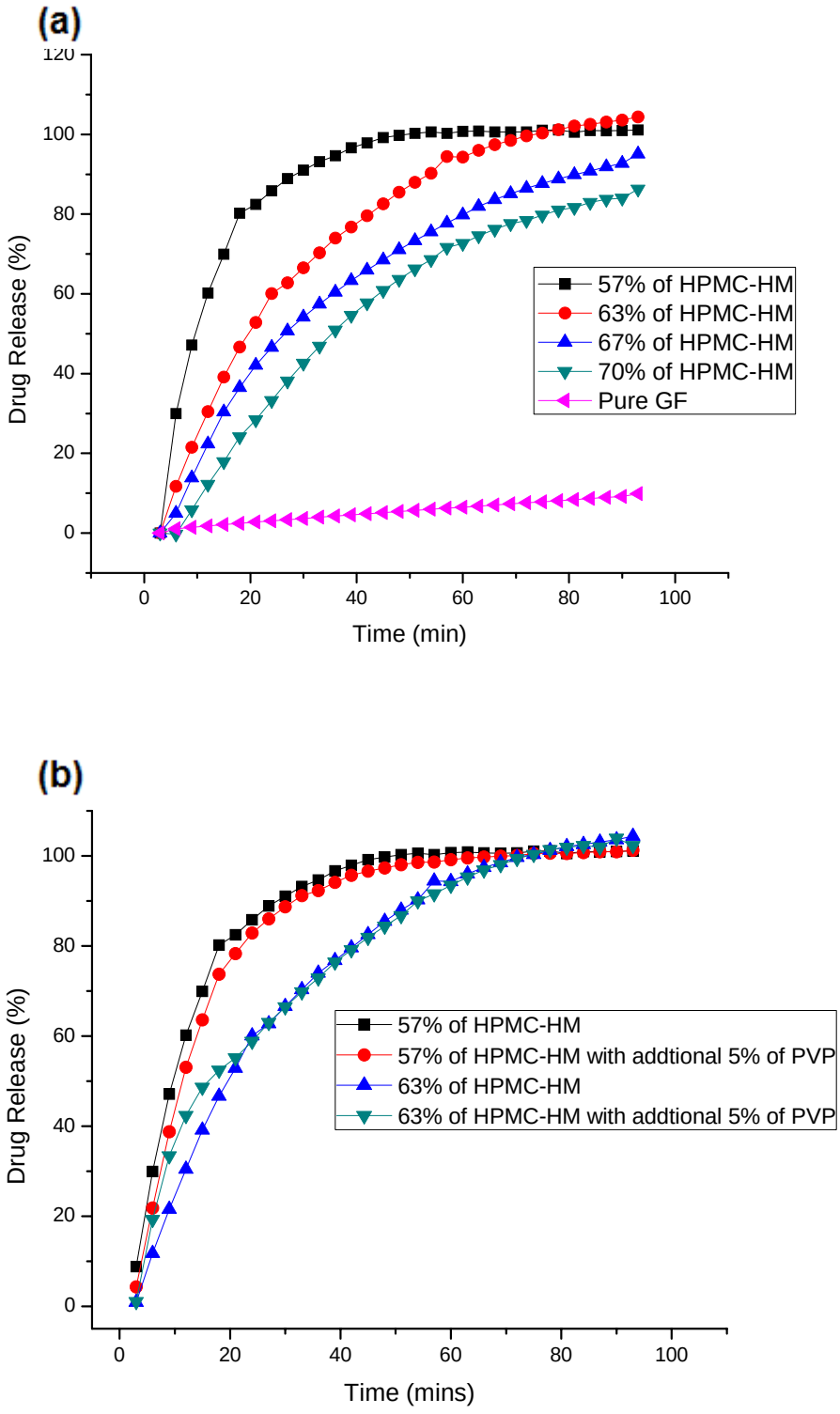

Figure 4.8 Drug release profiles of GF-loaded polymer films.

4.4 Summary

The integration of anti-solvent synthesis of micron-scale particles, their stabilization in the suspension and subsequent film formation was accomplished. While HPMC-LM was an excellence at stabilizing GF in suspension, HPMC-HM and PVP were necessary for making continuous films with good mechanical properties. In vitro drug release profiles showed compelete drug released at the end of 50 minunts. Typically, the release rate decreased with an increase in HPMC content of the film. It is found that first-order and Hixson-Crowell model were most suited for describing the drug release rate, which suggested that the release was concentration dependent and depended on the surface area.

CHAPTER 5

ANTI-SOLVENT PARTICLE FORMATION AND FILM FORMATION WITH CYCLODEXTRINS

5.1 Introduction

Poor water solubility has always been a key obstacle in achieving adequate bioavailability for many hydrophobic drug molecules being developed by the pharmaceutical industry (Merisko-Liversidge et al., 2003; Yu et al., 2006). Dissolution in the gastrointestinal (GI) tract is a limiting factor for these compounds and increasing their dissolution rate has been a great interest in drug development processes (Tho et al., 2010). The purpose of the present investigation is to study the effects of β-cyclodextrin and its derivatives, as well as the combination use with surfactant on the anti-solvent synthesis of hydrophobic drug particles with simultaneous suspension stabilization and the formation of films for drug delivery. The Griseofulvin particles were produced with anti-solvent precipitation, while β-cyclodextrin, Methyl-β-cyclodextrin and Hydroxypropyl-β-cyclodextrin were used to stabilize the GF suspension, and encapsulation into polymer films was carried out with high molecular weight hydroxypropyl methyl cellulose. The interaction between cyclodextrins and griseofulvin has been investigated in both solid and liquid state.

5.2 Experimental Section

5.2.1 Materials

Three cyclodextrins (β-Cyclodextrin, methyl-β-cyclodextrin and hydroxypropyl-β-cyclodextrin) were chosen to study their influence over the physicochemical properties of drug-cyclodextrin systems in term of drug-cyclodextrin interactions in both solid state (physical stability) and aqueous solution (inclusion complexation).

Griseofulvin (GF, 95% purity), β-Cyclodextrin (BCD), methyl-β-Cyclodextrin (MBCD), hydroxypropyl-β-Cyclodextrin (HPBCD) and sodium dodecyl sulfate (SDS) were purchased from Sigma Aldrich (St Louis, MO). High molecular weight hydroxypropyl methyl cellulose (HPMC-E4M) was purchased from Dow Chemical Company (Midland, MI). All these materials were used as received. The water used in the experiments was purified with a Milli-Q Plus system.

5.2.2 Methods

Anti-solvent precipitation was carried out at room temperature and the anti-solvent was prepared by dissolving cyclodextrins and SDS in water. The solvent solution was prepared by dissolving GF in acetone (GF: CD: SDS = 10:10:1, w/w). The mixing of anti-solvent and solvent was carried out under ultrasonic agitation for 30 min (water: acetone =. 5:1, v/v), which was followed by 15 min stirring. For preparation of the solid complexes, the drug suspensions were filtered through 0.45 μm PTFE membrane filters and the water was removed from aqueous drug/cyclodextrin solutions by evaporation. Film-forming suspensions were obtained by adding additional HPMC-E4M into the stabilized drug suspensions. Film-forming suspensions were cast on a stainless steel plate with a Film Casting Knife (BYK Additives & Instruments, Columbia, MD) and then

dried at 50 °C in a vacuum oven for 5 hours. This was followed by an additional 4 hours of drying at room temperature. Finally, the films were peeled off and stored in a dessicator.

Particle size analysis was carried out by static and dynamic light scattering. Static light scattering was carried out using Coulter Particle Size Analyzer LS230 (Beckman Coulter Inc., Miami, FL). Dynamic light scattering was carried out using Beckman Coulter, N4 Plus Submicron Particle Size Analyzer (Beckman Coulter Inc., Miami, FL) at 23^{o} fixed detector angle. Zeta potential measurements were determined using a DelsaNano (Beckman Coulter Inc., Miami, FL). Differential scanning calorimetry (DSC) was used to determine the melting point of GF particles. Approximately 6 mg of samples were weighed and sealed in an aluminum pan and then scanned using a Pyris-1 DSC instrument (Perkin Elmer Inc., San Jose, CA) with a temperature speed of 5 °C/min from 25 to 300 °C.

Sedimentation was monitored as a function of time by measuring the weight percentage of the solid remaining in the suspension. This was accomplished as follows. Each suspension was divided equally into four subsamples and transferred to separate tubes and stored at 25^{o}C. The solid sediments were collected at 2, 4, 7 and 10 hour intervals, dried in the oven at 40 °C in a vacuum to remove the solvent and weighed.

Scanning electron microscopy (SEM) was performed using a LEO 1530 (LEO Electron Microscopy Inc., Thornwood, NY) to study the morphology of particles and films. A Nicolet Almege XR Dispersive Raman with Olympus BX51 Confocal Microscope (Thermo Fisher Scientific Corp., Madison, WI) using a laser at 532nm was applied in the Raman imaging mode. The infrared analysis was performed using Perkin-

Elmer spectrometer (PerkinElmer, Boston, USA). The infrared spectra for inclusion complex were detected in KBr pellets in the transmission mode.

GF-loaded polymer films were stored in a dessicator at 25 °C for two months. Their redispersion was studied by dissolving the GF film in the water with magnetic stirring. The drug release studies were performed using the USP basket method at a rotational speed of 100 rpm using a Varian VK 7010 dissolution apparatus (Varian Inc., Cary, NC). The dissolution medium was 900 ml of 5 % SDS solution and the temperature was maintained at 37±0.5 °C. At appropriate time intervals, the samples were directed to analysis using a Cary 50 UV-visible spectrophotometer (Cary Inc., Canoga Park, CA) at 291nm.

5.3 Results and Discussion

The most common cyclodextrins are α, β and γ -cyclodextrins, which consist of six, seven and eight glucopyranose units respectively. Of these three cyclodextrins, β-cyclodextrin is the most common pharmaceutical excipients due to its cavity size, availability in pure form and efficiency of drug complexation. However, the parent β-cyclodextrin has limited aqueous solubility that was much lower than chemically modified β-cyclodextrin. For example, methyl-β-cyclodextrin has solubility of about 2000 mg/mL in aqueous solution at room temperature, which is significantly higher than that of the parent β-cyclodextrin (18.5 mg/ml) (Charoenchaitrakool et al., 2002). The higher aqueous solubility for cyclodextrin derivatives enhance effectiveness as drug carriers, and it has been reported that cyclodextrin derivatives such as methyl-β-cyclodextrin and

hydroxypropyl-β-cyclodextrin are the best candidates for incorporation into drug formulation for hydrophobic drugs (Charoenchaitrakool et al., 2002; Rogers et al., 2002).

5.3.1 Solid State Characterization

5.3.1.1 Particle Size Analysis for Drug Suspensions. It was observed that most of the GF underwent anti-solvent precipitation rather than be completely consumed in a soluble, aqueous complex. This is evident from the image presented in Figure 5.1. A clear drug solution containing GF in acetone is shown in Figure 5.1a, while a homogenous GF suspension in presence of HPBCD and SDS and the corresponding clear liquid phase (obtained from the filtration of the suspension) containing GF complex are shown in Figure 5.1b and c. Mass balance showed that 72% of the GF was present as a precipitate containing micron size particles.

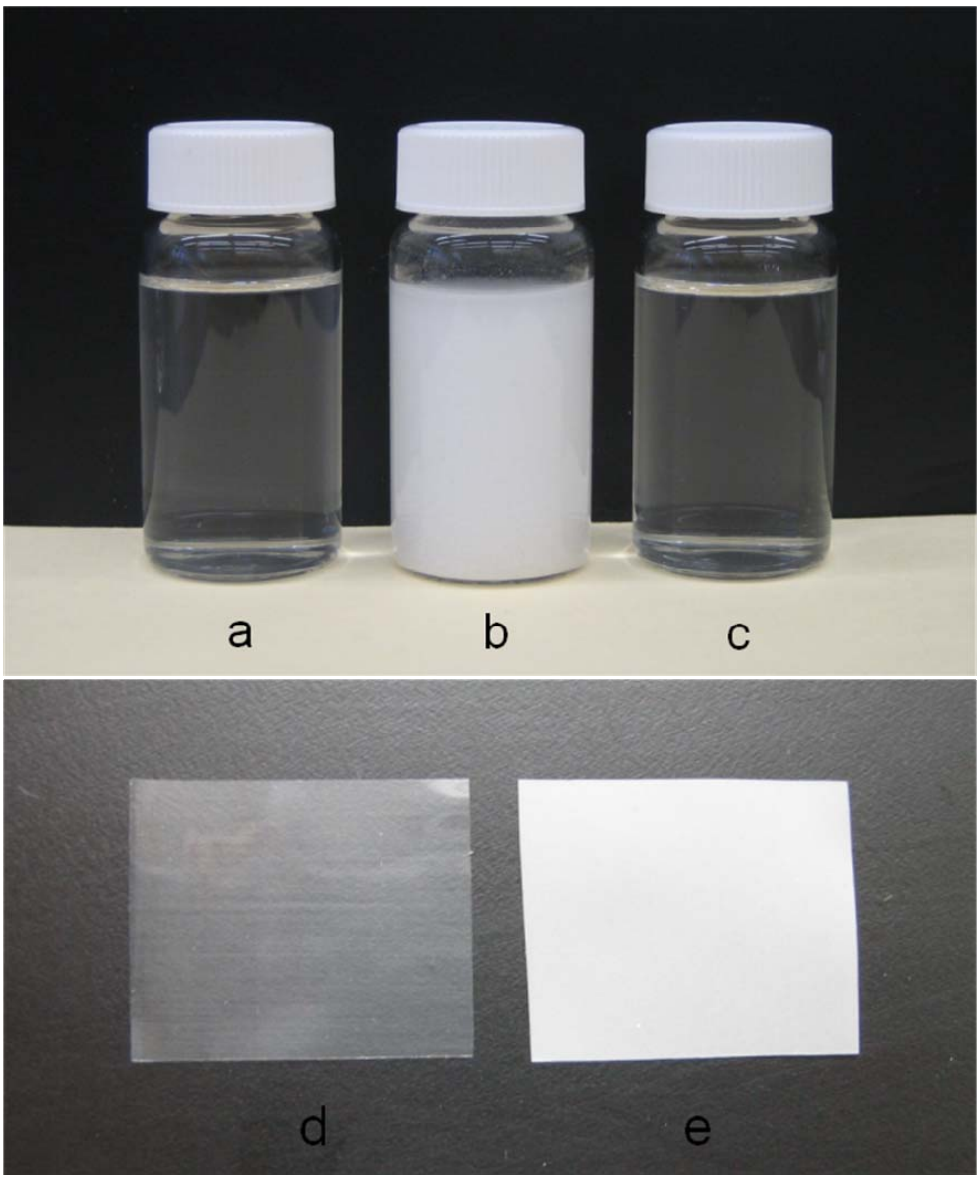

Figure 5.1 Photograph of (a) GF in organic solution (acetone); (b) GF suspension in presence of HPBCD and SDS; (c) liquid phase containing GF complex; (d) blank polymer film; (e) GF-loaded polymer film.

Dynamic light scattering or photon correlation spectroscopy (PCS) was used to selectively monitor the growth of the smaller particles. Figure 5.2 shows the change of the diameter of the smaller particles as a function of time for 30 hours. It is seen that the small particles grew with time, as the nanoparticles agglomerated into larger ones. The

growth of the smaller particles was faster when the combination of HPBCD and SDS were used in the formulation. The trend was similar for other cyclodextrins. The decrease in particle size in both systems may be attributed to Ostwald ripening.

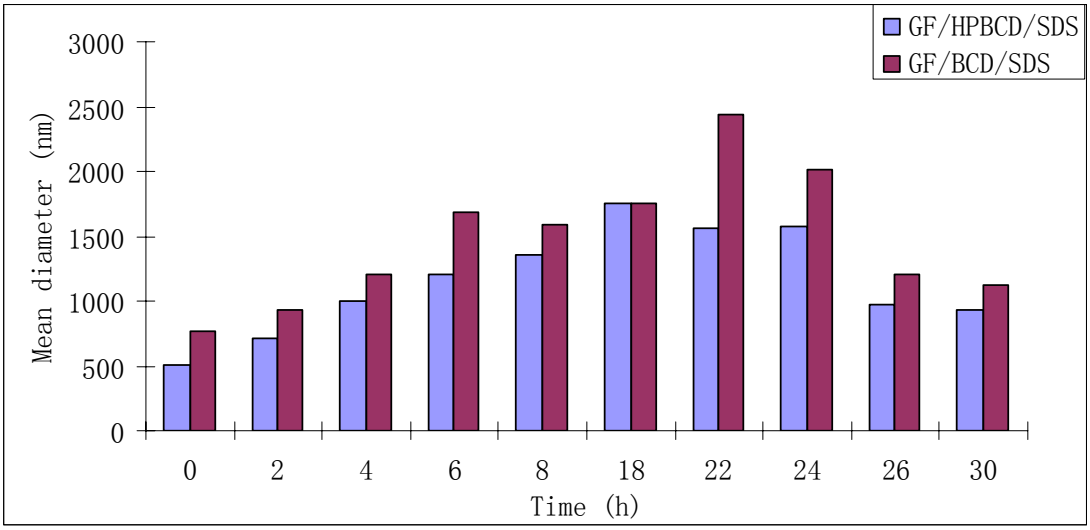

Figure 5.2 Dynamic light scattering measurement of stabilized suspension as a function of time (a) GF stabilized by HPBCD and SDS; (b) GF stabilized by BCD and SDS.

Typical particle size distribution (PSD) of pure GF and stabilized GF suspension with BCD are shown in Figure 5.3. Pure GF suspension was obtained by directly dissolving GF powder into water with stirring. The mean diameter in the aqueous suspension was 24.3 μm with a broad size distribution, where particles were as large as 76.4 μm. With anti-solvent precipitation and stabilization with HPBCD/SDS, the mean particle diameter decreased to 5.0 μm with a significantly narrow particle size distribution. Bimodal distributions were achieved during stabilization with all the cyclodextrins, which clearly showed the drug particles coagulated. The mean diameters of particle for different suspension systems are presented in Table 5.1 at the initiation of anti-solvent particle formation and four hours hence. All the cyclodextrins used here were effective in reducing the particle size. It was observed that the addition of SDS during

precipitation reduced the particle size between 8-20%. For example, the suspension of GF stabilized by HPBCD and SDS produced smaller particles (5.0 μm) compared with the one stabilized only by HPBCD (6.5 μm). The trend in particle diameter appeared to be in the order HPBCD<MBCD<BCD. MBCD and HPMBCD which contain methoxyl or hydroxypropyl groups are able to adsorb onto the hydrophobic solid surfaces, while BCD were found to be less effective. Among all the systems studied here, the combination of HPBCD/SDS generated the smallest particle size (5.0 μm).

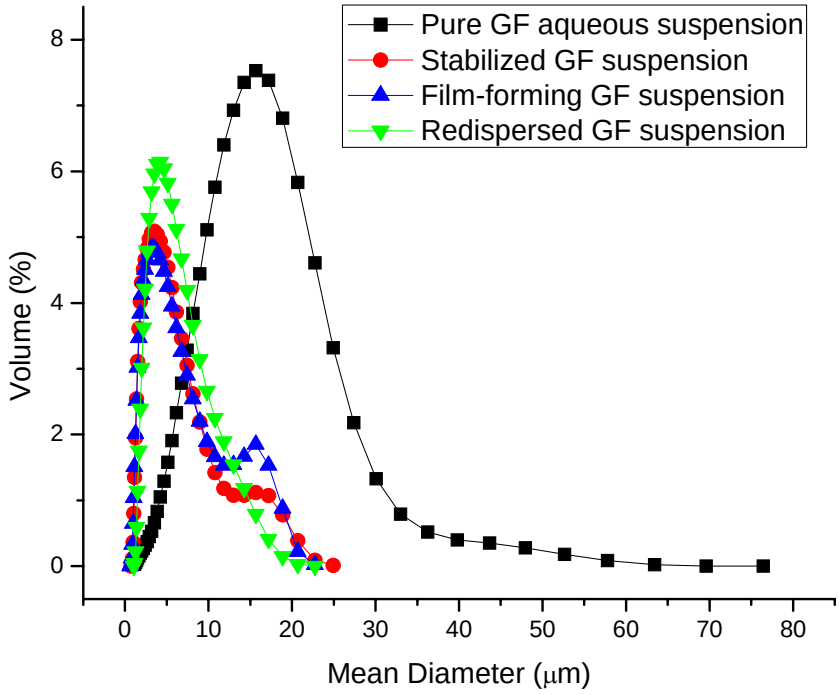

Figure 5.3 Particle size distribution of GF suspensions in presence of cyclodextrins and SDS.

Also seen from Table 5.1 is that as the suspension was allowed to stand, the larger particles settled, reducing the average particle diameter (dp) in the suspension. It is evident from Figure 5.4a that the presence of the cyclodextrins and SDS had stabilizing

effect. In presence of SDS, the variation in dp was significantly less because the settling rate was slower. In its absence dp dropped rapidly from 6.5 to 2.9 μm. While cyclodextrins provided steric stabilization, SDS provided an electrostatic energy barrier. Together they help maintain the distance between closely approaching solid particles in a suspension (Ain-Ai and Gupta, 2008). The selection of cyclodextrins was also important. According to Figure 5.4b, HPBCD showed a stronger stabilizing effect than MBCD and BCD. The trend was similar for all cases. Without SDS the average particle size in this suspension dropped to between 1.5-3.5 μm in 6-8 hours. Typically the drops were maximum in case of BCD and minimum for HPBCD.

Table 5.1 Stabilizing GF with Cyclodextrins and Surfactant

Suspension	Mean diameter (μm)		Percentage (%)	Percentage of particles in suspension (%)		Sedimentation rate (w %/h)		Zeta potential (mV)	Melting Point (°C)
	0 hour	4 hour	0 hour (<5 μm)	2 hour	7 hour	2 hour	7 hour		
GF/HPBCD/SDS	5.0	3.3	66.0	59.0	54.4	20.5	6.5	-16.3	217.8
GF/HPBCD	6.5	3.7	56.7	41.0	32.7	29.5	9.6	-7.5	220.6
GF/MBCD/SDS	5.6	3.5	57.0	56.2	41.9	21.9	8.3	-10.0	214.2
GF/MBCD	7.0	4.1	48.4	38.1	31.0	31	9.9	-4.8	219.6
GF/BCD/SDS	5.9	3.6	56.5	54.3	41.0	22.9	8.4	-7.3	214.8
GF/BCD	7.3	4.0	40.4	37.0	29.8	31.5	10.0	-4.5	219.1

Melting point for pure GF is 219.0 °C

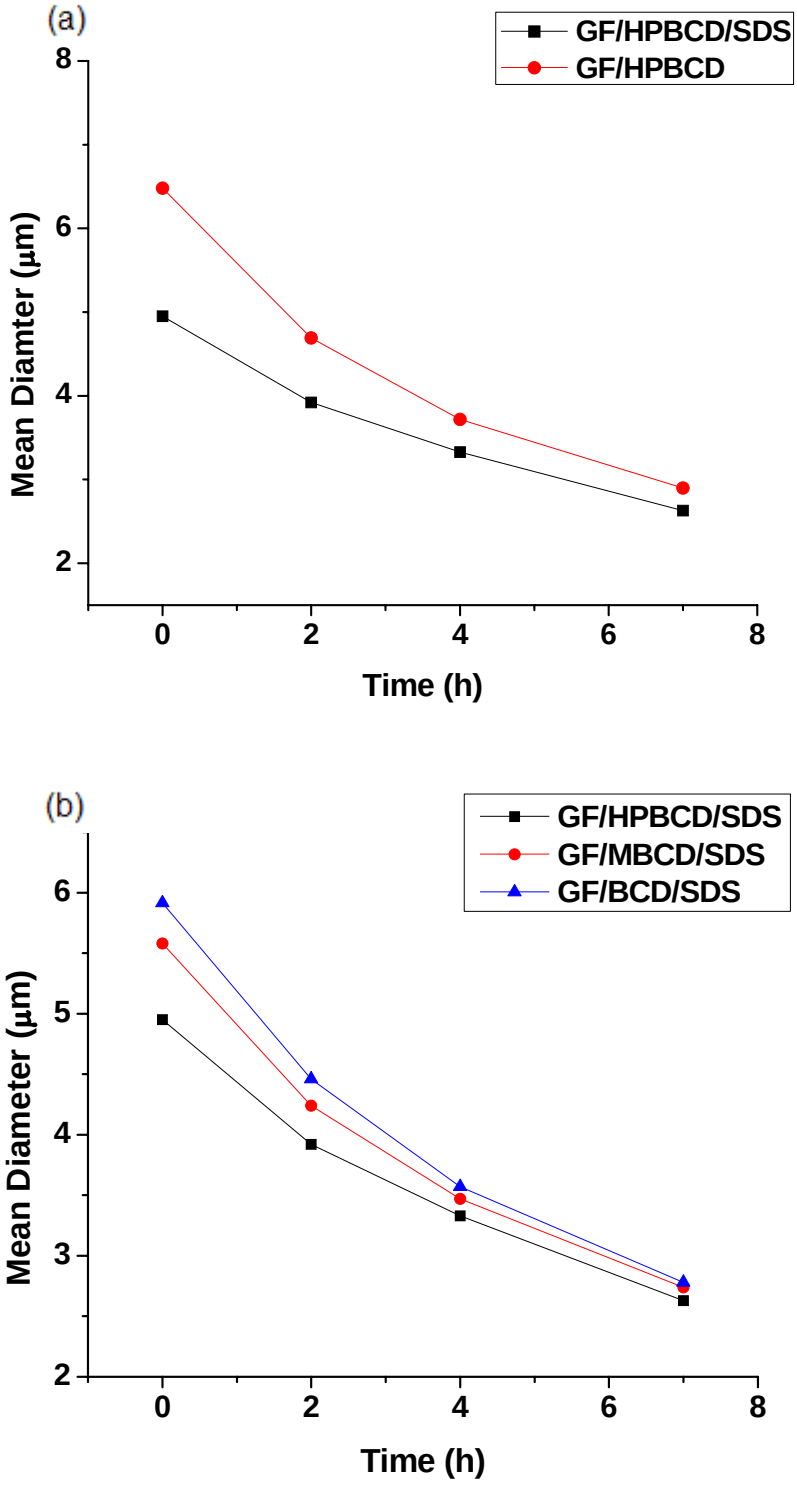

Figure 5.4 Mean diameter of drug particles as a function of time: (a) GF stabilized with HPBCD and SDS, FNB stabilized with HPBCD; (b) GF in presence of different cyclodextrins and SDS.

Zeta-potential measurements were used to study the stability of the drug suspension. The zeta potential values were measured after the preparation of the drug suspensions. Dispersed GF particles showed negative zeta potential in the range of -4.5 to -16.3 mV (Table 5.1). It has been found that both cyclodextrins and SDS contribute the stabilization of drug particles in the suspension and the addition of the anionic surfactant SDS probably led to a negative zeta potential. Melting point of the precipitated particles was measured to see if the cyclodextrins co-precipitated with GF particles. In all cases, the melting point did not increase significantly, which implied that the HPMC only formed a surface layer and was not a major component of the particle itself.

5.3.1.2 Sedimentation Rate. Sedimentation rate is a key factor in determining long term stability (Mersmann, 1999). Typically, the particles grow or aggregate to a larger size, which increases the overall setting rate. According to Stokes equation the rate of sedimentation depends upon the diameter of the dispersed particles, and the density and viscosity of the medium (Allen et al., 2005). Sedimentation rate was measured by calculating the weight percentage (wt%) of solid drug particles remaining in the suspension as a function of time.

The solid particles were uniformly distributed after the preparation of the suspension. The amount of the solid particles in the suspension decreased with time as they began to settle. These are presented in Figure 5.5. The results appear to be consistent with the Stokes Equation that the smaller diameter particles have slower settling rate. However, the rate of settling varied depending upon the cyclodextrins and SDS used. It was found that settling rate of GF/CD/SDS systems were slower than that of the GF/CD systems. At the end of 10 hours, 50.0% of the particles in the GF/HPBCD/SDS were still

in suspension as compared to 30.6% when the SDS was not added. As shown in Figure 5.5b, among HPBCD, MBCD and BCD, HPBCD were most suitable one where 50.0% of the drug stayed stabilized at the end of ten hours as compared to only 37.0%/37.6% in presence of MBCD and BCD. However, as seen from Figure 5.5c, trend in the GF/CD systems were not as obvious, as they were for the particle diameter. According to the Stokes equation, the density of the particles along with the medium plays an important role and may affect the precipitation of the particles.

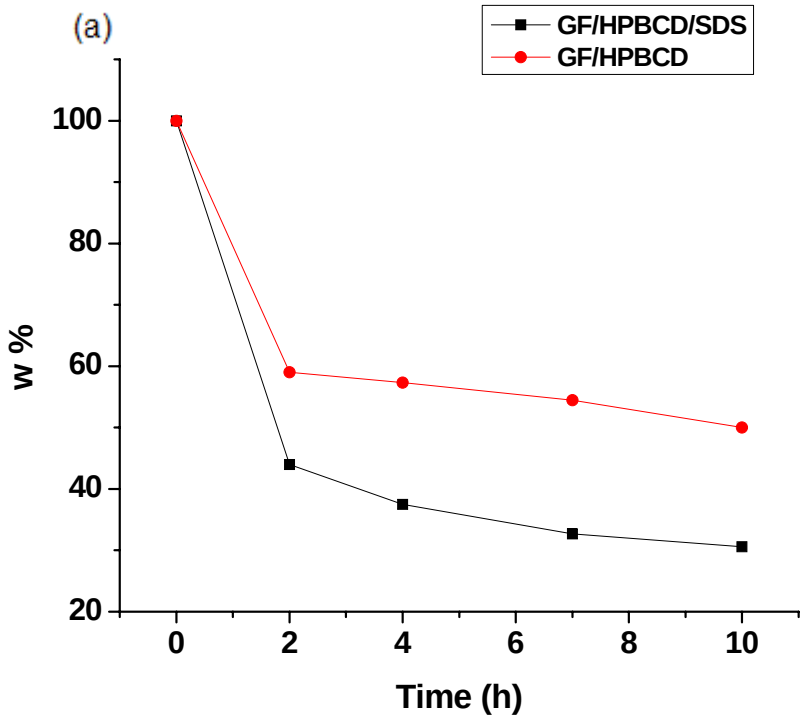

Figure 5.5 Weight percentage of stabilized drug particles in suspension: (a) GF in presence of HPBCD and SDS; (b) GF in presence of different cyclodextrins and SDS; (c) GF in presence of different cyclodextrins without SDS.

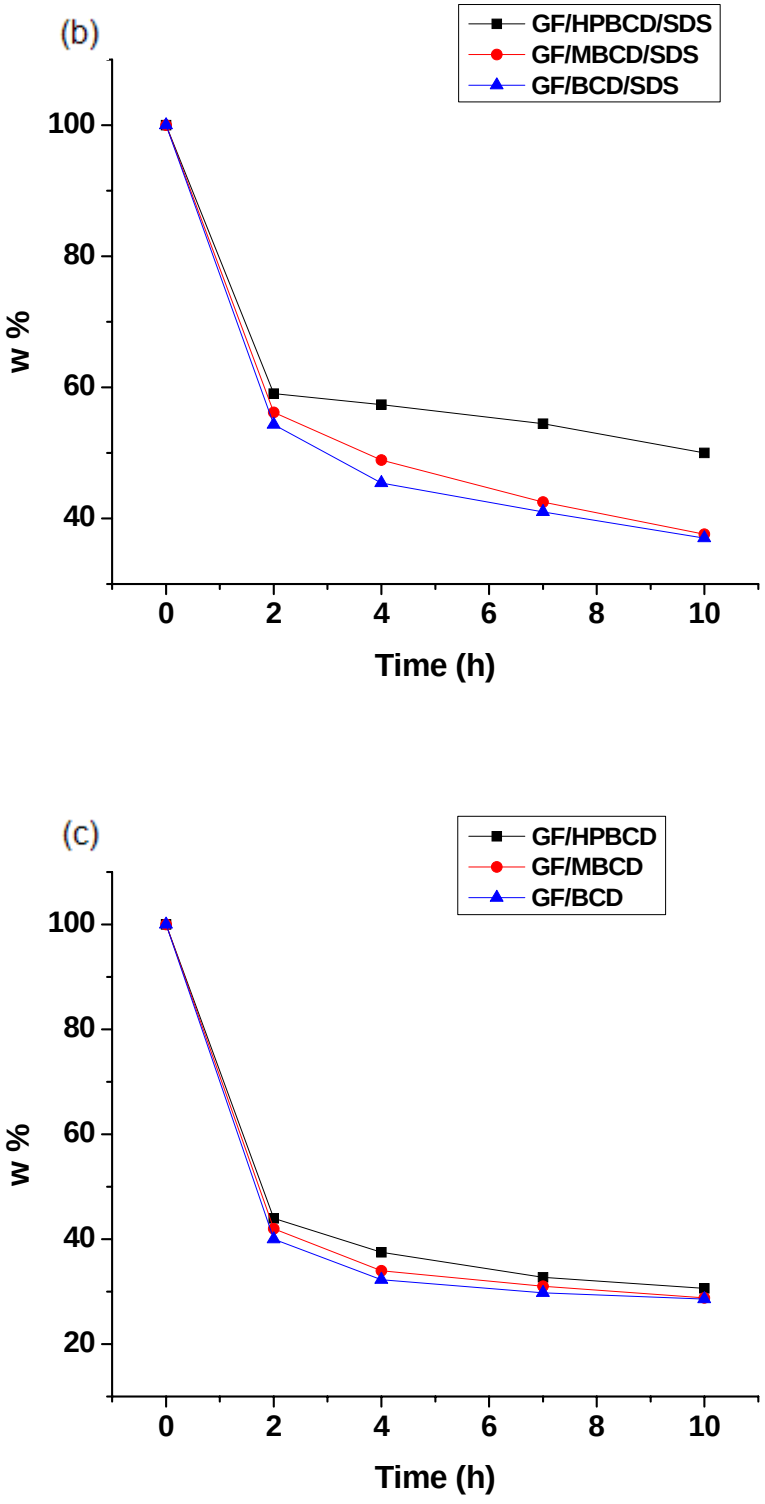

Figure 5.5 Weight percentage of stabilized drug particles in suspension: (a) GF in presence of HPBCD and SDS; (b) GF in presence of different cyclodextrins and SDS; (c) GF in presence of different cyclodextrins without SDS.(Continued)

The settling rate was computed as a function of time for all systems (Figure 5.6). It was evident that the settling rate increased rapidly within the first two hours and then dropped. The rate of settling was the slowest for HPBCD and fastest for BCD. In all cases, SDS was effective in lowering the settling rate. For example, in the case of GF/HPBCD/SDS system, the settling rate was reduced by more than 27% by the addition of SDS.

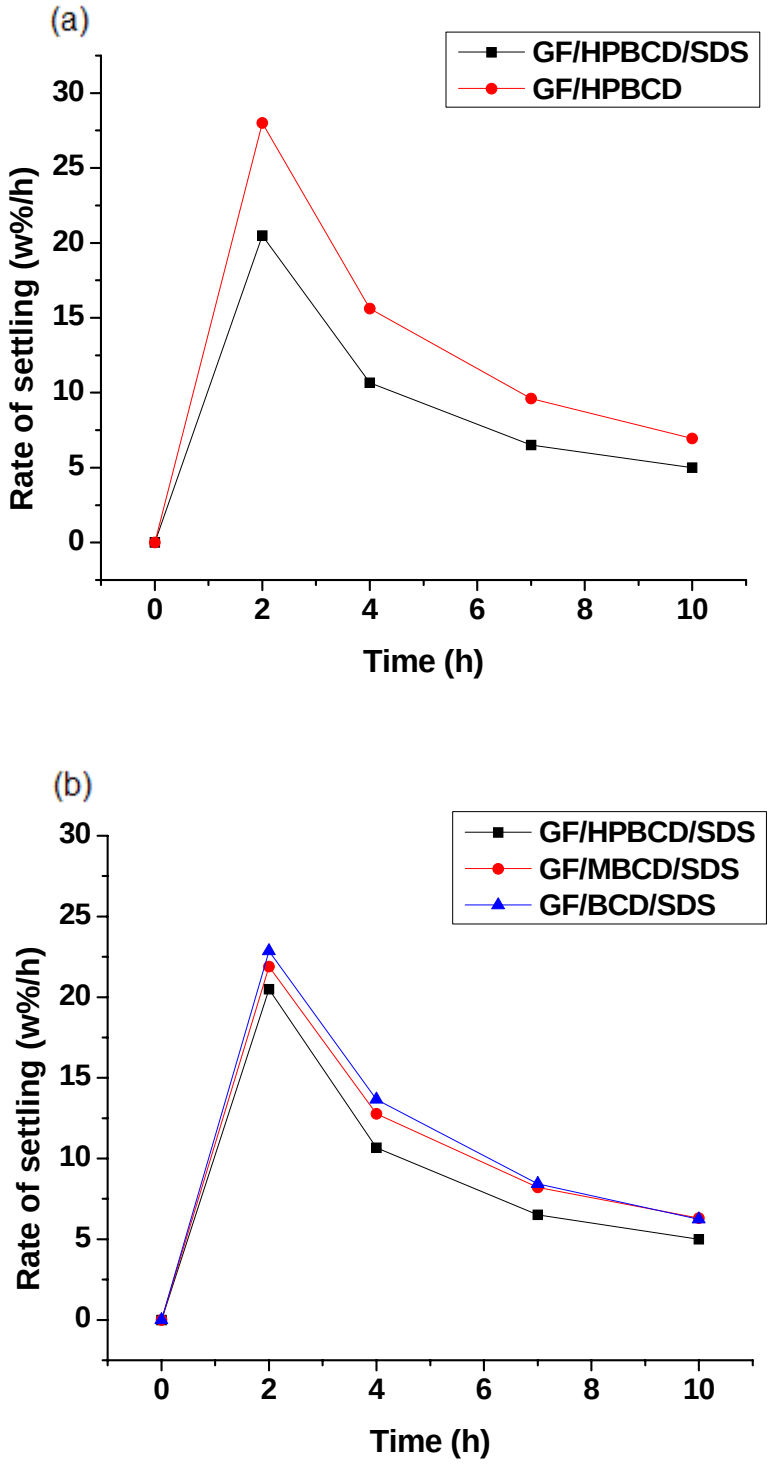

Figure 5.6 Rate of settling as a function of time for GF: (a) GF in presence of HPBCD and SDS; (b) GF in presence of different cyclodextrins and SDS.

5.3.1.3 Particle Morphology and Raman Spectroscopy Analysis. Figure 5.7 shows the comparison of SEM images of GF/CD/SDS systems and GF/CD systems. It was found that GF particles had crystal shapes in all the systems. In the case of GF/CD/SDS, the particles had relatively smaller diameter compared with those in GF/CD.

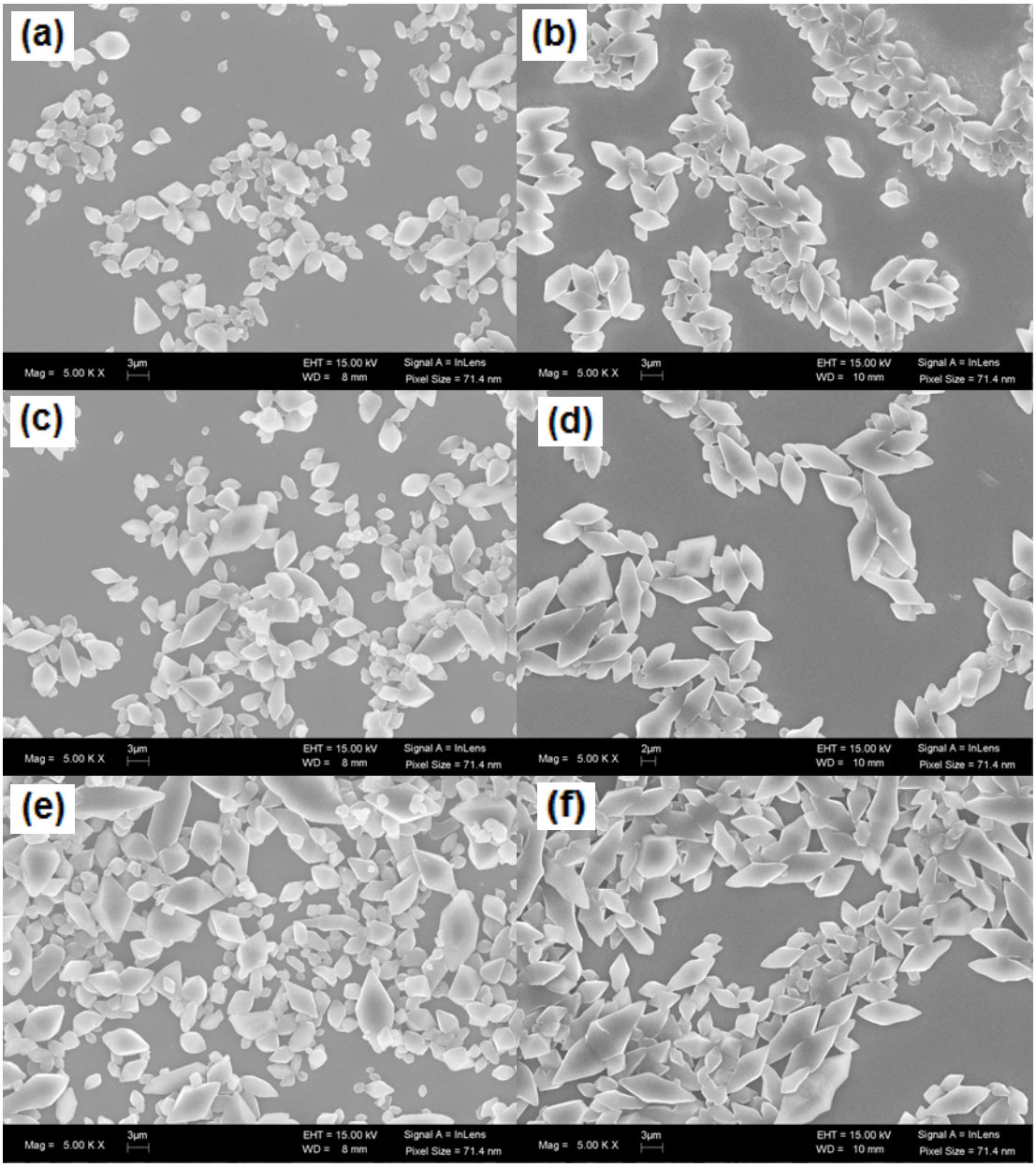

Figure 5.7 SEM images of GF particles**:** (a) GF stabilized by HPBCD and SDS; (b) GF stabilized by HPBCD; (c) GF stabilized by MBCD and SDS (d) GF stabilized by MBCD; (e) GF stabilized by BCD and SDS (f) GF stabilized by BCD.

Some of the solid drug particles were analyzed by Raman Microscopy. Figure 5.8a, b and d show the Raman images of GF drug particles stabilized with HPBCD and SDS. The Raman spectra of HPMC, pure GF and GF particles stabilized with HPBCD and SDS were compared. The C=O stretching of benzofuran ring of GF in the region

1550-1800cm^{-1} and C-H stretching in the region of 2800-3200 cm^{-1} were observed in both pure GF and it stabilized analog (Bolton and Prasad, 1981). The Raman results show that the crystals contained the respective drugs, but didn't show any interaction between the GF and HPBCD. The results suggest the absence of GF/CD inclusion complex formed in the solid state of drug suspension due to the insufficient affinity (low binding constant) of GF to enter the relatively apolar cavity of cyclodextrin (Miller et al., 2007).

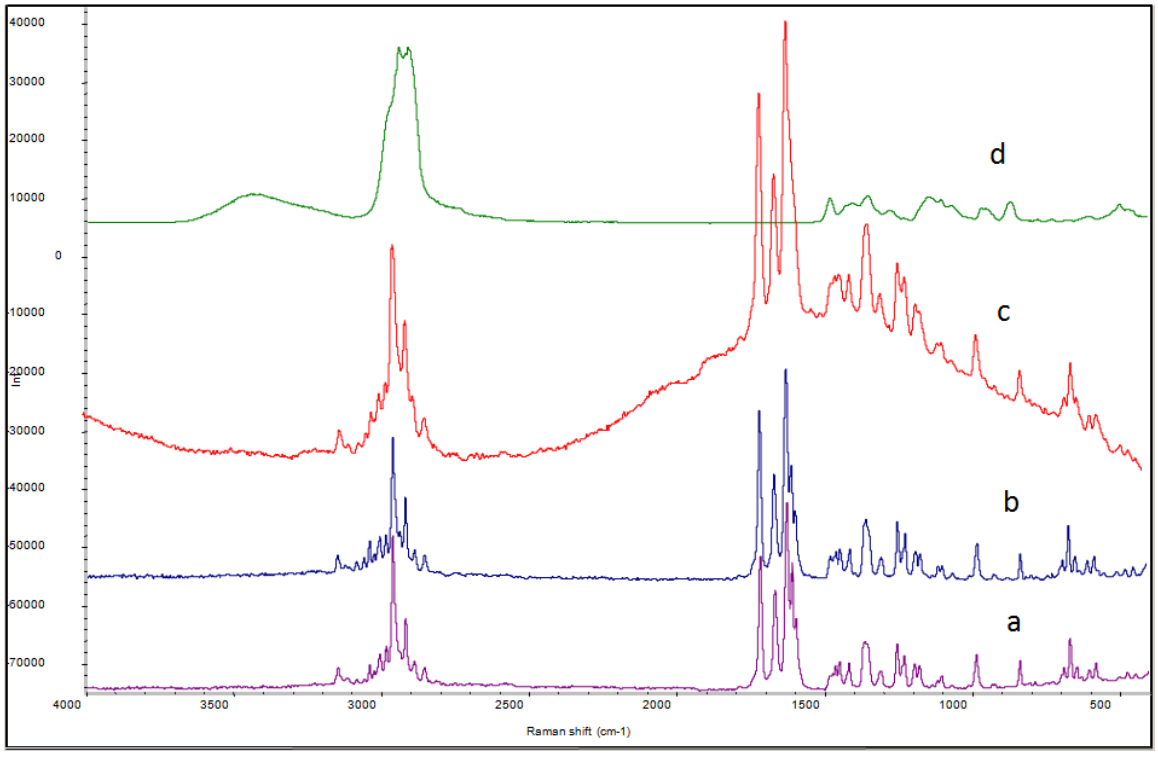

Figure 5.8 Raman spectra of (a) GF stabilized by HPBCD and SDS; (b) pure GF; (c) GF/HPBCD/HPMC film; (d) HPBCD.

5.3.2 Aqueous State Characterization

A relatively small percentage (28%) of the GF was found in the aqueous phase as soluble CD/GF complex. The complex formation was confirmed by FTIR and Raman spectroscopy. Figure 5.9 shows the Raman spectra of GF/HPBCD complex, HPBCD and pure GF. The C=O stretching of benzofuran ring of GF in the region 1550-1800 cm^{-1} was observed in both pure GF and GF/HPBCD complex. Compared with pure GF, the reduction of intensity of C=O stretching for GF/HPBCD complex indicated hydrogen bonding between cyclic keto group (oxygen) of GF and secondary alcoholic hydrogen of HPBCD. The IR spectra showed marked reduction in the intensity of the C=O group at 1708 cm^{-1} for GF complexes, suggesting the possible change in the environment of the C=O group of GF (Figure 5.10) (Dhanaraju, 1998).

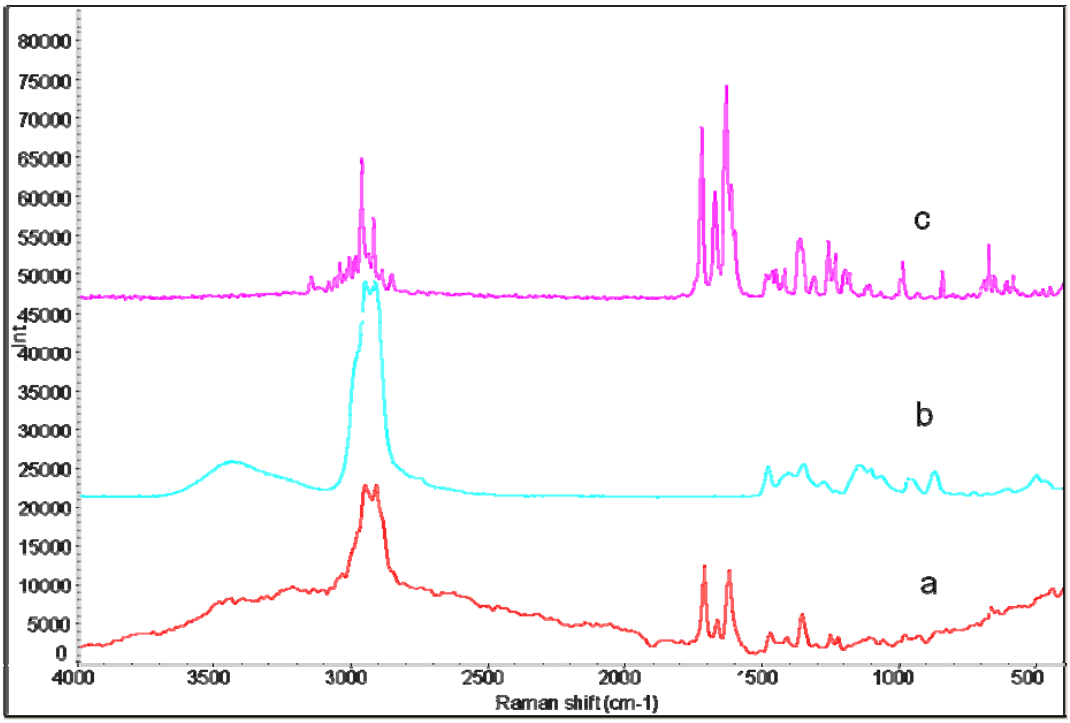

Figure 5.9 Raman spectra of (a) GF/HPBCD complex; (b) HPBCD; (c) pure GF.

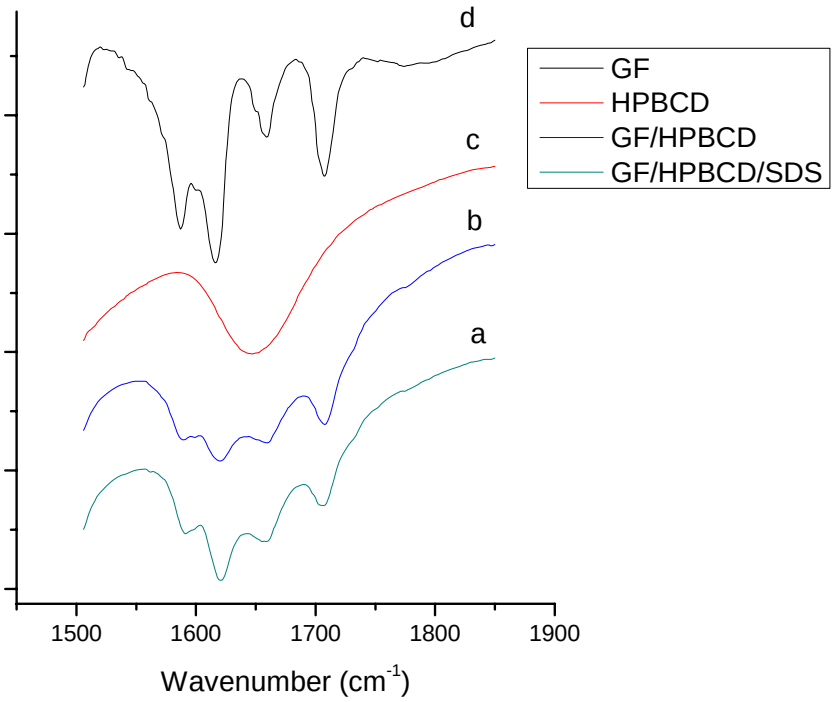

Figure 5.10 FTIR spectra of (a) GF/HPBCD complex from system GF/HPBCD/SDS; (b) GF/HPBCD complex from system GF/HPBCD; (c) HPBCD; (d) pure GF.

5.3.3 Drug Film Formation and Characterization

5.3.3.1 Characterization of film-forming suspensions and GF films. Hydroxypropyl methyl cellulose (HPMC), a semisynthetic derivative of cellulose, has been widely used in the pharmaceutical industry and is known to be a good film-forming agent (Cao et al., 2004; Hiremath, 2008). In this work, GF-loaded polymer films were casted from GF/CD suspensions with addition of high molecular weight of HPMC (HPMC-E4M) and the solvent was removed via solvent evaporation in a vacuum oven. HPMC-E4M films provided good mechanical properties compared to low molecular weight HPMC (Hardy et al., 2006). Films formed with low molecular weight HPMC were easy to crack (Nagarsenker, 1999). In our study, 41%-71% of HPMC-E4M were present in the final film and contributed to the optimization of films. Figure 5.3 shows the comparison of

stabilized GF suspension and final film-forming GF suspensions. The final film-forming suspension, which contained additional HPMC-E4M showed a slight shift in the size distribution compared with initial stabilized GF suspension. It was found that there was a 4-8% increase in mean particle diameter but it remained under 7.5 µm

SEM was used to study the surface morphology and GF particle distribution within the films. The goal was to obtain uniform distribution of the GF particles throughout the film. Figure 5.11 a and b show SEM images of GF-loaded film containing 16.4% of GF, 16.4% of HPBCD, 65.6% of HPMC and 1.6% of SDS. It can be seen that top surface showed the presence of large number of GF crystals. The SEM of the cross-section showed that the drug particles were uniformly distributed throughout the film.

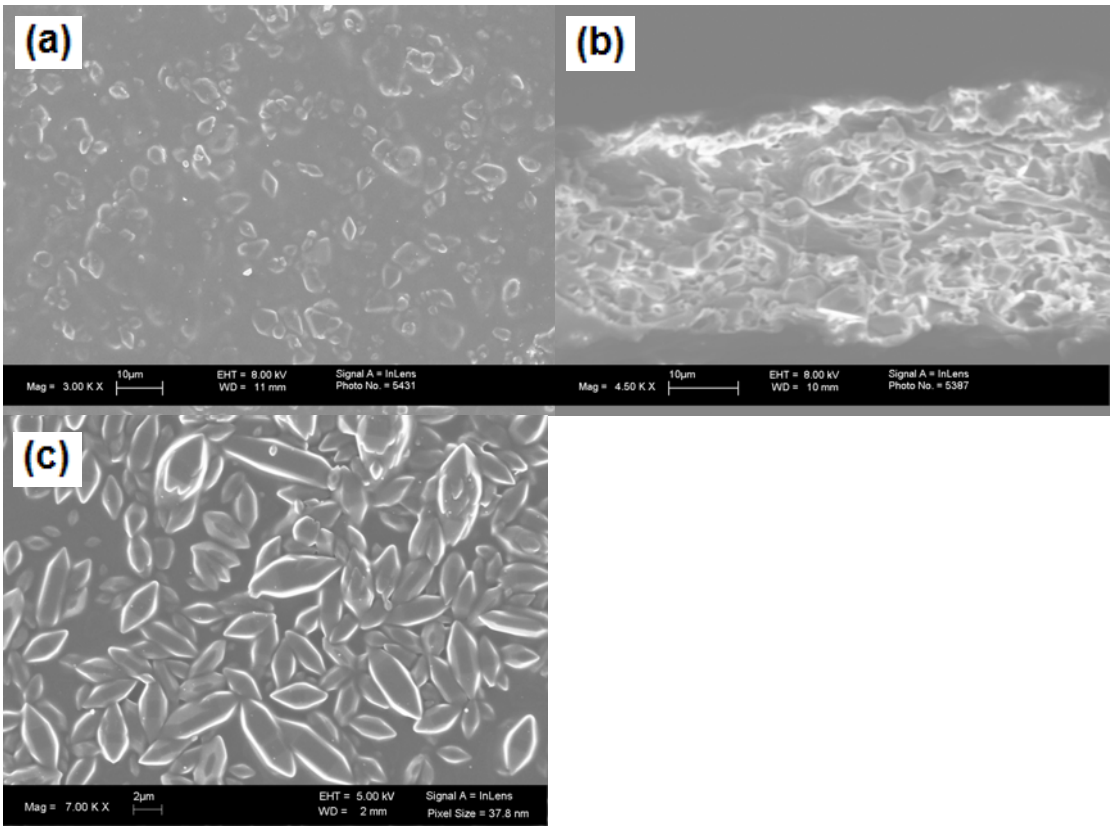

Figure 5.11 SEM images of (a) top surface of GF-loaded polymer film; (b) cross-section of GF-loaded polymer film; (c) GF particles in redispersed suspension.

Raman spectroscopy was used to image the film surface. It provided sensitive GF detection in polymer matrices and the well-resolved fundamental intra and intermolecular stretching and bending modes allowing determination in solid state. Figures 5.8b and c show the comparison of Raman spectra of pure GF and GF-loaded film containing 16.4% of GF. The GF spectra showed strong peaks in the region 1550-1800cm^{-1} and 2800-3200 cm^{-1}, which were attributed to the C=O stretching of benzofuran ring and C-H stretching of GF respectively (Bolton and Prasad, 1981). The same characteristic peaks were also observed in GF-loaded polymer film, which indicated the presence of the drug and no significant alteration of the GF molecule.

5.3.3.2 Redispersion of Drug Particles and In Vitro Drug Release Profiles. The GF films were stored at room temperature for two months prior to redispersion in aqueous medium. In all cases, the redispersion of the GF films regenerated the original particles (Figure 5.3). The SEM analysis of the dried GF particles from the film redispersions showed similar crystal shape (Figure 5.11c). Therefore it is concluded that the multiple steps of film formation, storage and redisperion did not alter the main properties of the drug.

The drug release profiles of pure drug substance and drug in the films was studied and are shown in Figure 5.12. It is apparent that all the films reached 100% of drug release within 80 minutes, which indicates that *in situ* drug/CD inclusion complex were formed in the aqueous dissolution medium. In terms of GF/CD, HPBCD and MBCD showed faster release rate than BCD system, which demostrated the stronger complexation and solubilzation effects for HPBCD and MBCD. However, no significant difference for the release rate were observed for GF/CD/SDS systems. Futhermore, the

addition of HPMC contribute to the enhancement of GF release rate in all the systems. It has been reported water-soluble polymers are known to enhance the complexation efficacy of a wide variety of guest molecules and aqueous solubility of cyclodextrins and free drug molecules (Ceschel et al., 2002; Nandi, 2003). For instance, Chowdary and Srinivas have evaluated the effect of polymers such as HPMC on the complexation, solubilizing efficiencies of HPBCD and dissolution rate of celecoxib from the HPBCD complexes and they found addition of those polymers significantly enhanced the complexation and solubilizing efficiencies of HPBCD (Chowdary, 2006).

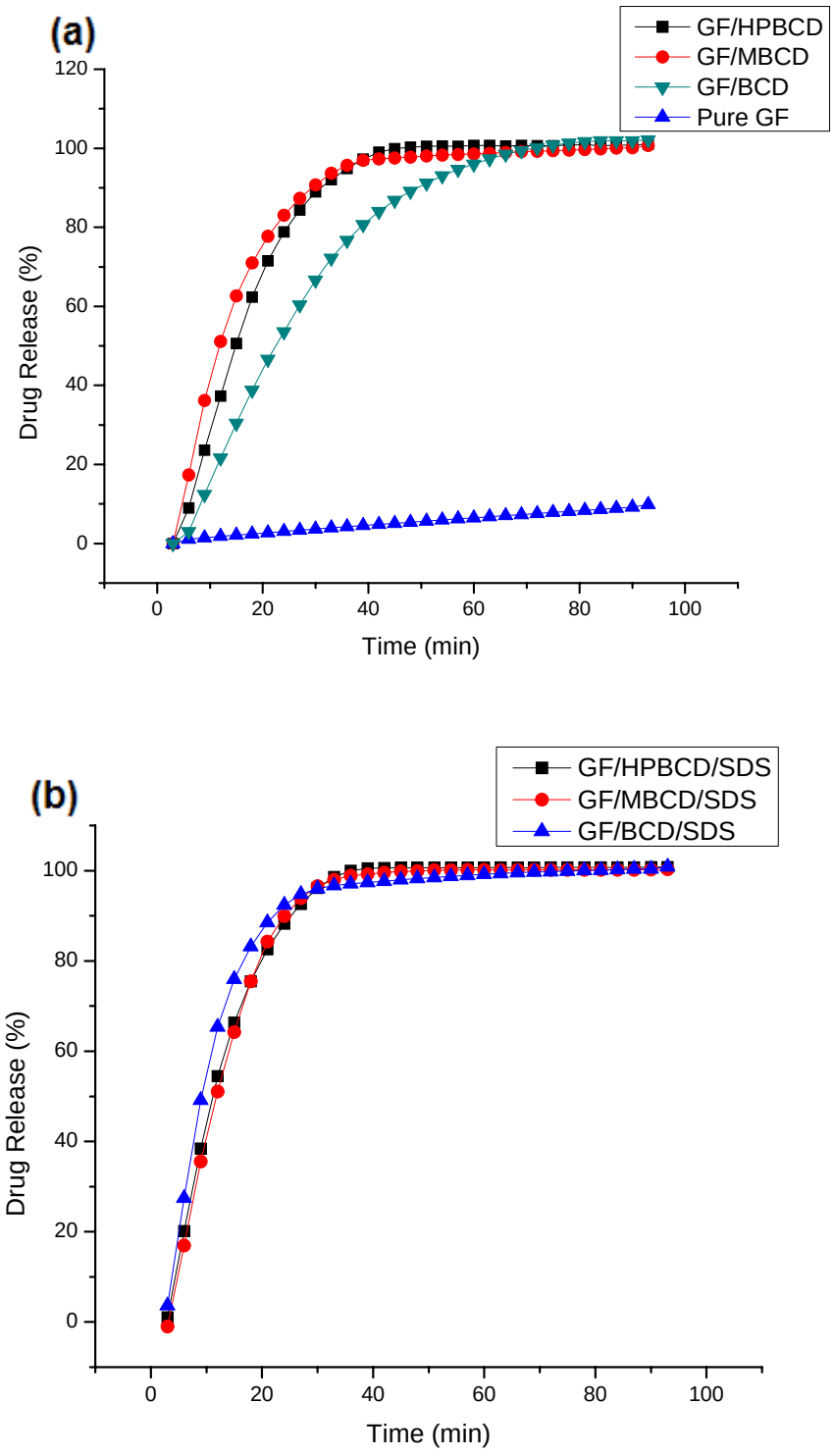

Figure 5.12 Drug release profiles of GF-loaded polymer films: (a) GF/CD system; (b) GF/CD/SDS system.

5.4 Summary

The integration of anti-solvent synthesis of micron-scale particles, their stabilization using cyclodextrins and subsequent film formation was accomplished. It has been found that the cyclodextrins were capable of inhibiting particle growth and stabilize the drug particles during anti-solvent precipitation. The solid phase of drug suspensions showed no evidence of inclusion complexation, but the complexes were found in the liquid phase. Drug-loaded polymer films were synthesized using high molecular weight HPMC. In vitro drug release profiles of films showed compelete drug released within 80 minunts, suggtesting strong interaction between the CD and the GF.

REFERENCES

Ain-Ai, A., Gupta, P.K., 2008. Effect of arginine hydrochloride and hydroxypropyl cellulose as stabilizers on the physical stability of high drug loading nanosuspensions of a poorly soluble compound. International Journal of Pharmaceutics. 351**,** 282-288.

Akhgari, A., Farahmand, F., Afrasiabi Garekani, H., Sadeghi, F., Vandamme, T.F., 2006. Permeability and swelling studies on free films containing inulin in combination with different polymethacrylates aimed for colonic drug delivery. European Journal of Pharmaceutical Sciences. 28**,** 307-314.

Akkar, A., Müller, R.H., 2003. Intravenous itraconazole emulsions produced by SolEmuls technology. European Journal of Pharmaceutics and Biopharmaceutics. 56**,** 29-36.

Al-Hamidi, H., Edwards, A.A., Mohammad, M.A., Nokhodchi, A., 2010a. To enhance dissolution rate of poorly water-soluble drugs: Glucosamine hydrochloride as a potential carrier in solid dispersion formulations. Colloids and Surfaces B: Biointerfaces. 76**,** 170-178.

Al-Hamidi, H., Edwards, A.A., Mohammad, M.A., Nokhodchi, A., 2010b. Glucosamine HCl as a new carrier for improved dissolution behaviour: Effect of grinding. Colloids and Surfaces B: Biointerfaces. 81**,** 96-109.

Allen, L.V., Popvich, N.G., Ansel, H.C., Section, V.I., 2005. Liquid dosage forms. Ansel's Pharmaceutical Dosage Forms and Drug Delivery Systems. 336-384.

Beck-Broichsitter, M., Gauss, J., Packhaeuser, C.B., Lahnstein, K., Schmehl, T., Seeger, W., Kissel, T., Gessler, T., 2009. Pulmonary drug delivery with aerosolizable nanoparticles in an ex vivo lung model. International Journal of Pharmaceutics. 367**,** 169-178.

Bodvik, R., Dedinaite, A., Karlson, L., Bergström, M., Bäverbäck, P., Pedersen, J.S., Edwards, K., Karlsson, G., Varga, I., Claesson, P.M., 2010. Aggregation and network formation of aqueous methylcellulose and hydroxypropylmethylcellulose solutions. Colloids and Surfaces A: Physicochemical and Engineering Aspects. 354**,** 162-171.

Bolton, B.A., Prasad, P.N., 1981. Laser Raman investigation of pharmaceutical solids: Griseofulvin and its solvates. Journal of Pharmaceutical Sciences. 70**,** 789-793.

Brewster, M.E., Vandecruys, R., Peeters, J., Neeskens, P., Verreck, G., Loftsson, T., 2008. Comparative interaction of 2-hydroxypropyl-[beta]-cyclodextrin and sulfobutylether-[beta]-cyclodextrin with itraconazole: Phase-solubility behavior and stabilization of supersaturated drug solutions. European Journal of Pharmaceutical Sciences. 34**,** 94-103.

Broman, E., Khoo, C., Taylor, L.S., 2001. A comparison of alternative polymer excipients and processing methods for making solid dispersions of a poorly water soluble drug. International Journal of Pharmaceutics. 222**,** 139-151.

Brown, M.B., Martin, G.P., Jones, S.A., Akomeah, F.K., 2006. Dermal and Transdermal Drug Delivery Systems: Current and Future Prospects. Drug Delivery. 13**,** 175-187.

Camino, N.A., Pérez, O.E., Sanchez, C.C., Rodriguez Patino, J.M., Pilosof, A.M.R., 2009. Hydroxypropylmethylcellulose surface activity at equilibrium and adsorption dynamics at the air-water and oil-water interfaces. Food Hydrocolloids. 23**,** 2359-2368.

Cao, Q.-R., Choi, H.-G., Kim, D.-C., Lee, B.-J., 2004. Release behavior and photo-image of nifedipine tablet coated with high viscosity grade hydroxypropylmethylcellulose: effect of coating conditions. International Journal of Pharmaceutics. 274**,** 107-117.

Ceschel, G.C., Mora, P.C., Borgia, S.L., Maffei, P., Ronchi, C., 2002. Skin permeation study of dehydroepiandrosterone (DHEA) compared with its α-cyclodextrin complex form. Journal of Pharmaceutical Sciences. 91**,** 2399-2407.

Chacón, M., Molpeceres, J., Berges, L., Guzmán, M., Aberturas, M.R., 1999. Stability and freeze-drying of cyclosporine loaded poly(D,L-lactide-glycolide) carriers. European Journal of Pharmaceutical Sciences. 8**,** 99-107.

Chan, L.W., Ong, K.T., Heng, P.W.S., 2005. Novel Film Modifiers to Alter the Physical Properties of Composite Ethylcellulose Films. Pharmaceutical Research. 22**,** 476-489.

Charoenchaitrakool, M., Dehghani, F., Foster, N.R., 2002. Utilization of supercritical carbon dioxide for complex formation of ibuprofen and methyl-[beta]-cyclodextrin. International Journal of Pharmaceutics. 239**,** 103-112.

Chien, Y.W., 1992. Oral drug delivery and delivery system. Novel drug delivery systems. 139-196.

Chowdary, K.P.R., Srinivas, S.V., 2006. Influence of Hydrophilic Polymers on Celecoxib Complexation With Hydroxypropyl β-Cyclodextrin. AAPS PharmSciTech. 7**,** 1-6.

Desai, C., Meng, X., Yang, D., Wang, X., Akkunuru, V., Mitra, S., 2011. Effect of solvents on stabilization of micro drug particles. Journal of Crystal Growth. 314**,** 353-358.

Dhanaraju, M.D., Senthil Kumaran, K., Baskaran, T., Sree Rama Moorthy, M. , 1998. Enhancement of Bioavailability of Griseofulvin by Its Complexation with Beta-Cyclodextrin. Drug Development and Industrial Pharmacy. 24**,** 583-587.

Dreis, S., Rothweiler, F., Michaelis, M., Cinatl Jr, J., Kreuter, J., Langer, K., 2007. Preparation, characterisation and maintenance of drug efficacy of doxorubicin-loaded human serum albumin (HSA) nanoparticles. International Journal of Pharmaceutics. 341**,** 207-214.

Duro, R., Alvarez, C., Martínez-Pacheco, R., Gómez-Amoza, J.L., Concheiro, A., Souto, C., 1998. The adsorption of cellulose ethers in aqueous suspensions of pyrantel pamoate: Effects on zeta potential and stability. European Journal of Pharmaceutics and Biopharmaceutics. 45**,** 181-188.

Ferrero, C., Massuelle, D., Doelker, E., 2010. Towards elucidation of the drug release mechanism from compressed hydrophilic matrices made of cellulose ethers. II. Evaluation of a possible swelling-controlled drug release mechanism using dimensionless analysis. Journal of Controlled Release. 141**,** 223-233.

Fulzele, S.V., Satturwar, P.M., Dorle, A.K., 2002. Polymerized rosin: novel film forming polymer for drug delivery. International Journal of Pharmaceutics. 249**,** 175-184.

Gao, Y., Li, L.B., Zhai, G., 2008. Preparation and characterization of Pluronic/TPGS mixed micelles for solubilization of camptothecin. Colloids and Surfaces B: Biointerfaces. 64**,** 194-199.

Grau, M.J., Kayser, O., Müller, R.H., 2000. Nanosuspensions of poorly soluble drugs -- reproducibility of small scale production. International Journal of Pharmaceutics. 196**,** 155-159.

Gun'ko, V.M., Klyueva, A.V., Levchuk, Y.N., Leboda, R., 2003. Photon correlation spectroscopy investigations of proteins. Advances in Colloid and Interface Science. 105**,** 201-328.

Haas Jimoh Akanbi, M., Post, E., Meter-Arkema, A., Rink, R., Robillard, G.T., Wang, X., Wösten, H.A.B., Scholtmeijer, K., 2010. Use of hydrophobins in formulation of water insoluble drugs for oral administration. Colloids and Surfaces B: Biointerfaces. 75**,** 526-531.

Hardy, I.J., Cook, W.G., Melia, C.D., 2006. Compression and compaction properties of plasticised high molecular weight hydroxypropylmethylcellulose (HPMC) as a hydrophilic matrix carrier. International Journal of Pharmaceutics. 311**,** 26-32.

Helfgen, B., Hils, P., Holzknecht, C., Türk, M., Schaber, K., 2001. Simulation of particle formation during the rapid expansion of supercritical solutions. Journal of Aerosol Science. 32**,** 295-319.

Hiremath, P.S., Saha, R. N. , 2008. Controlled Release Hydrophilic Matrix Tablet Formulations of Isoniazid: Design and In Vitro Studies. AAPS PharmSciTech. 9**,** 1171-1178.

Iervolino, M., Cappello, B., Raghavan, S.L., Hadgraft, J., 2001. Penetration enhancement of ibuprofen from supersaturated solutions through human skin. International Journal of Pharmaceutics. 212**,** 131-141.

Italia, J., Yahya, M., Singh, D., Ravi Kumar, M., 2009. Biodegradable Nanoparticles Improve Oral Bioavailability of Amphotericin B and Show Reduced Nephrotoxicity Compared to Intravenous Fungizone®. Pharmaceutical Research. 26**,** 1324-1331.

Itoh, K., Pongpeerapat, A., Tozuka, Y., Oguchi, T., Yamamoto, K., 2003. Nanoparticle formation of poorly water-soluble drugs from ternary ground mixtures with PVP and SDS. Chemical and Pharmaceutical Bulletin. 51**,** 171-174.

Jain, K.K., 2008a. Transdermal drug delivery system: skin perturbation devices. Drug delivery systems. 119-140.

Jain, K.K., 2008b. Drug delivery system- An overview. Drug delivery systems. 1-50.

Jongen, N., Bowen, P., Lemaître, J., Valmalette, J.-C., Hofmann, H., 2000. Precipitation of Self-Organized Copper Oxalate Polycrystalline Particles in the Presence of Hydroxypropylmethylcellulose (HPMC): Control of Morphology. Journal of Colloid and Interface Science. 226**,** 189-198.

Kesisoglou, F., Panmai, S., Wu, Y., 2007. Nanosizing -- Oral formulation development and biopharmaceutical evaluation. Advanced Drug Delivery Reviews. 59**,** 631-644.

Kipp, J.E., 2004. The role of solid nanoparticle technology in the parenteral delivery of poorly water-soluble drugs. International Journal of Pharmaceutics. 284**,** 109-122.

Kiratzis, N., Faers, M., Luckham, P.F., 1999. Depletion flocculation of particulate systems induced by hydroxyethylcellulose. Colloids and Surfaces A: Physicochemical and Engineering Aspects. 151**,** 461-471.

Larson, J.R., Gibson, G.A., Schmidt, S.P., 2002. Liquid Toner Materials. Handbook of Imaging Materials, 2nd Ed.**,** 239-264.

Li, C.L., Martini, L.G., Ford, J.L., Roberts, M., 2005. The use of hypromellose in oral drug delivery. Journal of Pharmacy and Pharmacology. 57**,** 533-546.

Loftsson, T., Masson, M., 2001. Cyclodextrins in topical drug formulations: theory and practice. International Journal of Pharmaceutics. 225**,** 15-30.

Loftsson, T., Másson, M., Brewster, M.E., 2004. Self-Association of Cyclodextrins and Cyclodextrin Complexes. Journal of Pharmaceutical Sciences. 93**,** 1091-1099.

Loftsson, T., Hreinsdóttir, D., Másson, M., 2005. Evaluation of cyclodextrin solubilization of drugs. International Journal of Pharmaceutics. 302**,** 18-28.

Marchisio, D.L., Rivautella, L., Barresi, A.A., 2006. Design and scale-up of chemical reactors for nanoparticle precipitation. AIChE Journal. 52**,** 1877-1887.

Martin, T., Bandi, N., Shulz, R., Roberts, C., Kompella, U., 2002. Preparation of budesonide and budesonide-PLA microparticles using supercritical fluid precipitation technology. AAPS PharmSciTech. 3**,** 16-26.

Martinac, A., Filipović-Grčić, J., Voinovich, D., Perissutti, B., Franceschinis, E., 2005. Development and bioadhesive properties of chitosan-ethylcellulose microspheres for nasal delivery. International Journal of Pharmaceutics. 291**,** 69-77.

Matteucci, M.E., Hotze, M.A., Johnston, K.P., Williams Iii, R.O., 2006. Drug nanoparticles by antisolvent precipitation: Mixing energy versus surfactant stabilization. Langmuir. 22**,** 8951-8959.

Maulding, H.V., Tice, T.R., Cowsar, D.R., 1986. Biodegradable microcapsules: Acceleration of polymeric excipient hydrolytic rate by incorporation of a basic medicament. Journal of Controlled Release. 3**,** 103-117.

Mehta, S.K., Kaur, G., Bhasin, K.K., 2007. Analysis of Tween based microemulsion in the presence of TB drug rifampicin. Colloids and Surfaces B: Biointerfaces. 60**,** 95-104.

Meng, X., Yang, D., Keyvan, G., Michniak-Kohn, B., Mitra, S., Synthesis and Immobilization of Micro-scale Drug Particles in Cellulosic Films. Colloids and Surfaces B: Biointerfaces. In Press, Accepted Manuscript.

Meng, X., Chen, Y., Chowdhury, S.R., Yang, D., Mitra, S., 2009. Stabilizing dispersions of hydrophobic drug molecules using cellulose ethers during anti-solvent synthesis of micro-particulates. Colloids and Surfaces B: Biointerfaces. 70**,** 7-14.

Meng, X., Yang, D., Mitra, S., 2011. Simultaneous synthesis, stabilization, and self-assembly of microscale drug particles in polymer films. Journal of Applied Polymer Science. 120**,** 2082-2089.

Merisko-Liversidge, E., Liversidge, G.G., Nanosizing for oral and parenteral drug delivery: A perspective on formulating poorly-water soluble compounds using wet media milling technology. Advanced Drug Delivery Reviews. In Press, Corrected Proof.

Merisko-Liversidge, E., Liversidge, G.G., Cooper, E.R., 2003. Nanosizing: a formulation approach for poorly-water-soluble compounds. European Journal of Pharmaceutical Sciences. 18**,** 113-120.

Mersmann, A., 1999. Crystallization and precipitation. Chemical Engineering and Processing: Process Intensification. 38**,** 345-353.

Miller, L.A., Carrier, R.L., Ahmed, I., 2007. Practical considerations in development of solid dosage forms that contain cyclodextrin. Journal of Pharmaceutical Sciences. 96**,** 1691-1707.

Mitragotri, S., 2005. Immunization without needles. Nature Reviews Immunology. 5**,** 905-916.

Mitragotri, S., 2008. Recent development in needle-free drug delivery Frontiers of engineering. 38**,** 5-12.

Muller, R.H., Moschwitzer, J., Bushrab, F.N., 2006. Manufacturing of Nanoparticles by Milling and Homogenization Techniques. 21-52.

Nagarsenker, M.S., Hegde, D.D., 1999. Optimization of the Mechanical Properties and Water-Vapor Transmission Properties of Free Films of Hydroxypropylmethylcellulose. Drug Development and Industrial Pharmacy. 25**,** 95-98.

Nagarsenker, M.S., Hegde, D. D., 1999. Optimization of the Mechanical Properties and Water-Vapor Transmission Properties of Free Films of Hydroxypropylmethylcellulose. Drug Development and Industrial Pharmacy. 25**,** 95-98.

Nair, L.S., Laurencin, C.T., Biodegradable polymers as biomaterials. Progress in Polymer Science. 32**,** 762-798.

Nandi, I., Bateson M., Bari M., Joshi, H.N., 2003. Synergistic Effect of PEG-400 and Cyclodextrin to Enhance Solubility of Progesterone. AAPS PharmSciTech. 4**,** 1-5.

Pérez, O.E., Carrera-Sánchez, C., Rodríguez-Patino, J.M., Pilosof, A.M.R., Adsorption dynamics and surface activity at equilibrium of whey proteins and hydroxypropyl-

methyl-cellulose mixtures at the air-water interface. Food Hydrocolloids. 21, 794-803.

Perrut, M., Jung, J., Leboeuf, F., 2005. Enhancement of dissolution rate of poorly-soluble active ingredients by supercritical fluid processes: Part I: Micronization of neat particles. International Journal of Pharmaceutics. 288, 3-10.

Pierigè, F., Serafini, S., Rossi, L., Magnani, M., 2008. Cell-based drug delivery. Advanced Drug Delivery Reviews. 60, 286-295.

Pongpeerapat, A., Itoh, K., Tozuka, Y., Moribe, K., Oguchi, T., Yamamoto, K., 2004. Formation and stability of drug nanoparticles obtained from drug/PVP/SDS ternary ground mixture. Journal of Drug Delivery Science and Technology. 14, 441-447.

Prow, T.W., Grice, J.E., Lin, L.L., Faye, R., Butler, M., Becker, W., Wurm, E.M.T., Yoong, C., Robertson, T.A., Soyer, H.P., Roberts, M.S., Nanoparticles and microparticles for skin drug delivery. Advanced Drug Delivery Reviews. In Press, Uncorrected Proof.

Raghavan, S.L., Trividic, A., Davis, A.F., Hadgraft, J., 2001. Crystallization of hydrocortisone acetate: influence of polymers. International Journal of Pharmaceutics. 212, 213-221.

Raghavan, S.L., Schuessel, K., Davis, A., Hadgraft, J., 2003. Formation and stabilisation of triclosan colloidal suspensions using supersaturated systems. International Journal of Pharmaceutics. 261, 153-158.

Rao, P.R., Diwan, P.V., 1998. Formulation and in Vitro Evaluation of Polymeric Films of Diltiazem Hydrochloride and Indomethacin for Transdermal Administration. Drug Development and Industrial Pharmacy. 24, 327-336.

Rasenack, N., Müller, B.W., 2002. Dissolution rate enhancement by in situ micronization of poorly water-soluble drugs. Pharmaceutical Research. 19, 1894-1900.

Rodriguez, C.F., Bruneau, N., Barra, J., Alfonso, D., Doelker, E., 2000. Hydrophilic cellulose derivatives as drug delivery carriers: Influence of substitution type on the properties of compressed matrix tablets. Handbook of Pharmaceutical Controlled Release Technology. 1-30.

Rogers, T.L., Nelsen, A.C., Hu, J., Brown, J.N., Sarkari, M., Young, T.J., Johnston, K.P., Williams, R.O., 2002. A novel particle engineering technology to enhance dissolution of poorly water soluble drugs: spray-freezing into liquid. European Journal of Pharmaceutics and Biopharmaceutics. 54, 271-280.

Sanganwar, G.P., Sathigari, S., Babu, R.J., Gupta, R.B., 2010. Simultaneous production and co-mixing of microparticles of nevirapine with excipients by supercritical antisolvent method for dissolution enhancement. European Journal of Pharmaceutical Sciences. 39, 164-174.

Sasa, B., Odon, P., Stane, S., Julijana, K., 2006. Analysis of surface properties of cellulose ethers and drug release from their matrix tablets. European Journal of Pharmaceutical Sciences. 27, 375-383.

Sawalha, H., Purwanti, N., Rinzema, A., Schroën, K., Boom, R., 2008. Polylactide microspheres prepared by premix membrane emulsification--Effects of solvent removal rate. Journal of Membrane Science. 310**,** 484-493.

Scherlund, M., Brodin, A., Malmsten, M., 2000. Nonionic Cellulose Ethers as Potential Drug Delivery Systems for Periodontal Anesthesia. Journal of Colloid and Interface Science. 229**,** 365-374.

Schmidt, C., Bodmeier, R., 1999. Incorporation of polymeric nanoparticles into solid dosage forms. Journal of Controlled Release. 57**,** 115-125.

Sepassi, S., Goodwin, D.J., Drake, A.F., Holland, S., Leonard, G., Martini, L., Lawrence, M.J., 2007. Effect of polymer molecular weight on the production of drug nanoparticles. Journal of Pharmaceutical Sciences. 96**,** 2655-2666.

Seppälä, O.P., Herrala, J., Hedman, J., Alanko, K., Liipo, K., Terho, E., Pietinalho, A., Nyholm, J.E., Nieminen, M.M., 1998. The bronchoprotective efficacy of salbutamol inhaled from a new metered-dose powder inhaler compared with a conventional pressurized metered-dose inhaler connected to a spacer. Respiratory Medicine. 92**,** 578-583.

Siepmann, J., Peppas, N.A., 2001. Modeling of drug release from delivery systems based on hydroxypropyl methylcellulose (HPMC). Advanced Drug Delivery Reviews. 48**,** 139-157.

Suzuki, K., Price, J.C., 1985. Microencapsulation and dissolution properties of a neuroleptic in a biodegradable polymer, poly(d,l-lactide). Journal of Pharmaceutical Sciences. 74**,** 21-24.

Talukdar, M.M., Michoel, A., Rombaut, P., Kinget, R., 1996. Comparative study on xanthan gum and hydroxypropylmethyl cellulose as matrices for controlled-release drug delivery I. Compaction and in vitro drug release behaviour. International Journal of Pharmaceutics. 129**,** 233-241.

Tantishaiyakul, V., Kaewnopparat, N., Ingkatawornwong, S., 1999. Properties of solid dispersions of piroxicam in polyvinylpyrrolidone. International Journal of Pharmaceutics. 181**,** 143-151.

Terayama, H., Okumura, K., Sakai, K., Torigoe, K., Esumi, K., 2001. Aqueous dispersion behavior of drug particles by addition of surfactant and polymer. Colloids and Surfaces B: Biointerfaces. 20**,** 73-77.

Terayama, H., Funakoshi, M., Torigoe, K., Esumi, K., 2002. Kinetics of formation of drug particles in the presence of surfactant/polymer. Colloids and Surfaces B: Biointerfaces. 23**,** 65-71.

Terayama, H., Inada, K., Nakayama, H., Yasueda, S., Esumi, K., 2004. Preparation of stable aqueous suspension of a hydrophobic drug with polymers. Colloids and Surfaces B: Biointerfaces. 39**,** 159-164.

Tho, I., Liepold, B., Rosenberg, J., Maegerlein, M., Brandl, M., Fricker, G., 2010. Formation of nano/micro-dispersions with improved dissolution properties upon dispersion of ritonavir melt extrudate in aqueous media. European Journal of Pharmaceutical Sciences. 40**,** 25-32.

Uekama, K., Ikegami, K., Wang, Z., Horiuchi, Y., Hirayama, F., 1992. Inhibitory effect of 2-Hydroxypropyl-β-cyclodextrin on crystal-growth of nifedipine during storage: Superior dissolution and oral bioavailability compared with polyvinylpyrrolidone K-30. Journal of Pharmacy and Pharmacology. 44**,** 73-78.

Van Eerdenbrugh, B., Froyen, L., Van Humbeeck, J., Martens, J.A., Augustijns, P., Van den Mooter, G., 2008. Drying of crystalline drug nanosuspensions--The importance of surface hydrophobicity on dissolution behavior upon redispersion. European Journal of Pharmaceutical Sciences. 35**,** 127-135.

Vippagunta, S.R., Wang, Z., Hornung, S., Krill, S.L., 2007. Factors affecting the formation of eutectic solid dispersions and their dissolution behavior. Journal of Pharmaceutical Sciences. 96**,** 294-304.

Wan, L.S.C., Heng, P.W.S., Wong, L.F., 1991. The effect of hydroxypropylmethylcellulose on water penetration into a matrix system. International Journal of Pharmaceutics. 73**,** 111-116.

Ward, G.H., Schultz, R.K., 1995. Process-Induced Crystallinity Changes in Albuterol Sulfate and Its Effect on Powder Physical Stability. Pharmaceutical Research. 12**,** 773-779.

Weber, M., Thies, M.C., 2002. Understanding the RESS process. Supercritical Fluid Technology in Materials Science and Engineering: Synthesis, Properties, and Applications. 387-437.

Willart, J.F., De Gusseme, A., Hemon, S., Odou, G., Danede, F., Descamps, M., 2001. Direct crystal to glass transformation of trehalose induced by ball milling. Solid State Communications. 119**,** 501-505.

Wischke, C., Schwendeman, S.P., 2008. Principles of encapsulating hydrophobic drugs in PLA/PLGA microparticles. International Journal of Pharmaceutics. 364**,** 298-327.

Wong, S.M., Kellaway, I.W., Murdan, S., 2006. Enhancement of the dissolution rate and oral absorption of a poorly water soluble drug by formation of surfactant-containing microparticles. International Journal of Pharmaceutics. 317**,** 61-68.

Xia, D., Quan, P., Piao, H., Piao, H., Sun, S., Yin, Y., Cui, F., 2010. Preparation of stable nitrendipine nanosuspensions using the precipitation-ultrasonication method for enhancement of dissolution and oral bioavailability. European Journal of Pharmaceutical Sciences. 40**,** 325-334.

Yagi, N., Terashima, Y., Kenmotsu, H., Sekikawa, H., Takada, M., 1996. Issolution behavior of probucol from solid dispersion systems of probucol-polyvinylpyrrolidone. Chemical and Pharmaceutical Bulletin. 44**,** 241-244.

Yalkowsky, S.H., Valvani, S.C., 1980. Solubility and partitioning I: Solubility of nonelectrolytes in water. Journal of Pharmaceutical Sciences. 69**,** 912-922.

Yasueda, S.I., Inada, K., Matsuhisa, K., Terayama, H., Ohtori, A., 2004. Evaluation of ophthalmic suspensions using surface tension. European Journal of Pharmaceutics and Biopharmaceutics. 57**,** 377-382.

Yasuji, T., Takeuchi, H., Kawashima, Y., 2008. Particle design of poorly water-soluble drug substances using supercritical fluid technologies. Advanced Drug Delivery Reviews. 60**,** 388-398.

Ye, Z.-w., Rombout, P., Remon, J.P., Vervaet, C., Van den Mooter, G., 2007. Correlation between the permeability of metoprolol tartrate through plasticized isolated ethylcellulose/hydroxypropyl methylcellulose films and drug release from reservoir pellets. European Journal of Pharmaceutics and Biopharmaceutics. 67**,** 485-490.

Young, T.J., Johnston, K.P., Pace, G.W., Mishra, A.K., 2003. Phospholipid-stabilized nanoparticles of cyclosporine A by rapid expansion from supercritical to aqueous solution. AAPS PharmSciTech. 5**,** 1-16.

Yu, Z., Johnston, K.P., Williams Iii, R.O., 2006. Spray freezing into liquid versus spray-freeze drying: Influence of atomization on protein aggregation and biological activity. European Journal of Pharmaceutical Sciences. 27**,** 9-18.

Yu. Shekunov, B., Baldyga, J., York, P., 2001. Particle formation by mixing with supercritical antisolvent at high Reynolds numbers. Chemical Engineering Science. 56**,** 2421-2433.

Yuan, H., Huang, L.F., Du, Y.Z., Ying, X.Y., You, J., Hu, F.Q., Zeng, S., 2008. Solid lipid nanoparticles prepared by solvent diffusion method in a nanoreactor system. Colloids and Surfaces B: Biointerfaces. 61**,** 132-137.

Zheng, W., Sauer, D., McGinity, J.W., 2005. Influence of hydroxyethylcellulose on the drug release properties of theophylline pellets coated with Eudragit® RS 30 D. European Journal of Pharmaceutics and Biopharmaceutics. 59**,** 147-154.

Zhu, W., Romanski, F.S., Meng, X., Mitra, S., Tomassone, M.S., Atomistic simulation study of surfactant and polymer interactions on the surface of a fenofibrate crystal. European Journal of Pharmaceutical Sciences. In Press, Corrected Proof.

Zili, Z., Sfar, S., Fessi, H., 2005. Preparation and characterization of poly-ε-caprolactone nanoparticles containing griseofulvin. International Journal of Pharmaceutics. 294**,** 261-267.

Zimmermann, A., Elema, M.R., Hansen, T., Müllertz, A., Hovgaard, L., 2007. Determination of surface-adsorbed excipients of various types on drug particles prepared by antisolvent precipitation using HPLC with evaporative light scattering detection. Journal of Pharmaceutical and Biomedical Analysis. 44**,** 874-880.